DYNAMIC RESPONSE OF A FRAMED OFFSHORE TOWER TO ICE FORCES CONSIDERING NONLINEAR SOIL-STRUCTURE INTERACTION

ASIM KUMAR HALDAR

NOTICE

The quality of this microfiche is heavily dependent upon the quality of the original thesis submitted for microfilming. Every effort has been made to ensure the highest quality of reproduction possible.

If pages are missing, contact the university which granted the degree.

Some pages may have indistinct print especially if the original pages were typed with a poor typewriter ribbon or if the university sent us a poor photocopy.

Previously copyrighted materials (journal articles, published tests, etc.) are not filmed.

Reproduction in full or in part of this film is governed by the Canadian Copyright Act, R.S.C. 1970, c. C-30. Please read the authorization forms which accompany this thesis.

THIS DISSERTATION
HAS BEEN MICROFILMED
EXACTLY AS RECEIVED

AVIS

La qualité de cette microfiche dépend grandement de la qualité de la thèse soumise au microfilmage. Nous avons tout fait pour assurer une qualité supérieure de reproduction.

S'il manque des pages, veuillez communiquer avec l'université qui a conféré le grade.

La qualité d'impression de certaines pages peut laisser à désirer, surtout si les pages originales ont été dactylographiées à l'aide d'un ruban usé ou si l'université nous a fait parvenir une photocopie de mauvaise qualité.

Les documents qui font déjà l'objet d'un droit d'auteur (articles de revue, examens publiés, etc.) ne sont pas microfilmés.

La reproduction, même partielle, de ce microfilm est soumise à la Loi canadienne sur le droit d'auteur, SRC 1970, c. C-30. Veuillez prendre connaissance des formules d'autorisation qui accompagnent cette thèse.

LA THÈSE A ÉTÉ
MICROFILMÉE TELLE QUE
NOUS L'AVONS REÇUE

DYNAMIC RESPONSE OF A FRAMED OFFSHORE TOWER TO ICE FORCES

CONSIDERING NONLINEAR SOIL-STRUCTURE INTERACTION

by

© Asim Kumar Haldar, B.E.

A Thesis submitted in partial fulfillment
of the requirements for the degree of
Master of Engineering

Faculty of Engineering and Applied Science
Memorial University of Newfoundland

April 1977

St. John's Newfoundland, Canada

To My Parents

ABSTRACT

The dynamic response to ice forces of a pile-supported framed offshore structure is studied for two types of foundation conditions: i) Rigid base and ii) Semi-Rigid base. The semi-rigid base is idealized in two ways: i) lumped parameter (also called half-space, continuum and soil spring) foundation model with linear soil springs, and ii) finite elemented foundation model with linear and nonlinear soil behaviour.

The structure analysed is an offshore tower supported by piles. The members are assumed to be rigidly connected and the added water mass is assumed equal to the mass of the water displaced. The structural modelling is based on a two-dimensional representation of the tower assuming a constant dimension equal to the base length perpendicular to the plane. The masses per unit length of the members in the plane of the frame are computed by summing up the structural mass, the mass of the water contained in the tube and the mass of the water displaced. The masses of the members perpendicular to the plane are assumed to be lumped at the horizontal cross-brace level joints.

Linear analysis is carried out for the fixed base condition. For the lumped parameter foundation model, the foundation is idealized by linear horizontal and rotational springs at the mudline level and, for the finite elemented foundation model, by two-dimensional isoparametric plane strain elements. For both models, the structural members and the piles are represented by two-dimensional beam elements. The

response is determined by modal superposition. The nonlinear behaviour due to shear deformations of the soil is handled by the equivalent linearization technique. Mode superposition facilitates an approximate solution in which the stiffnesses used are made compatible with effective shear strain amplitudes at the soil element centroids. The analysis uses the published data on strain-compatible soil properties for clays and sands, and the final values of the soil element stiffness properties are estimated by an iterative procedure. The investigation is carried out for two types of clay: a) Soft, and b) Stiff. In all the analyses, damping is expressed in terms of the modal damping ratio which includes structural damping, viscous damping due to fluid drag, and pile damping due to interaction with the soil.

The results of the study indicate that soil-structure interaction causes a complete redistribution of stresses in the structural members. For nonlinear soil behaviour, a typical member stress is 48% more than that for the rigid foundation model. Therefore, the study highlights the considerable need for including nonlinearity in soil-structure interaction studies. Recommendations are made to extend this investigation to other kinds of environmental forces on offshore structures, e.g. waves and currents.

ACKNOWLEDGEMENTS

The author is very grateful to his supervisor, Dr. D. V. Reddy, Professor of Engineering and Applied Science, Memorial University of Newfoundland, for his excellent guidance, valuable suggestions, encouragement and continuous support with the provision of reference material throughout the project. Without the painstaking effort and the time devoted by Professor Reddy for careful supervision and criticism at every stage, completion of the thesis in this form in a reasonably short period would not have been possible. Appreciation is expressed to Dr. A. S. J. Swamidas and Dr. M. Arockiasamy for their valuable ideas, references and enthusiastic support.

The author would like to thank Memorial University of Newfoundland for the award of a Graduate Fellowship. The support, in part, by Imperial Oil Ltd. under Grant No. 04-2025 to Professor D. V. Reddy is gratefully acknowledged.

Special thanks are due to Dean Dempster, Faculty of Engineering and Applied Science, Dean Aldrich, School of Graduate Studies, and Professor El Hawary, Chairman, Graduate Studies, Faculty of Engineering and Applied Science, for their constant advice and encouragement.

TABLE OF CONTENTS

LIST OF TABLES

Table | Page

LIST OF FIGURES

Figure | Page

NOTATION

σ_{ij} = Total stress tensor

ϵ_{ij} = Total strain tensor

κ = Bulk modulus

e = Volumetric strain

G = Shear modulus at any strain, ν

J''_2 = Second invariant of the stress deviation

τ_{xy} = Shear stress in x-y plane

ν_{xy} = Shear strain in x-y plane

$(\sigma_1-\sigma_3)_f$ = Compressive strength or stress difference at failure

$(\sigma_1-\sigma_3)_{ult}$ = Asymptotic values of stress difference

E_i = Initial tangent modulus

E_t = Tangent modulus

$\bar{\sigma}_o$ = Average effective confining pressure

τ_o = Octahedral shearing stress

G_o or G_{max} = Maximum shear modulus

τ_{max} = Maximum shear stress

σ'_m = Mean principal effective stress

K_o = Coefficient of lateral stress at rest

ν_r = Reference shear strain

ν_h = Hyperbolic shear strain

S_u = Undrained shear strength of soil

p = Lateral soil resistance on pile per unit length

y = Pile deflection

P_u = Ultimate soil resistance on pile per unit length

N_p = Dimensionless coefficient

C = Cohesion of clay in psi

ρ = Weight density of clay in pci

ρ_m = Mass density of soil

b = Pile diameter or width

ε_{50} = Strain corresponding to one-half of the ultimate deviator stress

P = Ice force

B = Width of the resisting structure

h = Thickness of ice-sheet

σ_o = Uniaxial compressive strength of ice

m = Shape coefficient

K_v = Lateral foundation stiffness

μ = Poisson's ratio

r_o = Radius of the footing

K_θ = Rotational stiffness

A = Pile cross-sectional area

K_{ip} = Axial stiffness of the pile

ω_{max} = Maximum frequency

Δt = Interval of digitization

λ_s = Wave length of the shortest shear wave

h_{max} = Vertical element size

M_{is} = Virtual mass of soil

ϕ_u, ϕ_v and ϕ_w = Soil pile interaction displacement field within the soil medium in x, y and z direction

E = Young's modulus

ϕ_y = Shear deformation of beam element

K_m = Element stiffness matrix

$\underline{K}_b$ = Assembled stiffness matrix for the structure

$\underline{K}_s$ = Assembled stiffness matrix for the soil medium

$[M^*]$ = Global mass matrix

$[C^*]$ = Global damping matrix

$[K^*]$ = Global stiffness matrix

$\{u\}$, $\{\dot{u}\}$ and $\{\ddot{u}\}$ = Displacement, velocity and acceleration vector

$\{P(t)\}$ = Time-dependent load vector

ω = Free vibration frequency

$[\phi]$ = Mode shape matrix

{X} = Generalised displacement

ΔT = Time step for integration

ABBREVIATIONS:

psi = pounds force per square inch

pci = pounds weight per cubic inch

CHAPTER I

INTRODUCTION

1.1 General Remarks

Different types of models are presented to determine the response to random ice loading of permanent offshore structures embedded in the ocean floor. In addition to the case of a rigid foundation model, two other models with yielding soil foundations are presented. The structures considered are plane frames.

1.2 Statement of the Problem

The purpose of this investigation is to determine the elastic response of a pile-supported offshore structure to dynamic ice forces considering linear and nonlinear soil behaviour (Fig. 1).

The time dependent variations of the displacements, axial forces and stresses of the soil-structure system are obtained at typical locations.

1.3 Layout

Chapter II reviews the literature on ice-structure-water-soil interaction under the following categories: measurement of forces and crushing strengths of ice, dynamic analysis of fixed offshore structures subjected to ice forces, static and dynamic analyses of the soil-pile medium with methods other than the finite element method, and the application of the finite element method to the solutions of problems related to the foundation-structure interaction including seismic excitation.

Chapter III presents the study of nonlinear stress-strain behaviour of soils under dynamic loading, constitutive equations, hysteretic stress-strain behaviour of soils under cyclic loading, dynamic lateral loading on piles and presentation by 'p - y' curves, and shear moduli for saturated clays. Different modelling criteria used in this analysis, and factors governing a true finite element representation of the soil-structure system are described. Evaluation of the added mass of soil and water on the response is also discussed.

Chapter IV presents the theory of the finite element formulation. It also describes the formulation and solution of the dynamic equilibrium equations for the entire soil-structure system with the application of the equivalent linear method to model the nonlinear soil-structure interaction.

Chapter V illustrates a numerical example for different kinds of models with finite element idealization.

Chapter VI compares the results obtained for different kinds of models and lists the conclusions. Several recommendations for further research are made at the end of the chapter.

CHAPTER II

LITERATURE REVIEW

2.1 Introduction

The topics reviewed are measurements of ice forces on structures, dynamic analysis of fixed offshore structures subjected to ice forces, static and dynamic analysis of soil-pile medium by procedures other than the finite element method, and the application of the finite element method to the solution of the foundation-structure interaction problem.

2.2 Analysis

2.2.1 Measurement of Forces and Crushing Strength of Ice

Zubov (166), Proskuryakov (112), Korzhavin (72), Drouin (33), and Drouin and Michel (34) carried out analytical, experimental and field studies on the determination of static ice pressures on structures, primarily due to the temperature fluctuations within the ice sheets. Korzhavin's comprehensive studies from 1933 - 1962 on the determination of ice pressures have been summarized by Michel (93). Peyton (104, 105, 106) made many useful recommendations for design based on his measurements of ice properties, and laboratory and field investigations of ice-structure interaction at Cook Inlet, Alaska. Blenkarn and Knapp (12) described the anticipated ice conditions and maximum ice forces in the Grand Banks off the Coast of Newfoundland. Nevel (96), Lavrov (79), Michel (93), Edwards et al. (37, 38), and Schwarz et al. (131) used dimensional analyses based on model and full-scale data to simulate the ice-structure interaction problem. Neill (94, 95) described measurements of ice forces

on several bridge piers in Alberta including the synchronization of force recording and movie photography at one site to study force fluctuations with the nature of the ice failure. Failure properties and strength deformation characteristics of ice and ice covers were studied by Weeks and Assur (152), Gold (47) and Lavrov (80). Danys (27, 28) investigated 22 offshore light piers in the St. Lawrence River waterway, seven of which had been damaged or destroyed by ice. The effect of ice pressures on offshore lighthouses in the Baltic Sea, with some reference to two structural failures, has been described by Reinius, Haggard and Ernstons (119).

Ice pressures based on the above two failures were estimated by Bergdahl (9). Kopaigorodski et al. (71) made model studies on ice sheets to determine the mean ice pressure and variation of the values around the mean. It was concluded that sheets with small h/d (i.e. thickness to indentor width) ratios fail by instability while shear failure occurs for sheets with large h/d ratios: Hirayama et al. (55, 56) and Schwarz et al, (132, 133) suggested an empirical formula for the ice pressure of ice which takes into consideration the indentor shape and diameter, ice thickness and the relative velocity between ice and the structure.

Kivisild (68) described the structural design of a year-round oil terminal in ice-covered waters of the St. Lawrence River. Afanas'er (1) developed an emperical equation for loading on vertical surfaces based on experimental and theoretical studies. Frederking and Gold (45) described a mathematical model for calculating ice forces against an isolated pile that takes into account the influence of the ice type,

strain rate, pilo geometry, and temperature. The Russian code of practice (149) presents formulae for the determination of static and dynamic ice loads on river structures. American Petroleum Institute (API) recommendations (3) indicate ice crushing strengths of 200-500 psi to determine ice forces. Croasdale (26) described a nutcracker ice strength tester in the Beaufort Sea which give ice-crushing strength values of (580.15 to 870.25 psi). Kennedy (64), Lazier and Maclachlan (81), and Lazier and Metge (82) investigated the deformations and movements in ice sheets due to temperature variation.

2.2.2 Dynamic Ice Forces on Structures

Blumberg and Strader (14) first analyzed an offshore monopod at Cook Inlet, Alaska, subjected to tidal current-driven ice loads for dynamic response. They replaced the moving ice loads by an equivalent static load at highest tide level and calculated the frequencies for the lumped mass model. It was suggested that i) soil-structure interaction may be quite important if the applied loads are very high, and ii) interaction effects will decrease the resonant period and may cause a shear failure in the supporting soils. Assuming the primary structural response to ice floe excitation to be in its fundamental mode of vibration, Matlock, Dawkins and Panak (90) analyzed a cantilever pier, idealized as a damped single-degree-of-freedom system and subjected to a postulated saw-tooth-type deterministic loading. The calculated response showed good agreement with earlier field measurements of Peyton (106). Sundararajan and Reddy (141) used the Matlock et al. model to study the stochastic response of a single-degree-of-freedom (SDOF) model

by spectral technique. The force records used were those of Blenkarn (13) at Cook Inlet, Alaska, from actual field data. It was observed that the system responded to excitation for $\omega \leq \omega_o$ (fundamental frequency of the structure) but filtered out the excitations for $\omega \geq \omega_o$. Peyton (106) concluded from field measurements of responses of a pile subjected to the action of uniformly-thick ice sheets that the force oscillations are predominant in the range of 1 Hz. Kivisild (67) estimated the natural frequencies of fluid-supported ice sheets, deforming laterally in dish-form, to be less than 1 Hz. Reeh (117, 118) derived relationships to determine the natural frequency and mode shapes of ice sheets vibrating in water and found that the frequency of rigid-body motion to be 1 Hz.

2.2.3 Dynamic Analysis of Fixed Offshore Structures to Ice Forces

Reddy and Cheema (114) used the power spectral density method for the determination of responses of an offshore structure modelled as multi-degree-of-freedom (MDOF) lumped mass system. The ice force records were those of Blenkarn (12) determined from two instrumented structural devices - a strain-gauged test pile driven into the ocean bottom adjacent to an existing temporary offshore drilling platform, and a field test beam hinged at both ends to the platform leg with a load cell measuring the reaction at the upper hinge. Observing the similarity between the flunctuating parts of ice force records and earthquake records, Reddy et al. (115) used the well-known response spectrum technique for analysing a three-dimensional offshore platform (modelled as a two-dimensional plane frame). They calculated the probable maximum dynamic response to impact loads of moving ice sheets. The added water mass was

taken into account by assuming it to be equal to the mass of water displaced as suggested by King (66). The ice-force records were digitised using the Nyquist criterion, and the stationarity of the chosen ice-force records was verified by using the Kolmogorov-Smirnov test. The work included an extensive literature review on ice-structure interaction. Reddy et al. (116) used the power spectral density method for the response analysis of a framed tower taking into account the three-dimensionality. Swamidas and Reddy (142) analysed an offshore monopod tower considering ice-structure interaction by the finite element method. Instead of assuming the added water mass to be equal to the displaced water mass, the frequency dependence of the added water mass was taken into account based on the substructure concept of EATSW, a programme for Earthquake Response of Axisymetric Tower Structures Surrounded by Water (83). The hydrodynamic interaction terms in the modal equations of motions of the structure are determined as solutions of the boundary value problems for the fluid domain. Ice-force records were generated artificially following a method suggested by Swamidas et al. (143) based on the similarity between the fluctuating parts of randomly varying ice-force records and seismic records. The work includes the study of the influence of soil properties on the frequencies and responses.

2.3 Soil-Pile Medium

2.3.1 Static Analysis

The true interaction problem between the structure and the soil system is still not well understood. Terzaghi (146) described an

approximate soil-structure interaction analysis which gives reasonable answers in most cases. Howe (57) suggested two procedures for modelling the soil restraints on the structure penetrating into the ocean floor: i) assumption of an equivalent point of fixity at some distance below the mudline with no soil restraints, and ii) assumption of the pile as a beam on elastic foundation simulated by a set of closely-spaced springs. The equivalent point of fixity was defined as that point of rigid fixity for a vertical cantilever without the surrounding medium which has the same bending moment as the actual pile with lateral soil restraints. Many research investigators used this concept of equivalent point of fixity, e.g. Anderson, Bartholomew and Wong (4), and Billington, Gaither and Ebner (11). The second method described by Ref. 57, which uses the concept of an elastic continuum by a set of closely-spaced springs, seems much more rational than the equivalent point of fixity. The continuum concept has been used widely to date in the analysis of offshore structures, particularly in the analysis of a laterally-loaded single pile to a known shear and moment at the mudline.

Using the Winkler foundation model, Reese and Matlock (120) presented a non-dimensional solution for laterally-loaded piles. They assumed the soil to behave as a series of separate elastic elements with the soil modulus varying linearly with the depth. Later, Matlock and Reese (85) incorporated the nonlinear behaviour of soil in the analysis of a laterally-loaded pile for static loading. The soil characteristics are presented by a set of 'p-y' (force-deformation) curves shown in Fig. 2(a) for different depths. The differential equation for

the beam on the elastic foundation model is solved by an iterative procedure using successive elastic approximations adjusting the soil modulus "E_s" (p/y) constants at each trial. Wilson (161) indicated three possible variations of the spring constants or the modulus of subgrade reaction, K_c: i) constant with depth, ii) linear with depth, and iii) less strength than that indicated by the second case down to the first point of zero deflection of a pile, X_T, as shown in Fig. 2(b). Case (i) is representative of normally consolidated clays, whereas the second and third cases are probably more suitable for sands, gravels and normally loaded silts. Feibusch and Keith (39) used the iterative technique of Ref. 85 to analyse an offshore structure supported by a pile foundation considering a nonlinear soil 'p-y' curve. A computer programme was developed which takes into consideration the elastic structural member and an inelastic soil 'p-y' curve for different depths. The results are printed at the end of the final iteration when convergence has been achieved for the computed and assumed soil moduli. It is pointed out that the inelastic soil behaviour will influence the deflection considerably compared to that for the case of assumed fixity. Therefore, neglecting the coupling effects in soil-structure-pile interaction can result in unconservative design values.

Spillers and Stoll (139) considered the soil medium interacting with a laterally-loaded pile and analysed two idealized models for static loading: i) an elastic pile in elastic half-space, and ii) an elastic pile in elasto-plastic half-space. The Mindlin Equation was used for determining the soil properties relating deformation at certain specific points to the resulting soil surfaces. Francis (44) analysed a

two-dimensional pile group for static loading by the influence coefficient method. The soil resistance was considered uniform or increasing proportionally with depth. Aschenbrenner (5) presented a three-dimensional study based on the influence coefficient method. Kubo (74) carried out an experimental study to determine the behaviour of laterally-loaded piles in both sandy and clayey soils. A new relationship between the soil reaction and pile deflection was proposed, and conversion factors were established to predict the behaviour of the prototype pile on the basis of the results or model tests. It was found that the soil reaction coefficient 'K' decreases for pile widths greater than 20 cm. Many field test values were processed to establish a unique relationship between the soil reaction coefficient 'K' and the standard penetration value 'N' for clayey and sandy soils. Saul (130) presented a general formulation of the matrix method for a three-dimensional foundation with rigidly connected piles. He indicated that the method could be extended to dynamically-loaded foundations. Robertson (128) and Parker and Cox (100) used the method formulated by Reese and Matlock (122, 123) for pile analysis subjected to lateral and axial loading. Reese and O'Neill (124) presented the theory for a general three-dimensional grouped pile foundation using matrix formulation. Basically, the method was an extension of the theory of Hrennikoff (58) in which the piles were presented as an assemblage of springs. Awoshika and Reese (6) presented the analysis of a foundation with widely-spaced battered piles for static loading considering soil nonlinearity through p-y curve. Piles subjected to lateral and axial loads were studied experimentally and analytically. Reese, O'Neill and Smith (125) presented

the generalized analysis of pile-supported structures by matrix formulation.

Model studies of laterally-loaded piles were carried out by Davisson and Salley (29) to develop criteria for the design of pile foundations. Matlock (89) carried out field tests on instrumented piles as well as laboratory model tests to establish the correlations between the two. Three types of loading conditions often used for the design of laterally-loaded piles in soft, normally consolidated marine clay were considered, namely, i) short-term static loading, ii) cyclic loading, and iii) subsequent reloading with forces less than the previous maxima. Since the design recommendations of Ref. 89 were based on a considerable amount of experience and experimental data, they seem to be the most reliable of the established procedures available for developing 'p-y' relationships for piles in soft clay.

Field tests on large diameter bored piles under axial and lateral loads were reported by Botea, Manoliu and Abramesey (15). Diaj (31) present a computer analysis for the determination of pile forces, displacements and soil reactions of a group of piles in soil with general elastic properties. He assumed elastic behaviour of piles and represented the pile as a linear elastic beam supported elastically by the soil. Interaction between different piles in the groups was neglected. Shrivastava (134) analysed a pile group subjected to vertical and lateral loads by developing a stiffness matrix relation between external forces and displacement vectors. The pile constants were determined from the Mindlin Equation for forces acting inside the elastic half-space. It was concluded that good results can be obtained from the elastic theory if

the soil properties are properly assessed and the magnitude of the loading is about one-third to one-half of the ultimate loading. Poulos (107, 108, 109) assumed that the soil surrounding the piles acts as an elastic half-space according to the elasticity theory. Procedures were presented to predict the lateral behaviour of isolated single piles, pile groups and socketed piles. Though the method indicates the possibility of analysis of any pile size and pile group, it is restricted by the assumptions of constant and uniform Young's moduli for the soils and piles, and constant section moduli for the piles. Other limitations are applicable to only fixed or free-headed piles and computation of only pile head response. Brod et al. (16) outlined a method for analysing an offshore structure on pile foundations considering nonlinear soil behaviour. The technique used for the solution was a 'reduced stiffness' method in which the structure and the pile foundation are first treated separately and then deflections and forces at the structure-pile head interface are matched by iteration to satisfy the final equilibrium condition. Focht and Koch (42) presented an approximate procedure for predicting the behaviour of laterally-loaded offshore pile groups. Subgrade (p/y) analysis was combined with the elastic half-space procedures incorporating the relevant modifications.

2.3.2 Dynamic Analysis

2.3.2.1 Methods other than Finite Element Method

One of the earliest studies in the dynamics of laterally-loaded piles was that of Gaul (46). He carried out extensive model tests of a pile subjected to lateral harmonic forcing function in an effort to

simulate a pile subjected to ocean waves. Testing of a vertical pile on a weak marine foundation indicated that for "relatively" low frequency of load oscillation no dynamic load factor is required. It was also pointed out that determination of the variable load factor by model studies would require testing with a wide range of frequencies, different types of piles and foundations. Instead of assuming a viscous soil medium, it was assumed that plastic flow will occur in soil during vibration making the damping negligible. The dynamic modulus differed from the static modulus by only 1%. From the analysis of the test data it was concluded that:

1. The pile vibrates in the form of a standing wave which is in phase with the oscillating load,

2. Soil damping is negligible,

3. At relatively low frequencies of oscillation, the maximum bending moment and the section where it occurs are not materially different from those obtained for a static case, and

4. Soil modulus is constant for montmorillonite clay, more commonly known as bentonite, under dynamic loading.

In this investigation, the rate of loading was kept constant at 1 Hz and the material considered was a special type of clay exhibiting unusual properties. Hence, the conclusions stated above cannot be accepted to be generally valid even for clays. Tucker (148) extended the Matlock model (86, 87) for dynamic analysis of laterally-loaded piles to the unsteady conditions of impulse and harmonic loadings. He extended Matlock's technique for solving a beam-column on foundation under static loading to the problem of dynamically-loaded pile. The

basic differential equation of motion for dynamic equilibrium was transformed to a set of finite difference equations. Viscous damping was included in the model and the results showed good agreement with those of Gaul. Ref. 148 observed that the true relationship between pile deflection and soil resistance is seldom linear due to nonlinearity of the stress-strain curve for soil. It was recommended that nonlinear springs be introduced to represent the soil force-deformation characteristics accurately and the iterative technique, as suggested by Ref. 122, be used for solution.

Hayashi and Miyajima (51) conducted tests on vertical steel H-piles embedded in sands and subjected to lateral static and dynamic loads. Their findings were: i) The natural frequency and resonant curves for single vertical piles can be calculated from idealised simple vibration systems, and ii) damping coefficients measured in the free vibration tests depend on the relative densities of the subgrade and the lengths of the free parts of piles. Lateral load and vibration test data on prototype pile groups consisting of vertical and battered piles were reported by Matsumoto and Tsuchiya (91). Penzien, Scheffey and Parmelee (102) analysed bridges on long piles subjected to seismic excitation in which the soil system was represented by a Kelvin-Voigt model. The inertia of the soil system was taken into consideration by means of a lumped mass model for evaluating the soil reaction to seismic excitation. The results from extensive soil tests on San Francisco Bay mud were used to determine the nonlinear hysteretic stress-strain relations, damping and creep characteristics of clay. The model developed initially was a coupled system which led to an extremely

complicated method of analysis requiring considerable computational effort. After a number of attempts it was decided to simplify the problem by using an uncoupled spring system often called the "Winkler" model. Another assumption made was to evaluate the uncoupled spring properties from the static stress and displacement fields within the clay medium, i.e. the Mindlin theory. The assumption was justified by the argument that the characteristic wave length in the clay medium, a shear wave length, was long compared to the horizontal distance across the zone of major influence resulting from interaction. The soil spring used was of the bilinear type and a step-by-step matrix analysis solution of Wilson and Clough (156) was used to solve the set of simultaneous differential equations for the soil and the pile displacements. This approach was also used for the analysis of an offshore platform which will be discussed later in this section.

Hayashi, Miyajima and Yamashita (52) proposed a new method for estimating the behaviour of piles under static and dynamic loading. They carried out many field tests on full-scale prototype piles and investigated the characteristics of horizontal subgrade reaction for different types of soil. Several "standard curves" were presented for different types of soil classified as "C-Type" and "S-Type" to predict the deflection of a pile above the soil surface, maximum bending moment and the necessary length of pile embedment for design purposes. The study also considered the response of a pile to lateral dynamic loading of the alternating type. The reports indicate the non-availability of adequate literature on piles subjected to random loading. Prakash and Aggarwal (110) reported the study of a vertical pile under lateral

dynamic loading, and compared the deflection with that for a static case. In another study involving earthquake excitation, Kubo (73) studied the response of a system having two degrees of freedom - one representing the superstructure and the other the subsoil. He suggested that, for structures modelled in the most simplified way, at least two degrees of freedom must be considered for dynamic analysis. The restoring force of the superstructure is the elastic property of the frame, and the spring force applied to the substructure is the horizontal resistance of the subsoil. The study includes the relationship between the structural response and the ground motions, damping constants, etc. Flemming et al. (41) described an analytical study which included soil-structure interaction. The superstructure was idealised by a conventional lumped mass model and the soil medium was represented by a flexible member attached to the above lumped mass model, having the same force-deformation relationship as the foundation. The soil properties were assumed to be linearly elastic and the soil damping was neglected in formulating the mathematical model. The results from parametric studies made on the variation of foundation stiffnesses indicated that, in earthquake analysis, completely erroneous results may occur due to neglect of foundation-superstructure interaction effects.

Forehand and Reese (43) studied the vertical motion of a pile during driving with the help of the wave equation. It was assumed that "... the resistance to driving is composed of the static resistance plus incremental resistance that develops under dynamic loading, and is expressed as a percentage of the static value ...". The load deformation characteristics of the soil are described as

$$R_D = R_S(1 + C_v\dot{u}) \qquad (2.1)$$

where R_D is the dynamic resistance, R_S is the static resistance, C_v is the viscous damping and $\dot{u}$ is the rate of displacement. Wu (1963) observed that soil resistance in the pile driving analysis is composed of two parts - the linear viscous damping on the outside surface and the restoring force at the pile end. Barkan (7) indicated that, in clays, the pile natural frequency remains nearly constant while being driven and increases after a week. It was concluded from this observation that resistance during driving is due to end bearing, and resistance after driving is due to the shear on the outside surface. Chan and Hirach (22) presented a detailed report of available publications up to 1977 on soil dynamics and soil rheology. Parmelee (101) investigated the building-foundation interaction phenomenon by utilizing the solutions for the steady state vibration of a rigid plate on an elastic half-space. He used Bycroft's (19) results for this study with the main assumption that the ground or foundation medium is a semi-infinite, isotropic, linearly elastic body. Edge (36) made a detailed analytical study of an off-shore structure with pile foundations, subjected to wave loading. Both deterministic and stochastic models were considered in the analysis assuming a Winkler-type foundation. The soil was replaced by three types of springs at each level of pile below mudline: i) Lateral springs for bending, ii) Vertical springs for shear, and iii) Torsional springs for twist. The Young's modulus for soil was assumed to be varying with depth and the analysis was carried out for a linear elastic system. Kubo (75) carried out a model test for vibrations of

a pile-supported structure. A large-size shaking table was used since a small-size one will hardly satisfy the similarity law between the model and prototype. From tests with a very large shaking table at the Chiba Experiment Station, University of Tokyo, in 1967, the following results were obtained by Ref. 75: i) maximum bending stress occurs at a period of about 1.3 sec in the prototype, and ii) as the frequency of the shaking table increases, ground movement becomes larger and the surrounding soil pushes the pile horizontally. Ross (129) developed an analytical model for the response analysis of an offshore pile subjected to wave loading. The pile analysed was a single one embedded in the ocean floor and the superstructure was replaced by a lumped mass connected to the pile top by two springs, lateral and rotational. Both soil nonlinearity and pile geometric nonlinearity were considered. Interaction between the pile and the soil was simulated by a modified Kelvin-Voigt-type model placed at nodes below the mud line. Nonlinear soil properties were simulated by placing a dashpot placed in parallel with a spring friction block system. Damping was represented at each node by a dashpot. The equation of motion was solved by the Runge-Kutta Method, and the results compared with laboratory test values on a model pile.

Agarwal (2) formulated a method for analysing the dynamic response for a pile using the discrete-element method as suggested by Matlock et al. (88) for a linearly-elastic beam-column. The physical model consisted of rigid bars, connected end to end with pin joints and elastic springs to input the required flexural stiffness. The soil medium was represented by infinitely closely-spaced springs, i.e. the Winkler foundation, mass and dashpot damping. Although only linear

analysis was carried out, the method gives an option to use a nonlinear soil spring by an equivalent combination of a force and a linear spring. The damping behaviour of soil medium was treated similarly by a dashpot. Comparison of the analytical results with test values for two different kinds of loading, i) harmonic and ii) transient, indicated fairly good agreement. Prakash and Chandrasekharan (111) studied the dynamic response of a pile under lateral loading analytically and experimentally. Based on a full-scale field test on several piles both bearing and frictional types, an easier method of analysis was suggested for predicting pile response to lateral dynamic load. Szilard (144) reported the dynamic response of multilevel guyed towers subjected to earthquake excitations considering the nonlinearity of the elastic supports. It was suggested that the soil nonlinearity of the stress-strain relationship can be handled in a manner similar to that for the prestressed cable supports. The Navier solution was used to solve the differential equation of motion for the forced part of the vibration. The nonlinearity of the cable supports was approximated by a piece-wise linearization technique. Tajimi (145) studied a structure embedded in an elastic stratum by the application of the three-dimensional wave propagation theory. Penzien (103) presented an analytical model for evaluating the response of an offshore tower to seismic excitation considering soil-pile-water-structure interaction. Three kinds of models were used to simulate the true interaction effect of soil around the structure; two of these were presented earlier in a paper on the analysis of a bridge structure supported on piles (Ref. 102). Deterministic and stochastic responses were presented for an elastic

half-space model and the results interpreted in terms of present design code requirements. It was suggested that, for deep pile foundations, the soil medium could be idealized by an elastic half-space because the lateral forces applied to the upper ends of the piles by the tower would be rapidly transferred to the surrounding soil with increasing depth, unless the foundation conditions are extremely soft. Bielak and Jennings (10) studied the dynamics of building-soil interaction by modelling the soil as a linear elastic half-space and the building structure as an n-degree-of-freedom oscillator. Both earthquake response and steady-state response were studied, and examples were given for one-storey, two-storey and ten-storey interaction systems. Results indicate that interaction effects may be important and must be included in the design and analysis of certain structures. Hasselman (50) studied the probabilistic response of an interactive soil-structure system to seismic excitation. The analysis was based on the linearised sub-system approach, the platform structure and pile foundation forming one sub-system, and the soil the other sub-system. The nonlinearity of the soil treated in terms of the secant shear modulus, following the suggestion of Hardin and Drnevich (48, 49), is represented by soil density and the hysteretic soil shear stress-strain curves which vary with strain and depth. The spring constants used were based on the lateral and vertical forces of soil corresponding to the strains developed at the different levels, and the response of the entire soil-structure system was calculated in an iterative manner. The results indicate that dynamic tuning between a soft soil and a platform structure can give a high level of response

and, for a very high input level, the soil column frequency may exceed the structure period causing a significant dynamic attenuation.

Hays (54) carried out a study of the nonlinear dynamic response of a framed structure with pile foundations to seismic excitation. The nonlinearity considered was of a geometric type due to large axial loads often called the 'PΔ' effect (where P is the axial load and Δ is the displacement between the structural joints). The method was based on the nonlinear discrete element method suggested by Hays and Matlock (53). A computer programme, CLOSE 11, was developed and the results checked well with those of Workman (162). Ref. 54 claimed that the same programme could handle soil nonlinearity (material) without further modification. Utt, Durning, Duthweiler, and Engle (150) analysed the recorded dynamic response of a monopod platform in Cook Inlet. The response was simulated with computer models to study the reason for observed changes in the fundamental frequency. It was observed that the platform frequency changed from 0.91 Hz in 1967 to 0.77 Hz in 1972 owing to changes in the soil conditions of the foundation. It was concluded that the platform's dynamic characteristics are insensitive to deck mass changes. The addition of a weight over 500,000 lbs. (6% of the deck mass) at one corner of the deck changed the fundamental period by only 1%, but the natural frequency was very sensitive to soil stiffness. Vandiver (151) presented a technique to detect the subsurface structural failure of a three-dimensional offshore structure (frame-type) by detecting changes in the natural frequency of the structure. It was indicated that a detected shift in natural frequency in successive measurements would

indicate a change in the mass or stiffness of the structure. The soil was replaced by vertical and lateral springs along the pile length and a statistical energy analysis made for predicting the seismic response and random wave response for fixed and floating offshore structures. Stockard (140) studied the model suggested by Ref. 129 for simulating the dynamic response of an offshore structure excited by an earthquake. The nonlinear soil properties were simulated by a Kelvin-Voigt-type model placed at the pile nodes below the mudline. The seismic excitation applied to the pile base was that of the 1040 El Centro earthquake. It was pointed out that pile-soil-water interaction has very significant effects on the dynamic response of an offshore platform subjected to earthquake excitation.

2.3.2.2 Finite Element Method (FEM)

Wilson (157) presented a method for analysing the foundation structure interaction by idealizing the structure and foundation by finite element modelling. Linear strain quadrilateral elements were used to represent a dam and its foundation, and seismic excitation was input at a remote distance from the structure. The analysis was purely elastic, and Rayleigh damping (damping matrix proportional to the mass and stiffness matrices) was considered. The coupled equations of motion were solved by a stable step-by-step integration procedure as suggested by Ref. 156. It was pointed out that the advantages of this method over mode superposition were: i) elimination of the large eigenvalue problem, ii) a faster step-by-step procedure, and iii) easy extension to include the effect of nonlinear material properties by modifying the stiffness

matrix in each time interval of increment during the step-by-step solution procedure. Khanna (65) used the finite element technique to evaluate the elastic soil-structure interaction of a building frame to seismic excitation. The frame was finite-elemented by a number of one-dimensional beam elements and plane strain elements were used for soil. Different types of foundation conditions were considered by varying the soil modulus and the depth. The results indicated that the fundamental frequency is hardly influenced by variations of the foundation condition. A deep pile foundation in soft soil gave a second mode value of one-third that for a rigid base which meant that the soil influenced only the higher modes. The effect of variation in the soil modulus and extent of participating soil on the vibration modes higher than the second was considerable, and the maximum base shear in the column (for E_s = 10 Ksi) is about 170% greater than that for the rigid case (for El Centro input). He concluded that, as the elastic modulus and the extent of soil can greatly influence the response, wrong results would be obtained by neglecting soil-structure interaction.

Kuhlemeyer (77) presented a finite element solution for the solution of statically- and dynamically-loaded piles using beam bending elements of circular cross section. The solution included up to two layers of soil, and flexibility coefficients were plotted in logarithmic scale against Young's modulus ratios (pile modulus/soil modulus). The analysis assumed that the soil and piles behave linearly elastically and the results were compared with those of Refs. 107, 108, 109 and Novak (99). Finn and Khanna (40) used the finite element method for evaluating seismic response of an earth-dam.

Yegian and Wright (163) first presented a finite element method for predicting the lateral soil resistance-displacement relationships (p-y curves) for single or grouped pile foundations under short-term static loading. They concluded that soil-pile interface properties may have a significant influence on the lateral soil resistance-displacement relationship. The finite element solution results were compared with results from conventional procedures for developing the p-y curves and predicting the lateral soil resistance as described by Ref. 89. The results showed reasonable agreement. The interesting parameter studied was the zone of pile influence (radius 'r'). At a sufficient distance 'r' away from the pile, the magnitude of soil displacements resulting from lateral movement will be relatively small and may be neglected for practical purposes. The fixed boundary was varied to establish a relationship between the zone of pile influence of radius 'r' and the pile diameter 'D'. It was found that the radius would have to be approximately eight times the pile diameter. In this analysis, the pile and the soil were represented by two-dimensional quadrilateral elements of the form described by Doherty, Wilson and Taylor (32) referred to as "QM5" elements. The soil-pile interface was represented by a special type of element called the "slip" element.

Idriss et al. (59) developed a computer programme, QUAD-4, for evaluating the seismic response of soil structures by variable damping finite elements. The soil behaviour was represented by a nonlinear shear stress-strain curve for cyclic loading (hysteretic-type) and the response evaluated by an iterative method after all the elements achieved strain compatibility. Chan and Matlock (21) presented a

"discrete element" method for analysing a beam column resting on a linear or nonlinear elastic or nonlinear-inelastic supports subjected to either static fixed loads or dynamic loads. The applications included studies of the dynamic response of offshore piles to wave-induced forces and earthquake-induced forces, and prediction of the hysteretic effect of inelastic support.

Kuribayashi and Lida (78) applied the finite element method to an actual bridge pier subjected to vibratory horizontal forces considering soil-foundation interaction. The estimation of the elastic moduli of soils was made from the Voigt solution and the values compared with those obtained from field tests. The damping ratio was set equal to 10% for each mode. Lysmer et al. (84) developed a computer programme, LUSH, for complex response analysis of soil-structure system by the finite element method. The programme takes into account the strong nonlinear effects which occur in soil masses subjected to seismic excitation. This is achieved by a combination of an equivalent linear method described by Seed and Idriss (135) and the method of complex response with complex moduli.

Carnahan, Zimmer and Carnahan (20) presented some aspects of anchor-pile design for marine environments using the finite element method. The pile, the soil and the pile/soil interface were modelled and the stresses and forces obtained using the programme, ANSYS. The analysis was completely elastic and a 'gap' element was used to represent the pile-soil interface.

Seed et al. (136) reported an extensive comparison of half-space and finite element analyses for soil-structure interaction under

seismic loading. The paper describes the limitations of both methods and indicates that, in finite element analysis, the approximation of a true three-dimensional problem to a two-dimensional plane strain problem will cause an error of approximately 20% to 30%, but the method is still advantageous because of its capability to include variable moduli and damping characteristics.

Desai (30) investigated the static load-deformation behaviour of axially-loaded pile foundation in sandy soils by the finite element method. The values of the bearing capacities obtained from finite element analysis were compared with those determined from field tests and limit equilibrium analysis. Quadrilateral isoparametric elements (axisymmetric) were used to model the pile and the surrounding soil media, and the deformation behaviour of sands was approximated by using hyperbolic stress-strain curve.

Isenberg (61) pointed out that, if the side boundaries are sufficiently far from the structure, the response at the boundary is almost the same as that for a free field analysis.

CHAPTER III

SOIL PROPERTIES

3.1 Introduction

This chapter discusses the nonlinear stress-strain behaviour for soils under dynamic loading and the different modelling techniques used for analysis of soil-structure interactions. Soil deformations due to dynamic loading, earthquake, wave, ice or severe machine-developed forces can vary from small to very large amplitudes, nearly elastic to plastic values. Particular attention is given to the effects of strain amplitudes, cyclic loading and the reduction in shear modulus due to cyclic loading. The variation of damping with strain amplitude is also discussed.

Two types of foundation conditions are discussed: i) Rigid Base and ii) Semi-Rigid Base. The Semi-Rigid Base is idealized in two ways: i) Lumped Parameter Foundation Model with Linear Soil Springs and ii) Finite Elemented Foundation Model with Linear and Nonlinear Soil Behaviour. The finite elemented foundation model also discusses several factors that need to be considered for better modelling such as the influence of the boundary, mesh size and the highest frequency to be included in the analysis.

3.2 Dynamic Stress-Strain Relations for Soils

3.2.1 Constitutive Equations

Jackson (62, 63) presented the general stress-strain relation for soils in the form of a constitutive equation as:

$$\sigma_{ij} = Ke\,\delta_{ij} = 2G\,(\varepsilon_{ij} - 1/3\,e\,\delta_{ij}) \qquad (3.1)$$

and the yield condition as:

$$\sqrt{J_2''} = f(\bar{\sigma}_o) \qquad (3.2)$$

where σ_{ij} = total stress tensor,

ε_{ij} = total strain tensor,

K = modulus of volume compressibility or bulk modulus,

$e = \varepsilon_x + \varepsilon_y + \varepsilon_z$ = volumetric strain,

G = Shear modulus,

δ_{ij} = Kronecker delta function ($\delta_{ij} = 1$ when $i = j$, $\delta_{ij} = 0$ when $i \neq j$),

J_2'' = second invariant of the stress deviation,

and $\bar{\sigma}_o$ = average effective normal stress or octahedral normal stress.

Eqn. (3.1) gives the stresses due to volume and shape changes. The discussion of J_2'' has been given by Newmark (98).

Soil deforming in one-dimensional compression may behave either in a strain-hardening or strain-softening manner depending on the stress level at which it is being tested. Fig. 3 gives the general behaviour but it has been found that, for stresses above 200 lb/in^2, soil exhibits a strain-hardening (Fig. 3, curve A) behaviour. Below this stress level the stress-strain curve may exhibit strain-hardening or strain-softening (Fig. 3, curve C) depending on the type of soil, degree of saturation

and degree of compaction. The primary goal of this investigation will be to study the influence of the nonlinear behaviour of soils on the response of an offshore structure. Particular attention will be given to the nonlinear shear stress-strain relationship of soils which is primarily of a strain-softening type. Therefore, the strain-hardening confined compression behaviour will not be considered.

For shearing stress-strain conditions, Eqn. 3.1 reduces to

$$\sigma_{ij} = 2 G \varepsilon_{ij} \qquad (3.3a)$$

or, in Cartesian coordinates,

$$\tau_{xy} = G \nu_{xy} \qquad (3.3b)$$

where τ_{xy} = shear stress

ν_{xy} = shear strain

and G = shear modulus.

3.3 Nonlinear Stress-Strain Behaviour

The stress-strain behaviour of any type of soil depends on a number of different factors including density, water content, structure, drainage conditions, strain conditions (i.e. plane strain, triaxial), duration of loading, stress history, confining pressure, and shear stress. The finite element method is a powerful tool for the incorporation of soil nonlinearity in analysis. Kondner and his co-workers (69, 70) approximated the nonlinear behaviour of soils for both clays and sands by a hyperbolic relationship. The equation for the hyperbolic stress-strain relationship in soil was proposed as:

$$(\sigma_1 - \sigma_3) = \frac{\varepsilon}{a + b\varepsilon} \qquad (3.4)$$

where σ_1, σ_3 = the major and minor principal stresses,

ε = axial strain,

and a and b = constants whose values may be determined by experiments.

The physical meaning of 'a' and 'b' may be seen from Figs. 4 and 5 where 'a' is the reciprocal of the initial tangent modulus, 'E_i', and 'b' is the reciprocal of the asymptotic value of the stress diference, ultimate deviator stress $(\sigma_1 - \sigma_3)$. Duncan and Chang (35) formulated the expression for tangent modulus for any stress condition as

$$E_t = \left[1 - \frac{R_f\,(1 - \sin\phi)(\sigma_1 - \sigma_3)}{2\,c\cos\phi + 2\,\sigma_3 \sin\phi}\right]^2 K\,p_a \left(\frac{\sigma_3}{p_a}\right)^n \qquad (3.5)$$

where $R_f = \frac{(\sigma_1 - \sigma_3)_f}{(\sigma_1 - \sigma_3)_{ult}}$, termed the failure ratio,

$(\sigma_1 - \sigma_3)_f$ = compressive strength or stress difference at failure,

$(\sigma_1 - \sigma_3)_{ult}$ = asymptotic values of stress difference,

p_a = atmospheric pressure expressed in the same pressure unit as E_i,

E_i = initial tangent modulus,

K = modulus number,

and n = exponent determining the variation of 'E_i' with 'σ_3'.

K and n are the pure numbers which can be determined readily from laboratory tests, and c and ϕ are the Mohr-Coulomb strength parameters.

3.4 Hysteretic Stress-Strain Behaviour for Soils

Soil stress-strain characteristics are nonlinear as mentioned before and, under constant cyclic loading, describe hysteresis loops such as those shown in Fig. 6. For loads producing high strains, the secant modulus decreases and the damping ratio (defined as a function of the area enclosed by the loop) increases as compared with loads producing smaller strains. It is readily apparent that each of these properties will depend on the magnitude of the strain for which the hysteresis loop is determined from Fig. 6. Thus, both shear moduli and damping factors must be determined as functions of the induced strains in a soil specimen.

3.4.1 Laboratory and Field Tests for Determining Shear Moduli and Damping Ratio

Several field and laboratory testing techniques have been developed to determine dynamic shear moduli and damping characteristics of soils which can be briefly classified as:

1) direct determination of stress-strain relationships,
2) forced vibration tests,
3) free vibration tests,
4) field measurements of wave velocities, and
5) analysis of ground response during earthquakes.

3.5 Effect of Test Variables on Shear Modulus and Damping

The shear modulus of soils is influenced by a number of quantities and has been described as a functional relationship by Richart (127) in the form:

$$G = f(\bar{\sigma}_o, e, H, S, \tau_o, C, A, f, t, \theta, T) \qquad (3.6)$$

where $\bar{\sigma}_o$ = average effective confining pressure,

e = void ratio,

H = ambient stress history and vibration history,

S = degree of saturation,

τ_o = octahedral shearing stress,

C = grain characteristics,

A = amplitude of strain,

f = frequency of vibration,

t = secondary effects that are functions of time and magnitude of stress increment,

θ = soil structure,

and T = temperature, including effects of freezing.

Refs. 48 and 49 made a comprehensive study of the factors that affect the shear moduli and damping of soil and suggested that the primary factors affecting moduli and damping factors as: i) strain amplitude, γ, ii) effective mean principal stress, σ'_m, iii) void ratio, e, iv) number of cycles of loading, N, and v) degree of saturation of cohesive soils, S. The less important factors were noted as: i) octahedral shear parameters, c and ϕ', and ii) time effects.

From the extensive series of reversed torsional tests on cohesive and cohesionless soils and the information already available in the literature, it was established that a modified hyperbolic curve will satisfactorily represent the shearing stress-shearing strain relation throughout the range of strain amplitudes up to failure. Fig. 7 shows

the factors which govern the basic hyperbolic shearing stress-shearing strain curve. At zero shearing strain, the tangent to the curve represents the maximum shear modulus, G_o. The secant modulus at any point along the curve - for example, point A - is designated as G, and the maximum shearing stress as τ_{max} (determined from a simple shear test). The horizontal line at the ordinate of τ_{max} is the second asymptote to the hyperbolic curve as described by Ref. 69. G_o and τ_{max} can be determined by field and/or laboratory tests. The general expression for evaluating G_{max} and τ_{max} is given by

$$G_{max} = 14760 \times \frac{(2.973 - e)^2}{1 + e} (OCR)^2 (\sigma'_m)^{\frac{1}{2}} \qquad (3.7)$$

where G_{max} = maximum shear moduli in psf at zero strain,

e = void ratio,

OCR = overconsolidation ratio,

a = parameter that depends on the plasticity index of soil,

σ'_m = mean principal effective stress in psf,

$$\tau'_{max} = \left\{\left[\frac{1 + K_o}{2} \sigma'_v \sin \phi' + C' \cos \phi'\right]^2 - \left[\frac{1 - Ko}{2} \sigma'_v\right]^2\right\}^{\frac{1}{2}} \qquad (3.8)$$

where K_o = coefficient of lateral stress at rest,

σ'_v = vertical effective stress,

and C',ϕ' = static strength parameters in terms of effective stress.

Refs. 48 and 49 found it convenient to normalize the strains by the use of the ratio ν/ν_r instead of constructing plots of G/G_o and damping as direct functions of the shearing strain, ν. The reference strain, ν_r,

is defined as the strain at the intersection of the initial tangent line, with slope, G_o, with the limiting shear stress, τ_{max}, as shown in Fig. 7. For thos representation, test data for shearing stress-strain fall into a narrow band for both cohesive and cohesionless soils.

Fig. 8 shows the shear-stress strain relationships for clay and sands. Fruther refinement made for representation of the test data resulted from a distortion of the strain scale to produce a "hyperbolic strain" described as:

$$\nu_h = \frac{\nu}{\nu_r}\left[1 + a \exp\left(-b \frac{\nu}{\nu_r}\right)\right] \qquad (3.9)$$

in which 'a' and 'b' are empirical quantities. For clean, dry sands, the values of 'a' and 'b' used to evaluate ν_h will be 0.5 and 0.16, respectively. Establishing the hyperbolic strain, a single curve was developed to illustrate the variation of the shear modulus ratio, G/G_o, and the damping ratio, D/D_{max}, with ν_h as shown in Fig. 9. The influence of the other parameters on the ν/ν_r-ν_h relationship was described in Ref. 49 by additional curves.

3.6 Bilinear Representation of Soil Stress-Strain Curve due to Cyclic Loading

Thiers and Seed (147) performed a series of simple shear experiments with cyclic loading on San Francisco Bay mud, a dark grey silty clay containing a little organic matter and some silt. The sample was taken from normally consolidated depths of 16 to 32 ft below the mudline, and the water content ranged from 85 to 96%. Modelling of the

stress-strain curves for cyclic loading was based on a bilinear relationship with shear moduli G_1 and G_2 and a yield strain of γ_r. These parameters were determined for variations of peak strain and a number of cycles. The conclusions are as follows:

1) If the stress-strain characteristics under cyclic loading conditions are represented by bilinear models defined by parameters, G_1, G_2 and γ_r, i) for a given cycle, the moduli, G_1 and G_2, decrease approximately 50% to 80% as the strain level increases from 0.5% to 2% shearing strain; for strains above 2%, the moduli are nearly constant, ii) the yield strain, γ_r, increases linearly with the strain level but remains essentially constant for a given strain up to 200 cycles, and iii) for a given value of peak strain, the moduli, G_1 and G_2, decrease about 30% in the first 50 cycles; above 50 cycles, G_1 and G_2 are nearly constant.

2) For samples subjected to cyclic strains of constant amplitude, there is a minimum shearing strain of the order of 1.5%, below which the static strength is virtually unaffected by 200 cycles of strain. Even a peak strain of 3% reduces the strength only by 10%.

3) The static modulus of the clay is reduced by cyclic strains of all amplitudes; the secant modulus at 1% strain is reduced by 20% for a peak strain of about 1%, and by 50% for a peak strain of about 3%.

3.7 Shear Modulus Values for Saturated Clays

Seed and Idriss (135) presented the results of an extensive series of tests on clayey soils (saturated), based on their test data and information already available in the literature since 1960. A

relationship was established between the shear modulus and undrained shear strength for a wide range of strain amplitudes. Their conclusion was based on the facts that i) stiffness increases, in general, with the soil strength, ii) for static load conditions, the ratio (E/S_u) for saturated clays does not vary widely from one soil to another, and iii) test data at very low strain levels indicates an approximately linear relationship between the shear modulus and shear strength for a number of clays as pointed out by Wilson and Dietrich. It seems reasonable to expect that variations in clay characteristics might be taken into account with a reasonable degree of accuracy by normalizing the shear modulus with respect to the undrained shear strength, S_u, and expressing the relationship $(G/S_u)_{max}$ as a function of shear strain (Fig. 10). For purposes of analysis, it was suggested that the maximum shear modulus, G_{max}, of any clay sample can be taken to be the undrained shear strength, S_u, of the clay sample times the value of $(G/S_u)_{max}$ at low strain levels (defined as 10^{-4}%). The data in Fig. 10 can be used to assess the influence of strain amplitude on the shear modulus of clays. For this, Idriss (60) expressed the ordinate in terms of the ratio of shear modulus at shear strain, γ, to the shear modulus at a shear strain of 10^{-4}%. The variations of the shear modulus and damping ratio for clays with strains are shown in Fig. 11. Reasonable estimates of the shear modulus of a clay at any strain amplitude can be obtained by determining the undrained shear strength of the soil sample and applying the reduction factors shown in Fig. 11 to determine the values at other shear strains. The data in Fig. 11, listed in Table 1, has been used for the response analysis.

3.8 Dynamic Lateral Loading of Piles

Many static and a few dynamic tests have demonstrated that the soil resistance vs deflection relationship developed on a pile face forced laterally against the soil is nonlinear. This nonlinearity is, of course, of the strain-softening type (Fig. 3, curve C) and can be approximated by hyperbolic curves similar to that shown in Fig. 7. Also, the resistance can be expressed as a function of deflection, y. Ref. 163 has used the hyperbolic stress-strain relationship for developing the 'p-y' curve by the finite element method. The determination of a suitable pressure vs displacement curve for a particular pile-soil system depends upon the dimensions of the pile, properties of the soil and the operating environment. Fig. 12(a) shows variations of pile displacement at three elevations for a pile forced horizontally into the soil. Fig. 12(b) indicates the pressure vs displacement for the first cycle of loading, and Fig. 12(c) indicates the hysteresis loops formed if the deformation is repeatedly reversed. It is seen from Fig. 12 that the strain-dependent soil reaction will give a varying stiffness along the pile. Hysteretic damping will also vary along the pile under vibratory loading.

3.8.1 Soil 'p-y' Curve

If laboratory stress-strain curves are available, then the soil-pile interaction could be represented by the 'p-y' curve. McClelland and Focht (92) developed a procedure for constructing the 'p-y' curve for soil with several layers of clay deposits of different shear strength characteristics from triaxial tests with the following relationships:

$$p = 5.5b\,\sigma_{\Delta} \qquad (3.10a)$$

and

$$y = 1/2\,b\,\varepsilon \qquad (3.10b)$$

where p = lateral soil resistance on pile per unit length of pile in pounds/inch,

b = pile diameter or frontal size in inches,

σ_{Δ} = deviator stress in a triaxial test with the confining pressure as close as possible to the actual overburden pressure,

and ε = strain in the triaxial test.

3.8.1.1 Development of the Soil 'p-y' Curve

Ref. 89 established a relation between the lateral soil resistance around a pile and deflection from both field and laboratory tests. The ultimate soil resistance per unit length of the pile was expressed as:

$$P_u = N_p\,cb \qquad (3.11)$$

in which N_p = dimensionless coefficient for the depth where only 'flow around' failure occurs, usually assumed to be '9' except near the ground surface where it is given by

$$N_p = 3 + \frac{px}{c} + J\frac{x}{b} \qquad (3.12)$$

in which x = depth in inches,

p = weight density of clay in pci,

c = cohesion of clay in psi,

b = pile diameter or width in inches,

J = dimensionless constant determined from the type of clay, and P_u = ultimate soil resistance in pounds per inch.

The final expression for the 'p-y' curve was obtained as a cubic non-dimensional curve, shown in Fig. 13(a):

$$p/P_u = 0.5 \left(\frac{y}{y_{50}}\right)^{1/3} \qquad (3.13)$$

between $0 \leq p/P_u \leq 1$ where $y_{50} = 2.5\ \varepsilon_{50} b$ in which y_{50} is the deflection corresponding to the strain, ε_{50}; ε_{50} is the strain corresponding to one-half of the ultimate deviator stress, $\sigma_{\Delta f}$, or one-half of the unconfined compression strength. Typical values of ε_{50} are available from Skempton's work (138) if laboratory stress-strain curves are not available. An important finding of Matlock (89) was that repetitive or cyclic loading causes a softening of the soil resistance. The value of the peak resistance is only about 70% of the resistance offered for a single static load.

Reese (121, 126) gave an expression for determination of the ultimate soil resistance for a wedge-type of failure near the ground surface considering the equilibrium of forces on the wedges as:

$$P_u = \rho bH + 2\ cb + 2.83\ \sigma H \qquad (3.14)$$

where ρ = effective unit wt, of soil in pci,

H = depth in inches,

b = diameter or width of pile in inches,

c = cohesion of clay in psi,

and P_u = ultimate lateral soil resistance for wedge-type failure in pounds per inch.

For deriving the expression for ultimate-soil reaction of a 'flow around'-type failure,

$$P_u = N_c cb \qquad (3.15)$$

where P_u = ultimate soil resistance in pounds per inch

and N_c = coefficient of bearing capacities, the value of which is usually assumed to be 11.

The lower of these two values of 'P_u' as evaluated from the above equations will be the ultimate soil resistance, 'P_u'. Details for developing the 'p-y' curve for both static and cyclic loading conditions are shown in Fig. 13(b).

3.9 Ice-Force Loading

Ice-force time history records are generated by modifying the available field records of Ref. 15 using the method outlined in Ref. 143. The method, based on the similarity between the fluctuating parts of randomly varying ice-force records and seismic records, uses a non-stationary random process obtained from filtering a shot noise through a second-order filter. The response of the structure can be studied using any appropriate time-history of ice-force loading obtained from either actual or computed records. In this investigation, artificial ice-force records are generated only to overcome the deficiencies due to the scantiness of available field records, and to obtain more realistic estimates of the loading function.

Both ice and earthquake loadings will induce significant cyclic stresses and strains in the soil. There are some important differences

in the nature of loading, such as the time scale and the number of cycles. The duration of a strong earthquake is measured in seconds with the periods ranging from 0.1 to 2 seconds, while the duration of ice loading may extend to hours, or even days, with periods ranging from 0.5 to 2 seconds. Hence, the number of significant loading cases may be larger for ice than for earthquakes in most cases, which may have an important effect for a site where both ice and earthquake loadings occur. Some of the methods which were originally developed for soil responses for earthquake loading by Seed and Idriss (135) are applied to study responses due to ice loading.

Afanas'ev's (1) formula is used in estimating the mean of the ice-force record. The maximum ice force developed when an ice-cover is cut through by the vertical column of the tower is given by:

$$P = m\, K\, B\, h\, \sigma_o \tag{3.16}$$

where m = shape coefficient equal to 0.90 for a semi-circular one

$$K = \left[5\,\frac{h}{B} + 1\right]^{\frac{1}{2}} \text{ for } 1 \leq \frac{B}{h} \leq 6 \tag{3.17}$$

[for $\frac{B}{h} > 1$, the values are obtained from the graph in Ref. 1]

B = width of the resisting structure,

h = thickness of the ice-sheet,

and σ_o = uniaxial compressive strength of ice.

The typical total (mean and fluctuating) force record for the framed tower is shown in Fig. 14. The mean part of the force on the framed tower is assumed to be produced by the impact of a moving ice floe of constant thickness of 1.5 ft. The random part is generated artifically

as described in Ref. 143, and superposed on the mean to give the total record.

3.10 Modelling Consideration

In the fixed base analysis, Fig. 15(a), the stiffness of the foundation is assumed to be rigid compared to the stiffness of the structure. For the half-space analysis, the foundation medium is idealized by interacting springs whose stiffness represents the force-deformation characteristics of the soil, Fig. 15(b). Finally, in the finite element idealization both the structure and the foundation are discretized with several elements of different types which allow a consistent representation of the stiffness and mass of the structural system, Fig. 15(c).

3.10.1 Half-Space or Semi-Fixed Type

Ref. 103 has determined the horizontal foundation stiffness using the elastic half-space analysis for a tower located on deep soil. If the foundation condition is not extremely soft, lateral forces applied at the upper end of the pile by the tower will be transferred to the surrounding soil with soil resistance increasing with depth. As such, it seems reasonable to assume the foundation to be the same as that for an equivalent rigid circular footing of radius, r_o, at the base of each leg of the tower and apply the elastic half-space theory to obtain the lateral foundation stiffness as

$$K_v = 18.2\, G r_o \frac{(1 - \mu^2)}{(2 - \mu)^2} \qquad (3.18)$$

where K_v = lateral stiffness per leg,

G = modulus of rigidity of the soil,

r_o = radius of the footing, here radius of the tower leg,

and μ = Poisson's ratio.

Ref. 103 also describes the evaluation of the rotational spring constant using the relation

$$K_\theta = \sum_i Y_i^2 K_{ip} \tag{3.19}$$

where Y_i is the y-coordinate position of pile, i, and K_{ip} is its vertical stiffness, i.e. equals the vertical force required at its upper end to cause a unit vertical deflection. K_{ip} is given as

$$K_{ip} = 3 \left(\frac{AE}{L}\right)_i \tag{3.20}$$

where L, A and E represent pile length, area and modulus of elasticity, respectively.

3.10.2 Maximum Frequency

Before modelling the structure-soil system by finite elements, the important factor which should be estimated is the choice of the maximum frequency, ω_{max}, to be included in the analysis. Choice of this frequency will influence more than anything the accuracy of the finite element dimensions and the cost of the analysis. Ref. 84 gives typical values for earth dams as 8 Hz and for nuclear power plants as 25 Hz (for seismic analysis). Typical values of frequencies for offshore structure have been established ranging from 0.2 to 3 Hz. According to the Nyqnist criterion, the interval of the digitization, Δt, for the force

record must be smaller than $\frac{1}{2}\omega_{max}$, where ω_{max} is the highest frequency specified above. In this analysis, $\Delta t = 0.01$ sec satisfies the digitization criterion.

3.10.3 Model Dimensions

The overall dimensions of the finite element mesh should be carefully determined, otherwise the response of the structure will be affected by reflections from the boundaries. The side boundaries should be placed outside the zone of influence of the structure to be analysed. It is usually sufficient to place the side boundaries away from the structure at a distance of 2.0 - 2.5 times the depth of the model.

3.10.4 Boundary Conditions

Ref. 84 has indicated that, if the input motion (seismic) is horizontal, it will correspond to vertically propagating shear waves in the free field, and the motion in the free field will be horizontal. The same interpretation will also be applicable for externally applied forces such as ice forces, and the best way to simulate the conditions is with horizontal rollers at the boundary to allow all modal points on the vertical boundaries to move in the horizontal direction only.

3.10.5 Mesh Size

The choice of element size has considerable influence on the higher frequencies. Kuhlmeyer and Lysmer (76) observed that the element dimension in the direction of wave propagation has a major influence on motion with high frequencies and correspondingly short wavelengths. Ref. 76 has given an empirical rule that the required mesh size for

effective transmission of any motion should be between one-quarter to one-eighth of the shortest wave length of motion. Ref. 84 has suggested that, because the significant part of the motion corresponds to vertical wave propagation, a good rule for the vertical element size is a value less than $h_{max} = 1/5\ \lambda_s$, where λ_s is the wave length of the shortest shear wave expressed as

$$\lambda_s = \frac{V_s}{\omega_{max}} = \frac{1}{\omega_{max}} \sqrt{\frac{G}{\rho_m}} \qquad (3.21)$$

where V_s is the shear wave velocity in the element, ω_{max} is the highest frequency in the analysis, G is the shear modulus of the layer, and ρ_m is the mass density of the soil. For the case of a lumped mass matrix, half the element size ($h_{max}/2$) should be used. It has also been pointed out by Ref. 84 that the computed response is less sensitive to the choice of the horizontal mesh size which may be several times longer than the dimensions indicated by Eqn. 3.21.

3.10.6 Thickness of the Soil Element

Ref. 65 has idealized the soil under the building frame by rectangular plane strain finite elements of 20 ft thickness. This is based on the concept that the frame is a part of a long building with 20 ft bays and is subjected to earthquake loading in the transverse direction causing only plane strain deformation. Later, Ref. 163 presented an approximation for the zone of influence of soil around a pile considering the soil and pile as a two-dimensional quadrilateral element. The zone of pile influence, as represented by the radius, r, is related directly to the diameter of pile, D, and found to be approximately eight

times the pile diameter. Based on this assumption, an equivalent thickness of the soil element has been used in this analysis which is approximately half the width of the base.

3.10.7 Added Mass of Soil

The effect of the soil mass on the movement of the pile should be considered. It is very difficult to estimate the effective mass which will participate in motion with the pile. Ref. 46 has assumed that, during vibration, the soil medium will behave like a fluid medium and the mass of the soil participating will be the mass of soil displaced by the pile volume. Ref. 103 obtained an expression using the Mindlin theory for elastic half-space, and stated that the effective mass of soil participating in the motion with the pile mass is given by

$$M_{is} \propto \int_{V_i} (\phi_u^2 + \phi_v^2 + \phi_w^2)\, \rho_m\, (x,y,z)\, dv_i \qquad (3.22)$$

where M_{is} = virtual mass of soil participating in motion at any level 'i'. ϕ_u, ϕ_v, ϕ_w represent the soil pile interaction displacement field within the soil tributary volume 'V_{is}' in the x-, y-and z-directions, respectively, due to a unit horizontal displacement of the pile groups in the x-directions at nodal point 'i'.

Instead of deriving the acceleration from the shear wave theory, Ref. 75 assumed the distribution curve for steady-state vibration as

$$a_i(t) = 100 \left\{1 + \frac{\omega^2}{p^2 - \omega^2} \left[\frac{di}{d}\right]^2\right\} \sin \omega t \qquad (3.23)$$

The virtual mass determined from the acceleration distribution curve was checked by comparing with experimental values and a parameter, β, termed additional mass ratio (= additional mass divided by the total mass of soil surrounded by 9 piles) was taken as the variable. β = 10% gave the best agreement between calculated and experimental values.

Ref. 140 derived an expression for the participating soil mass as

$$M_s = \left(C_s \rho_s \frac{\rho D^2}{4} L\right) \frac{(X_r - |P_{SET}|)}{L_u} \qquad (3.24)$$

where M_s = soil mass,

C_s = soil mass coefficient,

ρ_s = mass density of soil,

D = pile diameter,

L = length of segment above and below the node divided by two,

X_r = relative diaplacement of pile node with respect to the soil,

P_{SET} = permanent set of soil,

and L_u = ultimate displacement of soil, soil quake.

The present analysis assumes the mass of the soil in a rectangular element to be lumped equally at the four nodes following Ref. 65.

3.10.8 Added Mass of Water

A lumped mass approach has been used for the calculation of the added water mass assumed equal to the mass of water displaced by the structural member following Ref. 66. This assumption for the added water mass has been found to be reasonable for the first few modes, although there has been considerable discussion regarding possible frequency

dependence and modified values for flexible members. A refined analysis considering hydrodynamic interaction for an axisymmetric tower subjected to earthquake excitation was made by Liaw and Chopra (83) using a substructuring technique which was extended to the analysis of an offshore gravity platform as described in Refs. 142 and 143.

CHAPTER IV

THEORY

4.1 Introduction

This chapter describes the mathematical formulation of the dynamic analysis of the structure-soil system by the finite element method. As it is difficult, if not impossible, to obtain analytical solutions for the structure considered in view of the many complex cases, numerical analysis of a physical model based on certain approximations and simplified assumptions seems to be the only feasible approach. After the model is postulated, differential equations of motion are set up for the entire soil-structure systems and uncoupled. These equations are then solved by a step-by-step stable integration procedure and the responses obtained by modal superposition.

4.2 Idealization of Structure-Pile System

Structural members and piles are idealized by two dimensional beam elements. In the computer programme SAP-IV (158), the formulation is based on a three-dimensional approach as shown in Fig. 16(a), which considers torsion, bending about two axes, and the axial and shearing deformations. The element is prismatic and the development of its stiffness properties is standard as given in Przemieniecki (113). As the structure has been modelled as a two-dimensional frame, the beam elements need only six forces and six displacements.

4.2.1 Element Stiffness Matrix for Beam Elements

The stiffness matrix for a typical two-dimensional element is given as:

$$K_m = \begin{bmatrix} \frac{EA}{\ell} & & & & & \\ 0 & \frac{12\,EI_z}{\ell^3(1+\Phi_y)} & & & \text{Symmetric} & \\ 0 & \frac{6\,EI_z}{\ell^2(1+\Phi_y)} & \frac{(4+\Phi_y)EI_z}{\ell(1+\Phi_y)} & & & \\ \frac{-EA}{\ell} & 0 & 0 & \frac{EA}{\ell} & & \\ 0 & \frac{-12\,EI_z}{\ell^3(1+\Phi_y)} & \frac{-6\,EI_z}{\ell^2(1+\Phi_y)} & 0 & \frac{12\,EI_z}{\ell^3(1+\Phi_y)} & \\ 0 & \frac{6\,EI_z}{\ell^2(1+\Phi_y)} & \frac{(2-\Phi_y)EI_z}{\ell(1+\Phi_y)} & 0 & \frac{-6\,EI_z}{\ell^2(1+\Phi_y)} & \frac{(4+\Phi_y)EI_z}{\ell(1+\Phi_y)} \end{bmatrix} \quad (4.1)$$

where E, A, I_z, ℓ and Φ_y are the Young's modulus, cross-sectional area, moment of inertia, length, and shear deformations of the element, respectively. The geometric location of a typical element is defined by joint numbers, i and j. The location of the principal axis of the beam is defined by a third joint number k as shown in Fig. 16(a). The relationship between the local coordinates S_1, S_2 and S_3 obtained by the use of vector notation has been described by Wilson (159). The structure stiffness matrix K_b is assembled by the direct addition of element stiffness matrices as

$$\underline{K}_b = \Sigma K_m \tag{4.2}$$

The mass matrices for the element are computed on the basis of lumped mass idealization. Therefore, the assembled mass matrix for the entire structure-pile system is a diagonal one. Additional masses to account for the members perpendicular to the plane are lumped at the corresponding horizontal cross-brace level nodes.

4.3 Soil Medium

The soil under the structure (plane frame) is idealized by quadrilateral isoparametric plane strain finite elements with finite thickness "h". This assumption is based on the concept that frame is a part of a space frame of constant width, equal to the base length perpendicular to the plane, and the soil under the frame will undergo plane strain deformation only.

4.3.1 Stiffness Matrix for Two-Dimensional Isoparametric Elements

The local and global co-ordinate systems for a general quadrilateral element, as shown in Fig. 16(b), are related by

$$x = \sum_{i=1}^{4} h_i \, x_i \tag{4.3a}$$

and

$$y = \sum_{i=1}^{4} h_i y_i \tag{4.3b}$$

where the interpolation functions are

$$h_1 = 1/4\ (1-s)(1-t) \tag{4.4a}$$

$$h_2 = 1/4\ (1+s)(1-t) \tag{4.4b}$$

$$h_3 = 1/4\ (1+s)(1+t) \tag{4.4c}$$

and

$$h_4 = 1/4\ (1-s)(1+t) \tag{4.4d}$$

4.3.1.1 Strain-Displacement Equations

The above interpolation functions are used in the displacement approximation to take into account the rigid body displacement modes:

$$u_x\ (s,t) = \Sigma\, h_i\ u_{xi} \tag{4.5a}$$

and

$$u_y\ (s,t) = \Sigma\ h_i\ u_{yi} \tag{4.5b}$$

For two-dimensional analysis, the strain displacement equations are:

$$\varepsilon_{xx} = \frac{\partial u_x}{\partial x} = \Sigma\, h_{i,x}\, u_{xi} \tag{4.6a}$$

$$\varepsilon_{yy} = \frac{\partial u_y}{\partial v} = \Sigma\ h_{i,y}\, u_{yi} \tag{4.6b}$$

and

$$\varepsilon_{xy} = \frac{\partial u_x}{\partial y} + \frac{\partial u_y}{\partial x} = \Sigma\ h_{i,y}\, u_{xi} + \Sigma\ h_{i,x}\, u_{yi} \tag{4.6c}$$

The above expressions are written in matrix form as

$$\underline{\varepsilon} = \underline{a}(s,t)\underline{U} = \begin{bmatrix} \underline{H},x & 0 \\ 0 & \underline{H},y \\ \underline{H},y & \underline{H},x \end{bmatrix} \begin{bmatrix} \underline{U}x \\ \underline{U}y \end{bmatrix} \tag{4.7}$$

These strains are related to the eight nodal point displacements by a (3x8) matrix. The submatrices of the equation (4.7) are given by

$$\underline{H}_{,x} = [h_{1,x}\ h_{2,x}\ h_{3,x}\ h_{4,x}] \tag{4.8a}$$

$$\underline{H}_{,y} = [h_{1,y}\ h_{2,y}\ h_{3,y}\ h_{4,y}] \ . \tag{4.8b}$$

As the functions, h_i, are in terms of s and t, it is necessary to determine the derivatives with respect to the global system x-y. This is done by using the chain rule of partial differentiation:

$$h_{i,x} = h_{i,s}\ s_{,x} + h_{i,t}\ t_{,x} \ , \tag{4.9a}$$

and

$$h_{i,y} = h_{i,s}\ s_{,y} + h_{i,t}\ t_{,y} \ . \tag{4.9b}$$

In general, the chain rule is

$$\begin{bmatrix} \frac{\partial}{\partial s} \\ \\ \frac{\partial}{\partial t} \end{bmatrix} = \begin{bmatrix} x_{,s} & y_{,s} \\ \\ x_{,t} & y_{,t} \end{bmatrix} \begin{bmatrix} \frac{\partial}{\partial x} \\ \\ \frac{\partial}{\partial y} \end{bmatrix} \ , \tag{4.10}$$

which can be inverted as

$$\begin{bmatrix} \frac{\partial}{\partial x} \\ \\ \frac{\partial}{\partial y} \end{bmatrix} = \begin{bmatrix} s_{,x} & t_{,x} \\ \\ s_{,y} & t_{,y} \end{bmatrix} \begin{bmatrix} \frac{\partial}{\partial s} \\ \\ \frac{\partial}{\partial t} \end{bmatrix} \ . \tag{4.11}$$

The derivatives required in equation (4.9) are given by

$$\begin{bmatrix} s_{,x} & t_{,x} \\ s_{,y} & t_{,y} \end{bmatrix} = \frac{1}{J} \begin{bmatrix} y_{,t} & -y_{,s} \\ -x_{,t} & x_{,s} \end{bmatrix} \tag{4.12}$$

where the Jacobian J is

$$J = x_{,s}\, y_{,t} - x_{,t}\, y_{,s} \quad . \tag{4.13}$$

From equations (4.3a) and (4.3b),

$$\begin{aligned} x_{,s} &= \Sigma\, h_{i,s}\, x_i \quad , \\ x_{,t} &= \Sigma\, h_{i,t}\, x_i \quad , \\ y_{,s} &= \Sigma\, h_{i,s}\, y_i \quad , \end{aligned} \tag{4.14}$$

and

$$y_{,t} = \Sigma\, h_{i,t}\, y_i \quad .$$

For the given numerical values of s and t, the derivatives of the interpolating function can be evaluated. From equations (4.12) and (4.14), all required derivatives for the numerical evaluation of strain-displacement matrix of equation (4.7) can be computed.

4.3.1.2 Element Stiffness and Numerical Integration

For unit thickness, the element stiffness matrix is given by

$$\underline{K} = \int_{\text{Area}} \underline{a}^T\, \underline{c}\, \underline{a}\, dA \tag{4.15}$$

in which $\underline{c}$ is the stress-strain matrix and the integration is carried out over the area of the element. The matrix $\underline{c}$ is expressed as a (3x3) matrix for the plane strain element in the form

$$\underline{c} = \frac{E}{(1+u)(1-2u)} \begin{bmatrix} 1-\mu & \mu & 0 \\ -\mu & 1-\mu & 0 \\ 0 & 0 & \frac{1-2\mu}{2} \end{bmatrix} \qquad (4.16)$$

where E = Young's Modulus and μ = Poisson's Ratio. Equation (4.15) can be rewritten for the purpose of numerical integration in the s and t system as

$$\underline{K} = \int_{-1}^{1} \int_{-1}^{1} \underline{a}^T \underline{c}\, \underline{a}\, J \, ds \, dt \quad . \qquad (4.17)$$

Application of the one-dimensional integration formulae given in Zienkiewicz (164) yields

$$\underline{K} = \sum_j \sum_k W_j W_k J \underline{a}^T(s_j, t_k) \underline{c}\, \underline{a}\, (s_j, t_k) \qquad (4.18)$$

in which s_j and t_k are integration points, and W_j and W_k are the appropriate weight functions. In general, the element stiffness matrix derived in the above manner will lead to a (8x8) matrix. To improve the bending capacity of the element, additional internal degrees of freedom are provided at the element level. This can be done by improving the element displacement function in equation (4.5) with the addition of a few other terms as indicated below:

$$u_x = \Sigma\, h_i\, u_{xi} + h_5\, \alpha_1 + h_6\, \alpha_2 \quad , \tag{4.19a}$$

and

$$u_y = \Sigma\, h_i\, u_{yi} + h_5\, \alpha_3 + h_6\, \alpha_4 \tag{4.19b}$$

where α_i ($i = 1,2,3,4$) are the additional degrees of freedom. Functions h_5 and h_6 must be zero at the four nodes. The final stiffness matrix (8x8) is obtained by a static condensation procedure and will not be described here. The net results of the addition of the incompatible modes is the better satisfaction of microscopic equilibrium in the element.

Having formulated the stiffness matrix for a typical element, m, the stiffness matrix for the entire soil medium can be obtained by the direct stiffness method,

$$\underline{K}_s = \Sigma\, \underline{K}_m \tag{4.20}$$

where $\underline{K}_s$ = stiffness matrix for the soil medium

and $\underline{K}_m$ = stiffness matrix for the mth element.

The mass matrix is formulated in a similar manner. The lumped mass idealization makes the mass matrix diagonal. The small reduction in accuracy due to the approximation is justifiable in view of considerable saving in computer storage and time. In this investigation one-fourth of the mass of the quadrilateral element is assumed to be concentrated at each of the four nodal points.

4.4 Dynamic Equilibrium Equations

The dynamic equations of motion for a system of structural elements was expressed in the following matrix form as described by Clough and Penzien (24):

$$[M^*]\{\ddot{U}\} + [C^*]\{\dot{U}\} + [K^*]\{U\} = \{P(t)\} \qquad (4.21)$$

where $[M^*]$ = combined mass matrix for soil structure systems having only diagonal elements for lumped mass approximation,

$[C^*]$ = combined damping matrix for the soil-structure system,

$[K^*]$ = stiffness matrix for the soil-structure system being positive symmetric,

and $\{P(t)\}$ = load vector.

4.4.1 Response History Analysis by Mode Superposition

In the mode superposition analysis, it is assumed that the structural response can be expressed adequately by the p lowest vibration modes, where $p \leq n$ (maximum number of vibration modes which one may obtain considering all the degrees of freedom). For undamped free vibrations, the above matrix equation can be reduced to the generalized eigenvalue equation,

$$[K^*]\{\phi\} = \omega^2 [M^*]\{\phi\} \; ; \qquad (4.22)$$

where ω and ϕ are the free vibration frequency and mode shape, respectively. Using the transformation $\{U\} = [\phi]\{X\}$ where the columns in ϕ are the p M-orthonormalized eigenvectors, Eqn. 4.21 can be written in the following form as described in Ref. 158:

$$\{ \ddot{X} \} + [\Delta] \{ \dot{X} \} + [\Omega^2] \{ X \} = [\phi]^T \{ P(t) \} \qquad (4.23)$$

where

$$[\Delta] = \begin{bmatrix} 2\xi_1\omega_1 & & & & \\ & 2\xi_2\omega_2 & & & \\ & & 2\xi_3\omega_3 & & \\ & & & \cdots & \\ & & & & 2\xi_p\omega_p \end{bmatrix} \qquad (4.23a)$$

and

$$[\Omega^2] = \begin{bmatrix} \omega_1^2 & & & & \\ & \omega_2^2 & & & \\ & & \omega_3^2 & & \\ & & & \cdots & \\ & & & & \omega_p^2 \end{bmatrix} . \qquad (4.23b)$$

The above equation assumes that the damping matrix [C*] satisfies the modal orthogonality condition:

$$\{ \phi_i^T \} [C^*] \{ \phi_j \} = 0 \quad (i \neq j) . \qquad (4.24)$$

However, in soil-structure interaction problems, the assumption of the orthogonality condition for the damping matrix is not appropriate. Generally, the damping of the foundation medium will be relatively high

compared to that of the structure, and the damping forces cause coupling between the undamped free vibration modes. The coupling due to damping is particularly important in systems where the foundation medium is idealized by an elastic half-space model because very large viscous damping will be required to simulate the radiation energy loss. Besides this, the damping in soils is strain-dependent, and the damping values to be used in each element should be based on the strain developed in that element. This has been described in Ref. 59 and 84. For this investigation, a constant damping value, expressed in terms of the modal damping in each of the structural modes, has been assumed. This includes structural damping, viscous damping due to fluid drag, and pile damping due to interaction with the soil. Eqns. 4.23 represent a set of p uncoupled second-order differential equations. The solution of these second-order differential equations is accomplished by a step-by-step procedure as suggested by Ref. 8. The only approximation made is that the acceleration of each point in the system varies linearly within a small time interval, Δt. This assumption gives a parabolic variation of velocity and a cubic variation of displacement within the time interval, Δt. This step-by-step integration technique is accurate if the time step is small compared to the shortest period of the soil-structure system.

In the finite element idealization of the structure with complex geometries, the shortest period of vibration of the mathematical model may be several orders of magnitude less than the periods associated with the significant structural response. If the time step is long compared to the shortest period (normally allowed value is

one-tenth of the shortest period) the method will fail and instability will occur. Newmark (97) has studied this instability and recommended the constant acceleration method. This procedure is found to be stable when applied to finite element systems; however, some finite oscillations associated with the high frequencies are still present in the results. Several different unconditionally stable step-by-step methods have been used in the dynamic analysis of structural systems with large numbers of degrees of freedom. One of the simplest is the 'Wilson - θ' method suggested by Bathe and Wilson (8). This approach is based on the assumption that the acceleration varies linearly over an extended computational interval,

$$T = \theta \Delta T \quad \text{where } \theta > 1.37 \; . \tag{4.25}$$

The details of the computational procedure are well described in Ref. 24. The computer programme SAP-IV uses the 'Wilson - θ' method for the solution of Equation (4.23) to determine the response of the entire system.

4.5 Equivalent Linear Method

The normal mode method makes use of superposition which is only valid for linear systems. In the previous chapter, it was pointed out that shear deformation occurring in soils due to dynamic loading introduces nonlinear effects. This nonlinear deformation should be considered in the response analysis. Seed and Idriss (135) included it by introducing an equivalent linear method in which an approximate solution is obtained by a linear analysis, provided the stiffness and

damping used in each soil element are compatible with the effective shear-strain amplitudes developed in the element. Data on strain-compatible soil properties for clays and sands are published in Ref. 136. Typical variations of shear modulus and damping with shear strain are shown in Fig. 11 and summarized in Table 1.

In applying the above equivalent linear method, a set of shear moduli and damping values is estimated first for each soil element. Based on these variable properties, the structure is analyzed and the stress history is computed at each soil element centroid. Having computed the stress history, the effective shear-strain amplitudes for each element are estimated assuming that the effective shear-strain = Factor* $|\nu|$ maximum, where ν defines the shear strain, and Factor is a constant varying between 0.50 and 0.75.

The effective shear-strain amplitude computed at each element centroid is checked in Table 1 to ensure that the strain amplitude is compatible with the values of shear modulus and damping used in the response evaluation. If the soil properties are not compatible, modified values are estimated from Table 1, and the process repeated until convergence is achieved. The values obtained from the last iteration define the nonlinear response.

CHAPTER V

A NUMERICAL EXAMPLE

5.1 Introduction

This chapter presents an example to illustrate the applicability of the models described in the previous chapters to realistic situations. Detailed accounts of soil property values and the structural configuration of the tower are presented. The procedures for response computation for different kinds of models are described. The sequence of operations for the response calculation is summarized at the end of the chapter. Results for different kinds of models are given in the corresponding tables and figures.

5.2 Structural Geometry and Its Member Properties

The structure investigated is a welded tubular steel frame designed similar to that analysed by Corotis and Martin (25) for response to random wave forces. The welded tubular steel frame was designed for medium depth of water. Generally, the structure and the foundation should be treated as a continuous unit and the height of the structure will be set equal to the sum of the water depth, the foundation depth and the height above the water surface. In this example, a total height of 460 ft is assumed, with 100 ft below the mudline and 60 ft above the still water line; the water depth is 300 ft. A two-dimensional representation of the tower with three types of foundation conditions and sectional properties of the members are shown in Fig. 17. The structural members are assumed to be rigidly connected and the pile diameters assumed to be the same as

that of the tower leg. A constant dimension equal to the base length of the planar frame is assumed in the third direction. The masses per unit length of the members in the plane of the frame are computed by summing up the structural mass, the mass of the water contained in the tube and the mass of water displaced. The masses of the members perpendicular to the plane are assumed to be lumped at the horizontal cross base level joints and are shown in Fig. 17.

5.3 Ice Force Record

Ice force records are generated artificially as the continuous force vs. time records were not available. The procedure for generation of artificial ice force records has been described in Chapter III. The force vs. time ice force records are shown in Fig. 14. Ice force records were digitized with a time interval of 0.01 seconds and, knowing the filter properties and the interval of digitization, the predominant frequency of the record is estimated as 2.35 cps. In all the analyses, ice forces are applied at the M.S.L. level, and the total duration of the record is taken as 7.6 seconds.

5.4 Method of Analysis for Different Kinds of Models

The response analysis for different kinds of models was carried out by the computer programme SAP-IV (158). The preparation of input data and output commands will not be given as they are well-described in Ref. 158. The first five frequencies were considered for each individual model in the response evaluation by a modal analysis, and the modal damping in each of the structural modes was assumed to be 10%. While

this may seem a bit high for the fixed base analysis, it is reasonable when the yielding of the foundation is taken into consideration.

The important consideration in the analysis of the offshore structure is the soil condition. For the problem under investigation, the soil consists of approximately 100 ft of clay underlain by rock. In the finite element model, the side boundaries are located at a distance of approximately four times the base width to ensure free field motions. The soil medium has been represented by the finite element mesh (plane strain) shown in Fig. 15(c), which consists of 24 elements and 36 nodal points. In order to simulate a semi-infinite system, nodal points 18, 27, 36, 10, 19, and 28, were fixed in the vertical direction permitting movement only in the horizontal direction. Nodal points 1 to 8 (except 4 and 6) are fixed to the base. Forty-four beam elements were required to represent the structure. Two types of foundation layers were taken into consideration: i) soft and ii) stiff. Below the mudline, the basic soil properties vary with depth and are functions of unit weight, undrained shear strength and Poisson's ratio. Knowing the value of undrained shear strength for each layer, it is possible to find out the shear modulus at small strains (here defined as $\gamma = 10^{-4}\%$) from Fig. 10. This value is listed in Table 3(a) and 3(b) as G_{max} for each element. For an element in the clay medium, G_{max} would be equal to the undrained shear strength, S_u, of the clay within the element times the value of $(G/S_u)_{max}$, as suggested in Ref. 136. Typical values for the maximum Shear Modulus (G_{max} at strain $10^{-4}\%$) are given in Table 2 for different layers as calculated from the undrained shear strength of the sample.

For linear analysis, the shear modulus of each element is not dependent on the shear strain; it will be constant and analysis is carried out with the above values of G_{max} for two kinds of soil. The frequencies and the responses computed for the two different kinds of soils are shown in Table 4(a) to 4(d) and Figs. 18 to 25. For nonlinear finite element analysis, it is assumed that the shear modulus for each element is strain-dependent and the equivalent linear method described in Chapter IV is applied. The soil-structure system is analysed first using the properties as given in Table 2, i.e. a linear analysis is carried out first. Then the maximum shear strain is computed for each element from the stress history, and the effective shear strain calculated at the element centroid by the following relation:

$$\nu_{eff} = \text{Factor X } |\nu|_{max} \qquad (5.1)$$

where ν_{eff} = effective shear strain at element centroid

and ν_{max} = maximum shear strain computed from stress history.

The factor for effective shear strain is assumed to be 0.65. From the computed effective shear strain at each element centroid, the reduction factor for shear modulus is estimated from Table 1 and Fig. 11, and the new shear moduli for higher strain levels are computed as follows:

$$\text{Reduction Factor} = \frac{\text{Shear modulus at any strain } \nu}{\text{Shear Modulus at } 10^{-4}\% \text{ strain } (G_{max})} . \qquad (5.2)$$

Table 3(a) and 3(b) show the values of new shear moduli at the end of the first cycle of iteration. It is seen that the soil properties are not strain compatible. Also the differences between the assumed and computed

shear moduli is very high. Hence, a new iteration is carried out with the improved values of shear modulus for each element and the process is repeated until convergence has occurred. Final results are shown in Table 3(a) and 3(b). The values computed from the final iteration constitute the nonlinear response. The frequencies and the responses computed from the nonlinear analysis are presented in Table 5(a) to 5(d) and Figs. 26 to 33.

For the lumped parameter model, shown in Fig. 15(b), the soil medium is idealized by two kinds of springs at the structure base level, termed horizontal and rotational springs in Chapter III. The properties of these springs are given in Table 6. The structural model is represented by two kinds of element groups. These are: i) beam elements representing the structural members and ii) boundary elements representing the foundation springs for the lumped parameter model.

The total number of nodal points and elements necessary to complete the model are twenty-three and forty-two, respectively. The nodal points, 1 and 2, at the base level are assumed to be fixed in the vertical direction. The frequencies and the responses are presented in Table 7(a) to 7(c) and Figs. 34 to 39.

For the fixed base model shown in Fig. 15(a), the structure is represented by nineteen nodal points and thirty-eight elements (two-dimensional beam elements). The frequencies and the responses obtained are shown in Table 8(a) to 8(c) and Figs. 34 to 39.

5.5 Sequence of Operations

Finally, an outline of the sequence of operations required for the response evaluation is listed below:

1. Idealization of the soil-structure system as an assemblage of finite elements

   Input

   a) Nodal points
   b) Boundary conditions
   c) Elements
   d) Estimated material properties

2. Form Mass Matrix
3. Form Stiffness Matrix
4. Setup the equations of motion
5. Solution to evaluate nodal point displacements
6. Evaluation of stresses and strains.

For nonlinear analysis:

7. Determine effective shear strains in all soil elements as

$$\nu_{eff} = \text{Factor} \times |\nu|_{max}$$

8. Computation of strain-compatible soil properties
   a) Enter Table 1 for all soil elements
   b) Compare with properties used in the analysis
      i) If the difference is too large, the analysis is repeated from 1(d) with new properties.
      ii) If the difference is small, the computation is stopped.

CHAPTER VI

DISCUSSIONS AND CONCLUSIONS

6.1 Introduction

The results are presented in separate sets, each representing one of the problems investigated. The cases considered are: 1) Finite Elemented Foundation Model of the Soil-Structure System with i) Linear Soil Behaviour, and ii) Nonlinear Soil Behaviour; 2) Lumped Parameter (or Half-Space) Foundation Model with Linear Soil Springs; and, finally, 3) Fixed Base Model. The numerical results are presented at the end of this chapter.

6.2.1 Frequencies

It is seen from the above results that the fundamental frequencies of the frame are influenced significantly by soil-structure interaction. For example, the fundamental frequency of the lumped parameter model for the soft soil condition is 10.0% less than that for the rigid case. For the finite element model in soft soil with linear soil behaviour, the fundamental frequency is 6.67% less than that for the fixed base.

The variations are much larger for nonlinear soil behaviour, with the fundamental frequency 15.5% less than that for the rigid base condition. It is interesting to note that reduction in soil modulus, which, in effect, reduces the soil stiffness, affects the second and higher modes significantly for both linear and nonlinear analyses. For

example, it may be seen from Table 5(a) that, for the finite element model in soft soil with nonlinear soil behaviour, the third mode frequency is little more than a third of the corresponding frequency for the rigid foundation case.

6.2.2 Displacements

Due to the decrease in the fundamental as well as the higher frequencies, the flexible foundation has a major influence on the structural response. This can be easily seen from the results in Table 5(b). The maximum displacement at deck level is 4.373 in for the soft soil condition which is 36% more than that for the rigid case. Even for the case when soil nonlinearity is neglected, the displacement at deck level for the soft soil condition, as shown in Table 4(b) is 23% more than that for the rigid case. This variation in displacement is also noticeable for lumped parameter modelling of both types of soil condition. From Table 7(b), it is observed that the maximum displacement at deck level for the soft soil condition is 23% more compared to a rigid foundation.

6.2.3 Stresses

For the case of a flexible foundation, the displacement at the base level (mudline) of the tower is quite important. It is seen from Table 4(c) (linear analysis with finite element modelling) that the maximum stress in the vertical member, near base, is 10% less than that for a fixed base model, while the stresses in other members are higher. For example, the stresses in members 15 and 17 for the soft soil

condition are 23% more than that for the fixed base model, and 18% and 20% more for the stiff soil condition. The variation of stresses is even more when nonlinear soil behaviour is considered -Table 5(c). The stresses in members 15 and 17 are 48% more for the soft soil and 24% more for the stiff soil than that for the fixed base condition. In the former case, the stress in member 7 is 20% less than that for the rigid foundation condition. All these stress variations are due to the relative displacements of the floor levels with respect to the foundation. It is noticed that in all the cases with flexible foundation the relative displacement at the first floor level with respect to the foundation is less than that for the rigid foundation; therefore, the stresses are reduced in the bottom member. But the same situation was not observed for the higher levels, particularly at the M.S.L. level where the relative displacement is larger for the flexible foundation than that for the rigid one; therefore, stresses are increased in the top members.

For the lumped parameter model, the stresses in all the members - Table 7(c) - are 8-20% below those for the fixed base condition. This is a little surprising but not unrealistic when one considers the relative displacements between floor levels. One of the limitations of this kind of model is that, while computing the horizontal stiffness, K_y, the value of the shear modulus is taken only for the top layer of the soil. It is not known to what extent this will affect the overall response of the structure. Alternatively, in the finite elemented foundation model, the soil medium is represented consistently and the results seem to be more realistic than those for the half-space model.

6.3 Conclusions

The following conclusions are drawn from this study:

1. Fundamental and higher mode frequencies are influenced significantly due to structure-soil interaction.

2. Different kinds of soil conditions influence the structural response significantly inducing high stresses in certain members. In fact, redistribution of stresses takes place in the whole structure.

3. For the frame considered in this investigation, the stress in the pile member, 1, for the finite element model varies significantly due to soil behaviour. For nonlinear soil behaviour, with the stiff soil condition, the stress is 75% more than that for linear behaviour. Similarly, for soft soil, the difference is about 25%. The stresses in the other members are also affected significantly compared to the rigid base model.

4. It is seen from the different models used that soil stiffness is very important. For identical structures and same ice forces, the displacements occurring in the structure will vary quite a lot depending upon the relative stiffnesses of the foundation and the structure. It can also be shown that different foundation displacements will be obtained if the kind or stiffness of the structure is changed. Although this case has not been demonstrated specifically, the author feels that response analysis to dynamic loading may lead to erroneous results if the foundation-superstructure interaction is ignored.

6.4 Contributions

1. Application of the equivalent linear method to study nonlinear foundation-structure interaction of an offshore tower subjected to ice loading.

2. Study of the effects of different foundation conditions with varying soil properties.

3. Investigation of the influence of various modelling techniques on the dynamic responses of an offshore tower.

4. Study of the effects of soil-structure interaction on the fundamental and higher frequencies and modes.

5. Identification of the need for more field records for the artificial generation of realistic force record envelopes.

6. Indication of the necessity for obtaining strain-dependent soil properties, based on site field exploration and laboratory test programmes complemented by experience and available data for similar soils.

6.5 Recommenations for Further Research

1. Application to other kinds of environmental loading, e.g. wave forces.

2. Study of liquefaction of sandy soil foundation conditions due to repetitive loading.

3. Use of frequency-dependent springs instead of linear static springs for the lumped parameter foundation model.

4. Use of variable damping to ensure strain compatibility. (Note: The present analysis has neglected the variation of damping in the two systems - soil and structure.)

5. Model studies and System Identification ('massaging').

6. Extension to three-dimensional modelling for more realistic evaluation of the response.

TABLES AND FIGURES

TABLE 1: Strain-Compatible Soil Properties

(Ref. 84)

Effective Shear Strain γ_{eff} (%)	log (γ_{eff})	Shear Modulus Reduction Factor*		Fraction of Critical Damping (%)	
		Clay	Sand	Clay	Sand
$\leq 1 \times 10^{-4}$	-4.0	1.000	1.000	2.50	0.50
3.16×10^{-4}	-3.5	0.913	0.984	2.50	0.80
1.00×10^{-3}	-3.0	0.761	0.934	2.50	1.70
3.16×10^{-3}	-2.5	0.565	0.826	3.50	3.20
1.00×10^{-2}	-2.0	0.400	0.656	4.75	5.60
3.16×10^{-2}	-1.5	0.261	0.443	6.50	10.0
1.00×10^{-1}	-1.0	0.152	0.246	9.25	15.5
0.316	-0.5	0.076	0.115	13.8	21.0
1.00	0.	0.037	0.049	20.0	24.6
3.16	0.5	0.013	0.049	26.0	24.6
≥ 10.00	1.0	0.004	0.049	29.0	24.6

*This is the factor which has to be applied to the shear modulus at low shear strain amplitudes (here defined as 10^{-4} percent) to obtain the modulus at higher strain levels.

TABLE 2: Soil Properties for Different Layers

Soil Stratum Depth below Mudline	Soft Soil		Stiff Soil	
	Undrained (S_u) Shear Strength (psi)	G_{max}* (ksi)	Undrained (S_u) Shear Strength (psi)	G_{max}* (ksi)
0' - 30'	1.080	2.5	2.173	5.0
30' - 60'	1.521	3.5	3.043	7.0
60' - 100'	2.174	5.0	4.348	10.0

*Shear modulus at low strain level (here defined as 10^{-4} %)

TABLE 3(a). Iteration Cycles for Finite Elemented Foundation Model with Nonlinear Soil Behaviour (Soft Soil)

Soil Element	Mat. Type	Density (PCF)	Poisson Ratio	G_{Max} (KSI)	G_{Used} (KSI)	Iteration Cycle No. 1							
						σ_y (PSI)	σ_z (PSI)	τ_{yz} (PSI)	Max^m Shear Strain (10^{-4})	Eff. Shear Strain (10^{-4})	Reduction Factor	G_{New} (KSI)	Difference %
1,8	Soft Soil	120	0.47	5.0	5.0	.0675	.0016	.1192	.2472	.1607	.6802	3.401	32.0
2,7						.0974	-.0014	.2041	.4200	.2730	.5900	2.950	41.0
3,6						.4068	.7240	.2704	.6269	.4075	.5286	2.643	47.0
4,5						.0953	.5466	.2626	.6925	.4501	.5144	2.572	49.0
9,16		100	0.45	3.5	3.5	.0133	-.0774	.0520	.1972	.1282	.7187	2.515	28.0
10,15						.2073	.0763	.0898	.9809	.6376	.6376	2.231	36.0
11,14						.0535	.4301	.2726	.9466	.6153	.4696	1.643	53.0
12,13						.0513	-.433	.0660	.7172	.4662	.5094	1.783	49.0
17,24		80	0.40	2.5	2.5	.0125	.0130	.0186	.0748	.0486	.8563	2.140	14.0
18,23						.0362	-.0847	.0441	.2013	.1309	.7152	1.788	28.5
19,22						.3777	.4037	.3065	1.2271	.7976	.4324	1.081	56.0
20,21						.0749	.3597	.0621	.6214	.4039	.5299	1.325	47.0

TABLE 3(a), Continued

Soil Element	Mat. Type	Density (PCF)	Poisson Ratio	G_{Max} (KSI)	G_{Used} (KSI)	Iteration Cycle No. 2							
						σ_y (PSI)	σ_z (PSI)	τ_{yz} (PSI)	Max^m Shear Strain (10^{-4})	Eff. Shear Strain (10^{-4})	Reduction Factor	G_{New} (KSI)	Difference %
1,8	Soft Soil	120	0.47	5.0	3.401	.0309	-.0056	.1117	.3328	.2163	.6302	3.151	7.5
2,7					2.950	.0509	-.0400	.1511	.5349	.3477	.5514	2.757	6.5
3,6					2.643	.2889	.4735	.2049	.8508	.5530	.4849	2.424	8.5
4,5					2.572	.2501	.0765	.1170	.5665	.3682	.5432	2.716	-6.0
9,16		100	0.45	3.5	2.515	.0200	-.0386	.0671	.2912	.1893	.6523	2.283	9.0
10,15					2.231	.1217	.0150	.0739	.4085	.2655	.5948	2.081	6.69
11,14					1.643	.2218	.0502	.1749	1.1857	.7707	.4373	1.530	6.8
12,13					1.783	.1355	-.0056	.0588	.5154	.3350	.5567	1.948	-9.25
17,24		80	0.40	2.5	2.140	.0296	.0054	.0246	.1282	.0833	.7851	1.963	8.30
18,23					1.788	.0414	.0029	.0282	.1911	.1242	.7240	1.810	-.75
19,22					1.081	.2098	.2012	.1757	1.626	1.057	.3933	0.983	9.05
20,21					1.325	.2247	.0723	.0475	.6782	.4408	.5174	1.293	2.36

TABLE 3(a), Continued

Soil Element	Mat. Type	Density (P F)	Poisson Ratio	G_{Max} (KSI)	G_{Used} (KSI)	Iteration Cycle No. 3 σ_y (PSI)	σ_z (PSI)	τ_{yz} (PSI)	Max. Shear Strain (10^{-4})	Eff. Shear Strain (10^{-4})	Reduction Factor	G_{New} (KSI)	Difference %
1,8	Soft Soil	100	0.47	5.0	3.151	.0301	-.0058	.1159	.3722	.2419	.6106	3.053	3.15
2,7					2.757	.0511	-.0424	.1518	.5762	.3745	.5408	2.704	1.95
3,6					2.424	.2758	.4403	.2012	.8965	.5827	.4774	2.387	1.5
4,5					2.716	.0834	.2658	.1245	.5683	.3694	.5427	2.714	0.05
9,16		100	0.45	3.5	2.283	.0194	-.0371	.0710	.3348	.2176	.6286	2.20	3.6
10,15					2.081	.1157	.0107	.0775	.4498	.2924	.5784	2.024	2.75
11,14					1.530	.0568	.2082	.1689	1.2091	.7859	.4345	1.521	0.65
12,13					1.948	.0085	-.1469	.0713	.5412	.3518	.5497	1.924	1.2
17,24		80	0.40	2.5	1.963	.0302	.0053	.0281	.1474	.0958	.7667	1.917	2.35
18,23					1.810	-.0028	-.0349	.0302	.2443	.1588	.6822	1.7055	5.5
19,22					0.983	.2074	.1905	.1668	1.698	1.104	.3880	.9702	1.35
20,21					1.293	.0711	.2196	.0549	.7142	.4642	.5099	1.28	1.45

TABLE 3(b). Iteration Cycles for Finite Elemented Foundation Model with Nonlinear Soil Behaviour (Stiff Soil)

						Iteration Cycle No. 1							
Soil Element	Mat. Type	Density (PCF)	Poisson Ratio	G_{Max} (KSI)	G_{Used} (KSI)	σ_y (PSI)	σ_z (PSI)	τ_{yz} (PSI)	Max^m Shear Strain (10^{-4})	Eff. Shear Strain (10^{-4})	Reduction Factor	G_{New} (KSI)	Difference %
1,8	Stiff Soil	120	0.47	10.0	10.0	.07848	.01425	.1569	.1602	.1041	.7541	7.541	25.0
2,7						.15730	.03613	.2265	.2345	.1524	.6893	6.893	31.0
3,6						.8797	.4890	.2994	.3575	.2324	.6174	6.174	38.0
4,5						.1585	.6408	.3036	.3877	.2520	.6037	6.037	39.0
9,16		100	0.45	7.0	7.0	-.0150	-.0444	.0790	.1148	.0746	.7997	5.598	20.0
10,15						.2539	.1027	.1077	.1880	.1222	.7269	5.088	27.0
11,14						.1203	.6193	.3551	.6200	.4030	.5302	3.711	47.0
12,13						-.0314	-.5609	.1517	.4359	.2833	.5837	4.086	42.0
17,24		80	0.40	5.0	5.0	.0031	.0207	.0273	.0575	.0373	.8912	4.456	11.0
18,23						-.0333	-.1201	.0738	.1713	.1113	.7428	3.714	25.0
19,22						.5652	.4538	.3959	.7996	.5197	.4938	2.469	50.0
20,21						.1294	.554	.0244	.4269	.2775	.5872	2.936	41.0

TABLE 3(b), Continued

Soil Element	Mat. Type	Density (PCF)	Poisson Ratio	G_{Max} (KSI)	G_{Used} (KSI)	Iteration Cycle No. 2							
						σ_y (PSI)	σ_z (PSI)	τ_{yz} (PSI)	Max^m Shear Strain (10^{-4})	Eff. Shear Strain (10^{-4})	Reduction Factor	G_{New} (KSI)	Difference %
1,8	Stiff Soil	120	0.47	10.0	7.541	.06613	.00547	.1415	.1919	.1247	.7234	7.234	4.0
2,7					6.893	.1076	-.0284	.2153	.3275	.2129	.6323	6.323	8.0
3,6					6.174	.4383	.7563	.2864	.5306	.3449	.5526	5.526	11.0
4,5					6.037	.1426	.6378	.2742	.6120	.3978	.5321	5.321	12.0
9,16		100	0.45	7.0	5.598	.0110	-.0802	.0696	.1488	.0967	.7654	5.358	4.0
10,15					5.088	.2743	.0763	.0904	.2635	.1713	.6694	4.686	8.0
11,14					3.711	.1182	.4455	.2770	.8668	.5634	.4823	3.375	9.0
12,13					4.086	.0124	-.5379	.0730	.6966	.4528	.5136	3.594	12.0
17,24		80	0.40	5.0	4.456	.0323	.0206	.0254	.0586	.0381	.8886	4.442	0.5
18,23					3.714	-.0223	-.1037	.0565	.1875	.1219	.7272	3.636	2.0
19,22					2.469	.3796	.4125	.3143	1.2748	.8286	.4270	2.134	13.0
20,21					2.936	.0620	.3737	.0673	.5783	.3759	.4544	2.272	22.0

TABLE 3(b), continued

Soil Element	Mat. Type	Density (PCF)	Poisson Ratio	G_{Max} (KSI)	G_{Used} (KSI)	Iteration Cycle No. 3							
						σ_y (PSI)	σ_z (PSI)	τ_{yz} (PSI)	Max^m Shear Strain (10^{-4})	Eff. Shear Strain (10^{-4})	Reduction Factor	G_{New} (KSI)	Difference %
1,8	Stiff Soil	120	0.47	10.0	7.234	.0646	-.0014	.1419	.2014	.1309	.7172	7.172	0.85
2,7					6.323	.1087	-.033	.2071	.3462	.2250	.6229	6.229	1.5
3,6					5.526	.4363	.7474	.2768	.5746	.3735	.5411	5.411	2.0
4,5					5.321	.1061	.5622	.2794	.6772	.4404	.5175	5.175	2.75
9,16		100	0.45	7.0	5.358	.0151	-.0838	.0716	.1623	.1055	.7515	5.263	1.75
10,15					4.686	.2372	.0716	.0851	.2535	.1648	.6760	4.732	-1.0
11,14					3.375	.1127	.4231	.2678	.9171	.5961	.4741	3.319	1.6
12,13					3.594	-.0094	.4606	.0666	.6797	.4418	.5171	3.619	0.71
17,24		80	0.40	5.0	4.442	.0364	.0194	.0261	.0619	.0402	.8820	4.410	0.7
18,23					3.636	.0178	-.1003	.0527	.1846	.120	.7305	3.653	-0.45
19,22					2.134	.3690	.3917	.3010	1.411	.9172	.4124	2.062	-3.53
20,21					2.272	.0573	.3034	.0767	.6383	.4149	.5261	2.630	-15.75

TABLE 4(a): Natural Frequencies - Finite Element Model with Linear Soil Behaviour

(Unit: Hertz)

Type of Soil	Mode 1	Mode 2	Mode 3
Soft	0.945	1.161	1.732
Stiff	0.968	1.621	1.820

TABLE 4(b): Maximum Values for Horizontal Displacement in Joints 47, 49, and 51 - Finite Element Model with Linear Soil Behaviour

(Unit: Inches)

Type of Soil	Displ. at Joint 47	Time (sec.)	Displ. at Joint 49	Time (sec.)	Displ. at Joint 51	Time (sec.)
Soft	1.993	0.500	3.769	0.500	3.930	0.500
Stiff	1.867	0.400	3.619	0.500	3.773	0.500

TABLE 4(c): Maximum Values of Stresses (σ_{max}) in Members 1, 7, 15, and 17 - Finite Element Model with Linear Soil Behaviour

Type of Soil	Member 1					Member 7					Member 15					Member 17				
	Axial Force (kips)	Time (sec.)	Bending Moment (k-inch)	Time (sec.)	σ_{max} (ksi)	Axial Force (kips)	Time (sec.)	Bending Moment (k-inch)	Time (sec.)	σ_{max} (ksi)	Axial Force (kips)	Time (sec.)	Bending Moment (k-inch)	Time (sec.)	σ_{max} (ksi)	Axial Force (kips)	Time (sec.)	Bending Moment (k-inch)	Time (sec.)	σ_{max} (ksi)
Soft	356.9	0.4	58.0	3.7	1.820	696.9	0.5	876.9	0.5	3.28	95.69	0.6	14,390.0	0.6	14.57	3.49	0.6	5890.0	0.6	5.65
	350.0	3.7	53.7	0.4		618.0	3.7	1014.0	3.7											
Stiff	195.0	0.4	18.9	0.4	0.817	639.0	3.7	1082.0	0.4	3.49	91.75	0.6	13,810.0	0.6	13.98	3.39	0.5	5658.0	0.6	5.43
						691.0	0.4	1134.0	3.7											

TABLE 4(d): Maximum Response of Stresses in Soil Element No. 20 - Finite Element Model with Linear Soil Behaviour

Type of Soil	Normal Stress σ_y (psi)	Time (sec.)	Normal Stress σ_z (psi)	Time (sec.)	Shear Stress τ_{yz} (psi)	Time (sec.)
Soft	0.108	0.5	0.396	0.5	0.062	3.7
Stiff	0.141	0.5	0.396	0.4	0.025	0.6

TABLE 5(a): Natural Frequencies - Finite Element Model with Nonlinear Soil Behaviour

(Unit: Hertz)

Type of Soil	Mode 1	Mode 2	Mode 3
Soft	0.855	0.941	1.326
Stiff	0.946	1.278	1.762

TABLE 5(b): Maximum Values for Horizontal Displacement in Joints 47, 49, and 51 - Finite Element Model with Nonlinear Soil Behavior

(Unit: Inches)

Type of Soil	Displ. at Joint 47	Time (sec.)	Displ. at Joint 49	Time (sec.)	Displ. at Joint 51	Time (sec.)
Soft	1.961	0.5	4.181	0.5	4.373	0.5
Stiff	1.998	0.5	3.772	0.5	3.935	0.5

TABLE 5(c): Maximum Values of Stresses (σ_{max}) in Members 1, 7, 15, and 17 - Finite Element Model with Nonlinear Soil Behaviour

Type of Soil	Member 1					Member 7					Member 15					Member 17				
	Axial Force (kips)	Time (sec.)	Bending Moment (k-inch)	Time (sec.)	σ_{max} (ksi)	Axial Force (kips)	Time (sec.)	Bending Moment (k-inch)	Time (sec.)	σ_{max} (ksi)	Axial Force (kips)	Time (sec.)	Bending Moment (k-inch)	Time (sec.)	σ_{max} (ksi)	Axial Force (kips)	Time (sec.)	Bending Moment (k-inch)	Time (sec.)	σ_{max} (ksi)
Soft	441.0	0.6	106.6	0.6	1.897	434.9	0.5	434.9	0.5	2.954	14.0	0.5	17,120.0	0.5	17.33	4.06	0.5	7011.0	0.5	6.73
Stiff	313.0	0.3	85.6	0.3	1.34	688.4	0.6	854.0	0.5	3.28	95.72	0.6	14,390.0	0.6	14.56	3.49	0.6	5900.0	0.6	5.66

TABLE 5(d): Maximum Response of Stresses in Soil Element No. 20 - Finite Element Model with Nonlinear Soil Behaviour

Type of Soil	Normal Stress σ_y (psi)	Time (sec.)	Normal Stress σ_z (psi)	Time (sec.)	Shear Stress τ_{yz} (psi)	Time (sec.)
Soft	0.073	0.5	0.222	0.5	0.055	0.6
Stiff	0.100	0.5	0.368	0.5	0.077	0.6

TABLE 6: Spring Properties for Lumped Parameter Foundation Model

Type of Soil	Horizontal Spring, K_v (Pound/Inch)	Rotational Spring, K_θ (Inch-Pound)
Soft	2979.0×10^2	3761.0×10^6
Stiff	5958.0×10^2	3761.0×10^6

TABLE 7(a): Natural Frequencies of Idealized System - Lumped Parameter Foundation Model

(Unit: Hertz)

Type of Soil	Mode 1	Mode 2	Mode 3
Soft	0.910	1.543	3.158
Stiff	0.963	1.669	3.277

TABLE 7(b): Maximum Values for Horizontal Displacements in Joints 1, 13, 15, and 17 - Lumped Parameter Foundation Model.

(Unit: Inch)

Type of Soil	Displ. at Joint 1	Time (sec.)	Displ. at Joint 13	Time (sec.)	Displ. at Joint 15	Time (sec.)	Displ. at Joint 17	Time (sec.)
Soft	0.618	0.4	2.405	0.6	3.785	0.6	3.931	0.6
Stiff	0.307	0.4	2.086	0.4	3.371	0.6	3.518	0.6

TABLE 7(c): Maximum Values of Stresses (σ_{max}) in Members 1, 9, and 11 - Lumped Parameter Foundation Model

Type of Soil	Member 1					Member 9					Member 11				
	Axial Force (kips)	Time (sec.)	Bending Moment (k-inch)	Time (sec.)	σ_{max} (ksi)	Axial Force (kips)	Time (sec.)	Bending Moment (k-inch)	Time (sec.)	σ_{max} (ksi)	Axial Force (kips)	Time (sec.)	Bending Moment (k-inch)	Time (sec.)	σ_{max} (ksi)
	783.0	0.6	118.4	0.6							5.51	5.4	1143.0	5.4	
Soft					3.33	73.0	0.6	10,030.0	0.6	10.21					3.9
	469.0	0.2	372.6	0.2							0.766	0.6	4098.0	0.6	
Stiff	766.0	0.4	325.4	0.2	3.26	77.1	0.6	10,580.0	0.6	10.77	0.8027	0.6	4322.0	0.6	4.13

TABLE 8(a): Natural Frequencies of Idealized System - Fixed Base Foundation Model

(Unit: Hertz)

Type of Soil	Mode 1	Mode 2	Mode 3
-	1.012	1.874	3.509

TABLE 8(b): Maximum Values for Horizontal Displacements in Joints 1, 13, 15, and 17 - Fixed Base Model

(Unit: Hertz)

Type of Soil	Displ. at Joint 1	Time (sec.)	Displ. at Joint 13	Time (sec.)	Displ. at Joint 15	Time (sec.)	Displ. at Joint 17	Time (sec.)
-	0.0	-	1.898	0.4	3.055	0.6	3.201	0.6

TABLE 8(c): Maximum Values of Stresses (σ_{max}) in Members 1, 9, and 11 - Fixed Base Foundation Model

Type of Soil	Member 1					Member 9					Member 11				
	Axial Force (kips)	Time (sec.)	Bending Moment (k-Inch)	Time (sec.)	σ_{max} (ksi)	Axial Force (kips)	Time (sec.)	Bending Moment (k-Inch)	Time (sec.)	σ_{max} (ksi)	Axial Force (kips)	Time (sec.)	Bending Moment (k-Inch)	Time (sec.)	σ_{max} (ksi)
	745.0	1.4	1068.0	1.4							5.7	1.0	2429.0	1.0	
					3.70	83.57	0.6	11,630.0	0.6	11.83					4.59
	815.0	0.4	627.0								0.25	0.6	4749.0	0.6	

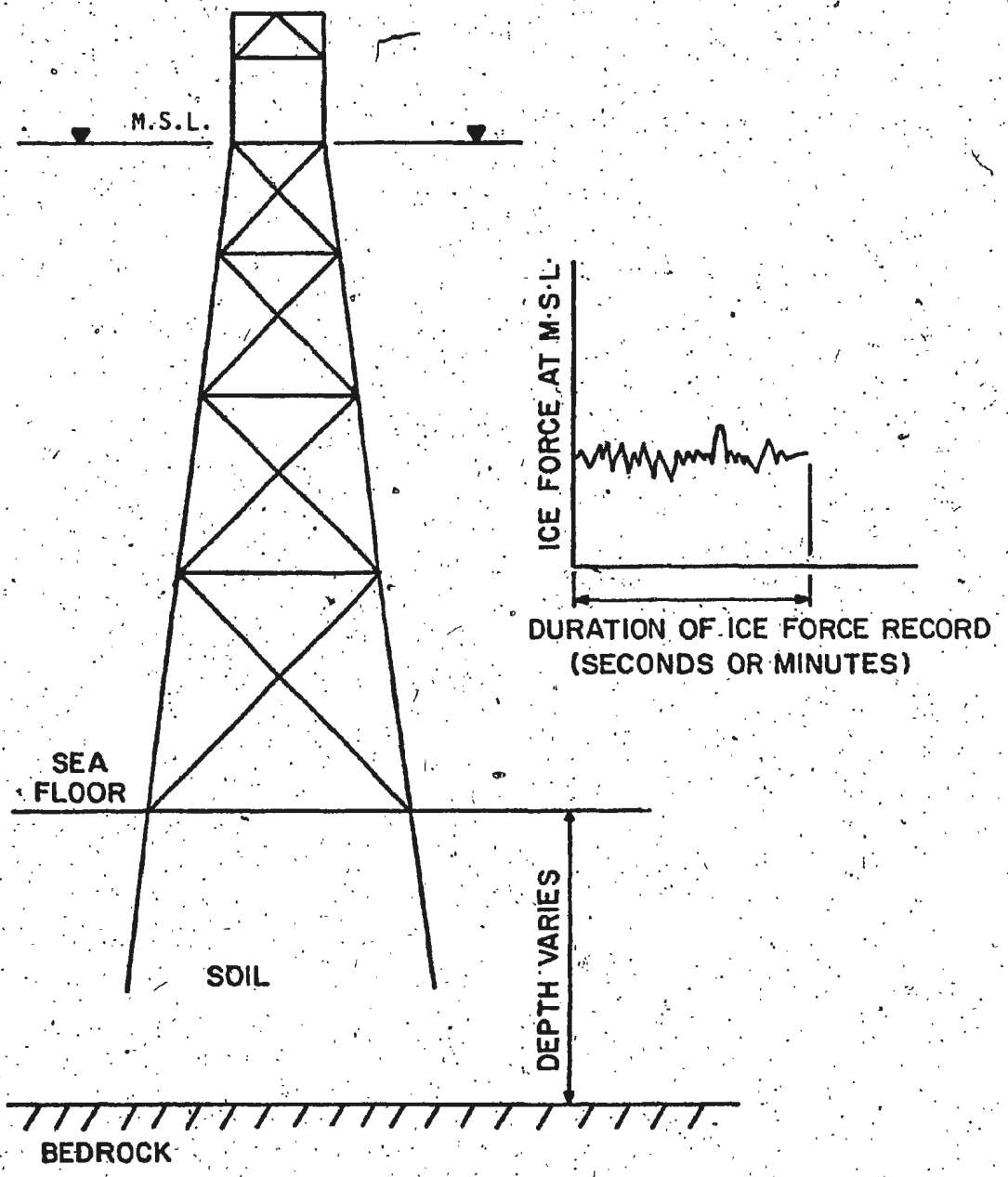

Fig. 1. Ice Loading on Soil-Structure-Pile Systems.

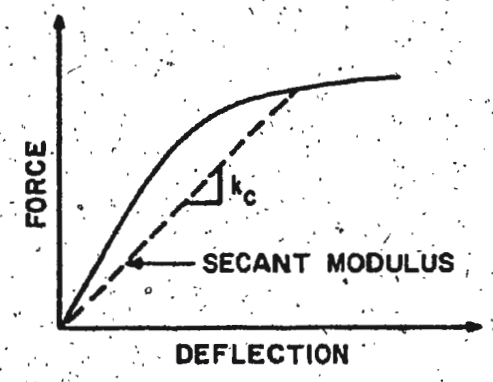

Fig. 2(a). Nonlinear Soil Reaction (Ref. 36).

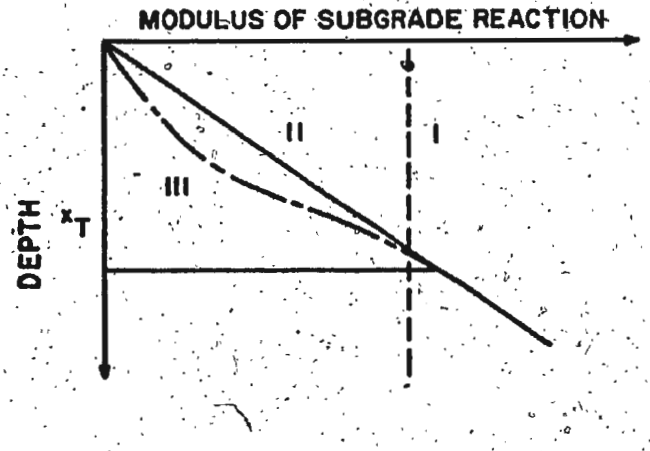

Fig. 2(b). Variation of the Modulus of Subgrade Reaction with Depth (Ref. 36).

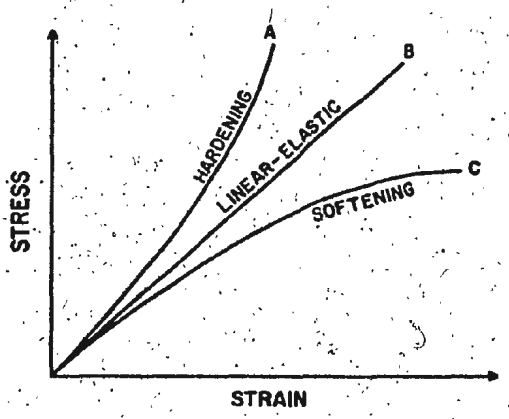

Fig. 3. Types of Stress-Strain Curves (Ref. 127).

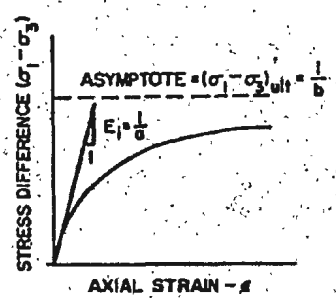

Fig. 4. Hyperbolic Stress-Strain-Curve (Ref. 69).

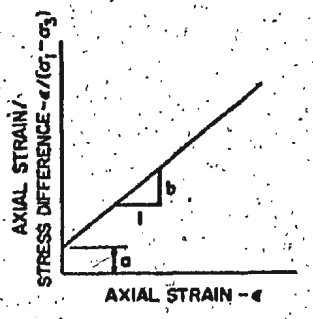

Fig. 5. Transformed Hyperbolic Stress-Strain Curve (Ref. 69).

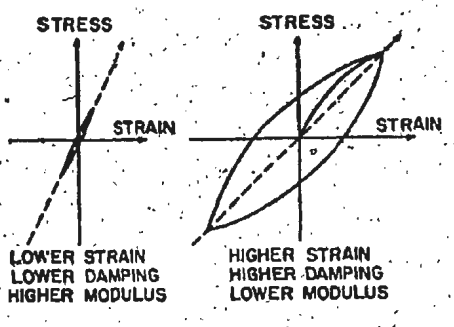

Fig. 6. Illustration of Strain-Dependency of Moduli and Damping in Soils (Ref. 136).

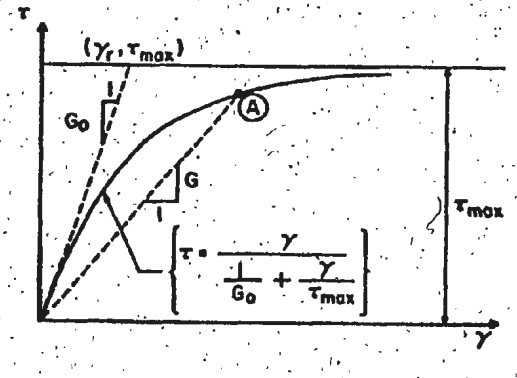

Fig. 7. Basic Parameters for Hyperbolic Shear Stress-Strain Curves (Refs. 48, 49).

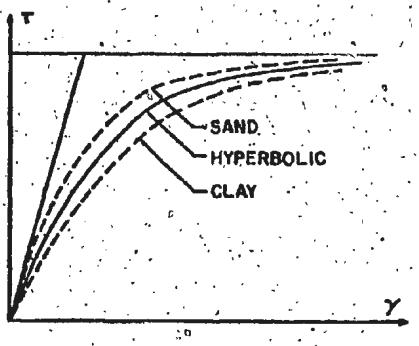

Fig. 8. Hyperbolic Shear Stress-Strain Curves for Sand and Clay (Refs. 48, 49).

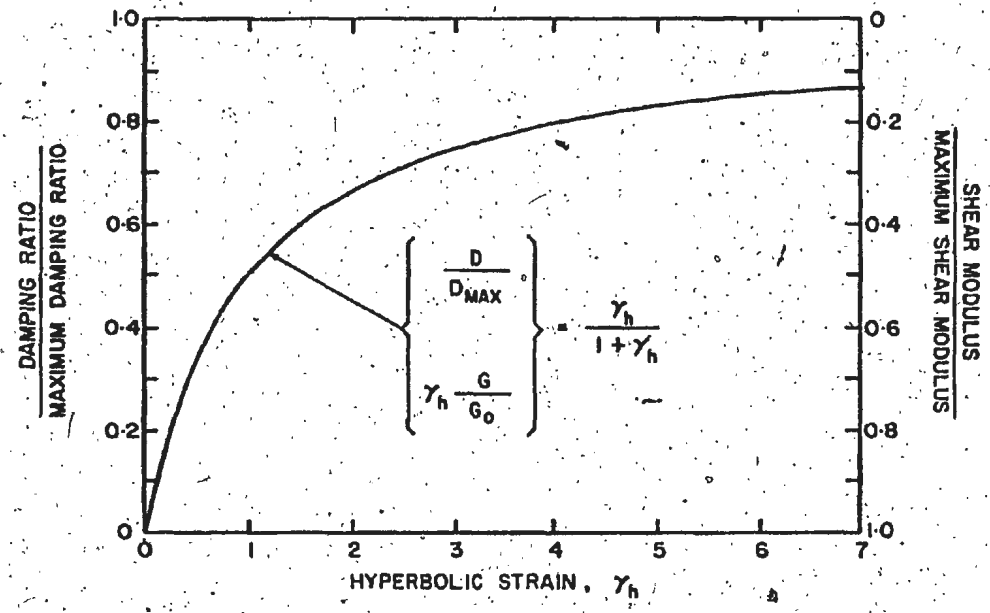

Fig. 9. Normalized Shear Modulus and Normalized Damping Ratio for All Soils vs. Hyperbolic Strain (Refs. 48, 49).

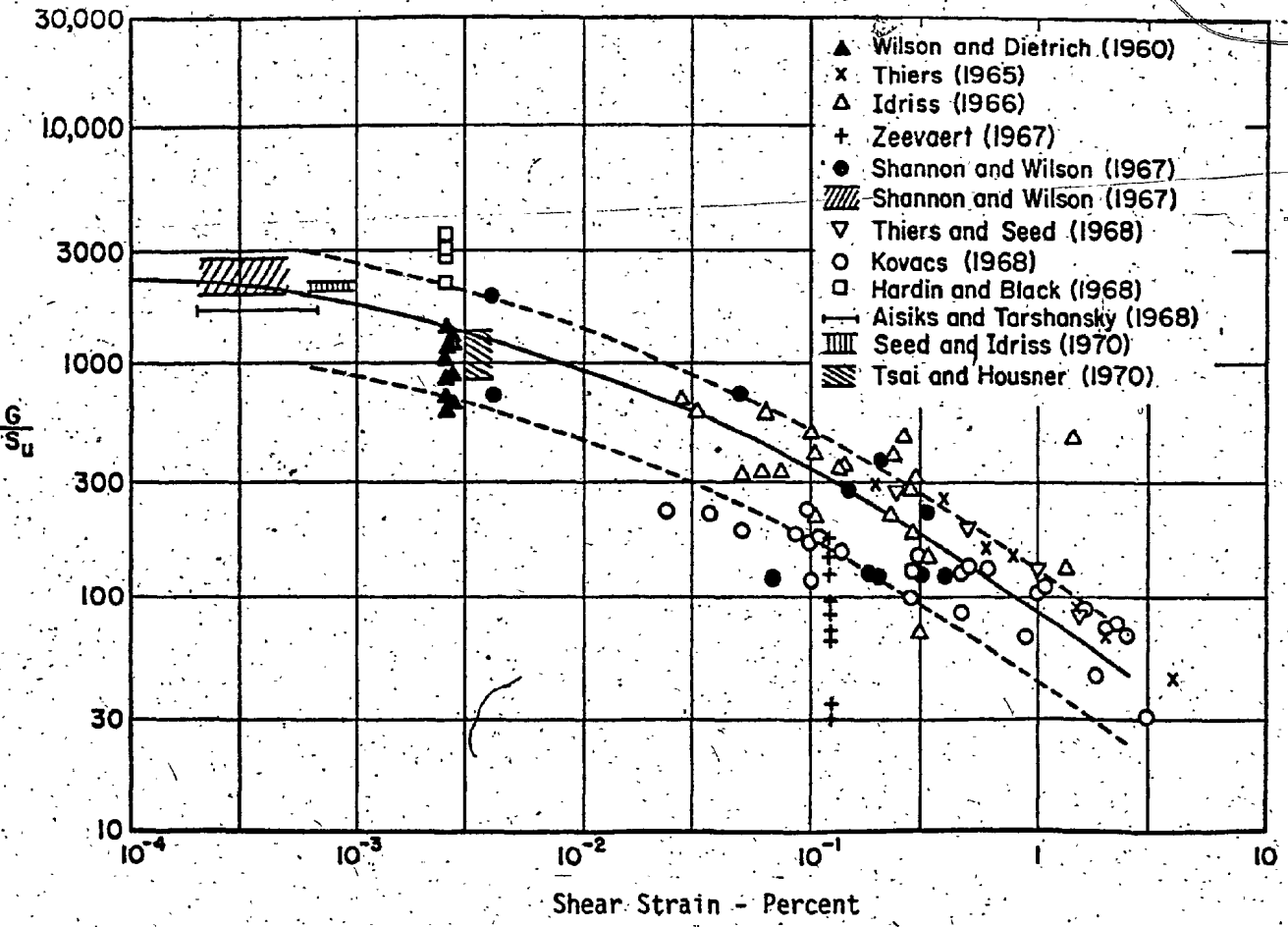

Fig. 10. In-Situ Shear Moduli for Saturated Clays (Ref. 136).

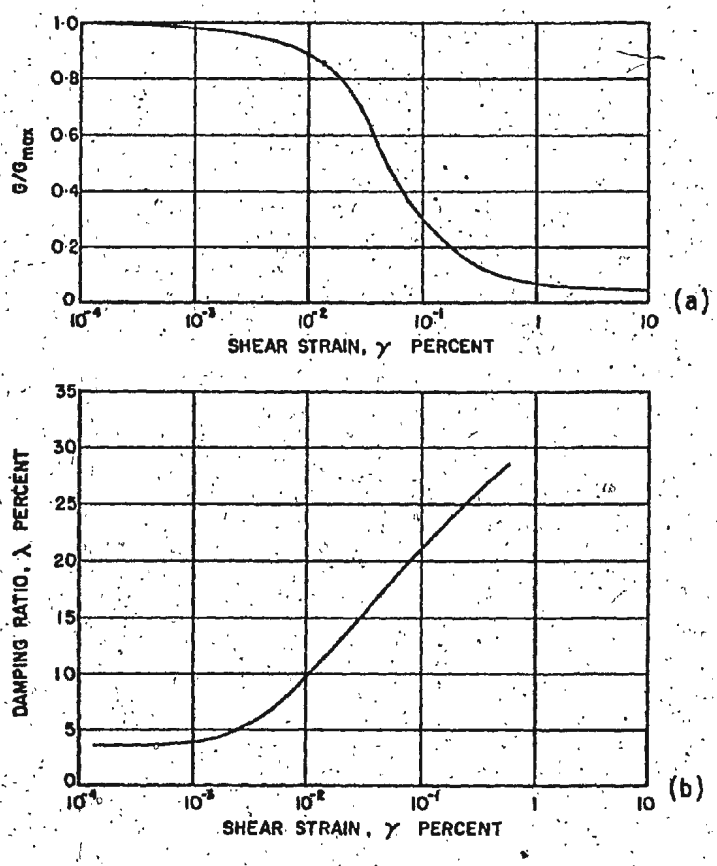

Fig. 11. (a) Example Relationship - Reduction in Modulus vs. Shear Strain, Clays, and (b) Example Relationship - Damping Ratio vs. Shear Strain, Clays (Ref. 60).

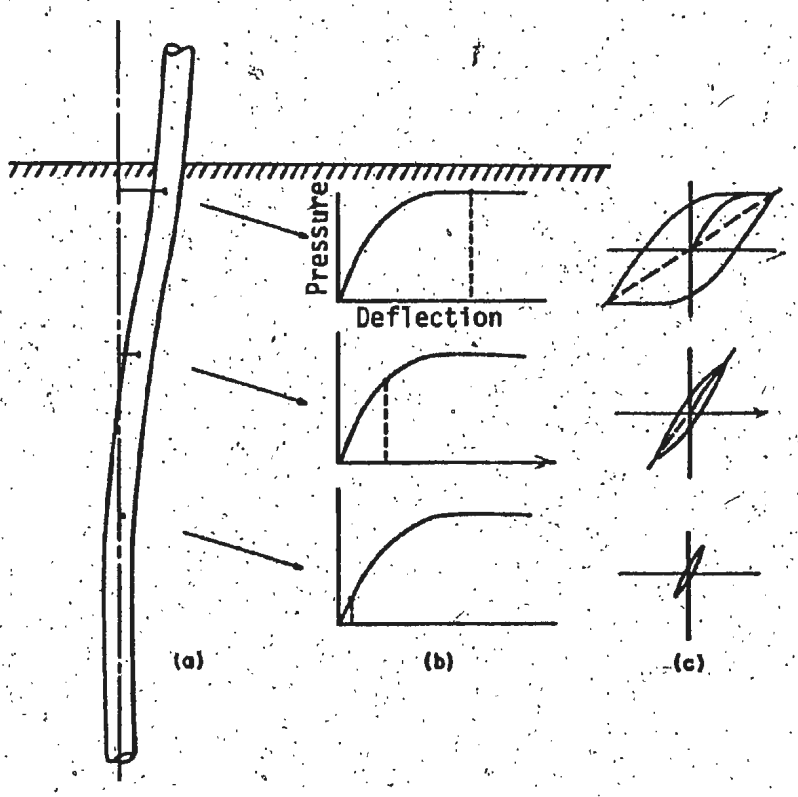

Fig. 12. Soil Structure Interaction for Laterally-Loaded Pile: (a) Pile Displacement, (b) Lateral Pressure vs. Deflection for First Loading, and (c) Lateral Pressure vs. Deflection for Reversed Loading (Ref. 127).

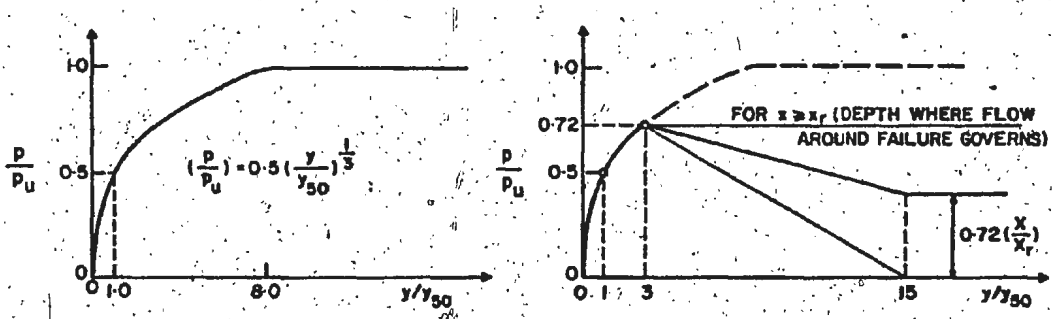

Fig. 13(a). Matlock's Criteria for 'p-y' Curves in Soft Clays (Ref. 100).

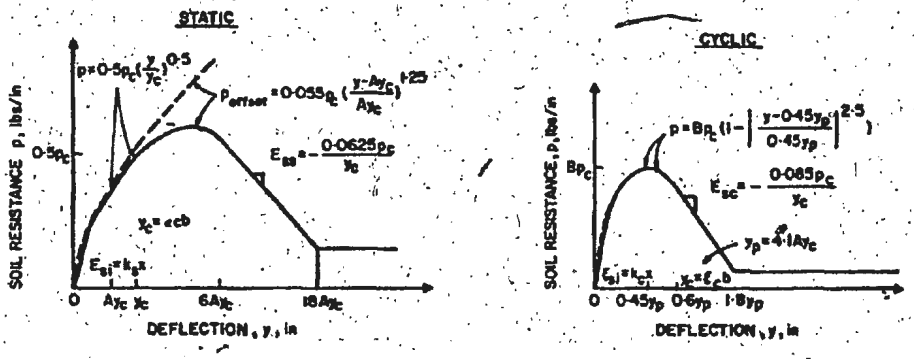

Fig. 13(b). Reese's Criteria for 'p-y' Curves in Stiff Clays (Ref. 126).

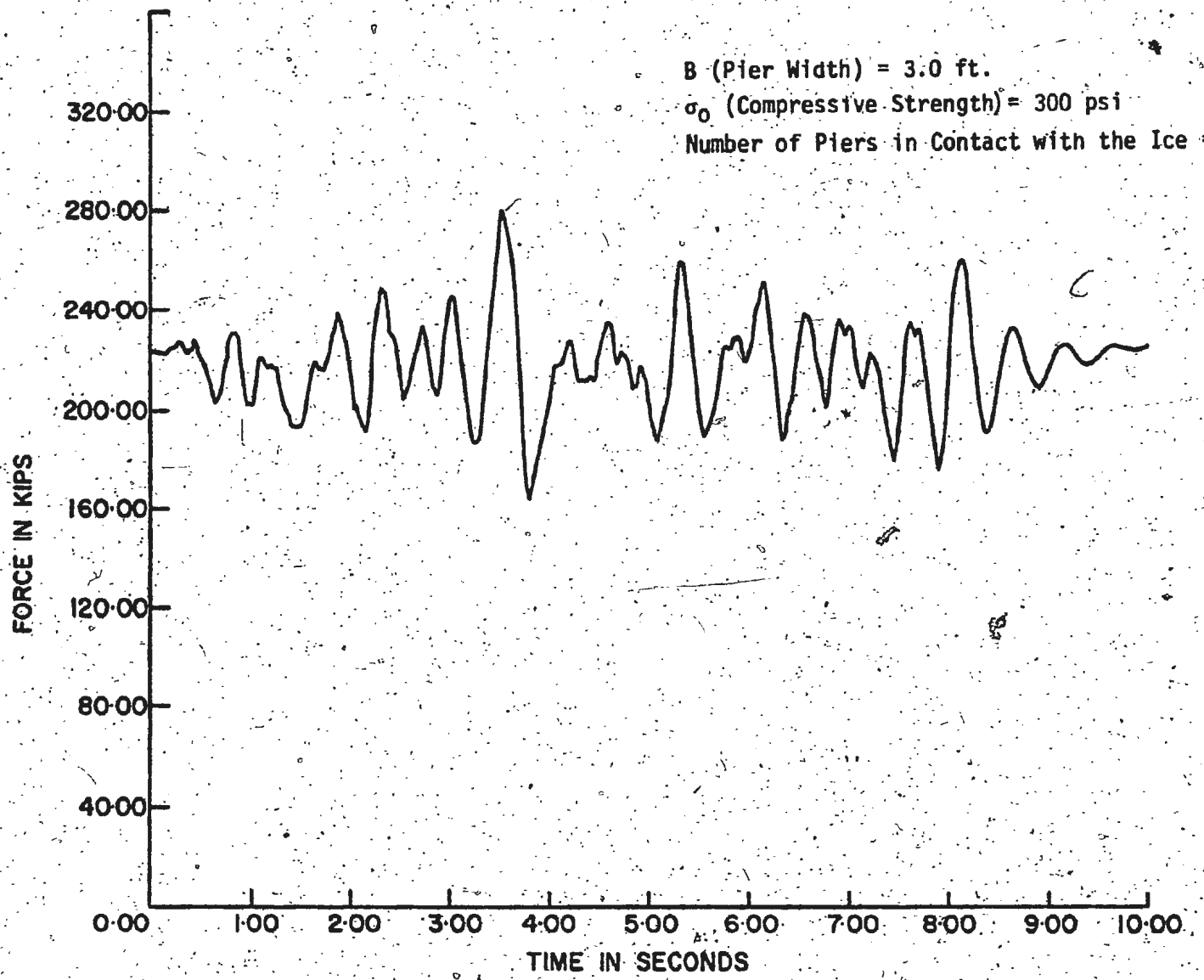

Fig. 14. Typical Artificially-Generated Ice-Force Records (Force vs. Time).

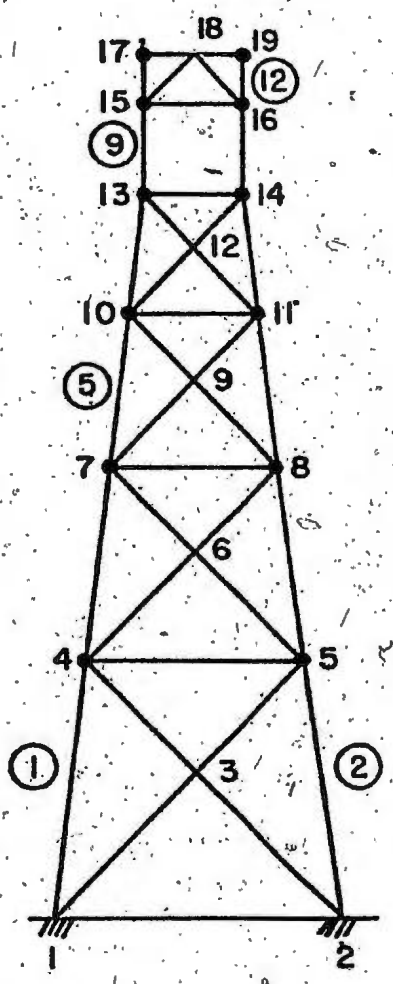

NODAL POINTS: 4,5, · · ·

ELEMENT NUMBER: ①, ②, · ·

Fig. 15(a). Fixed Base Model.

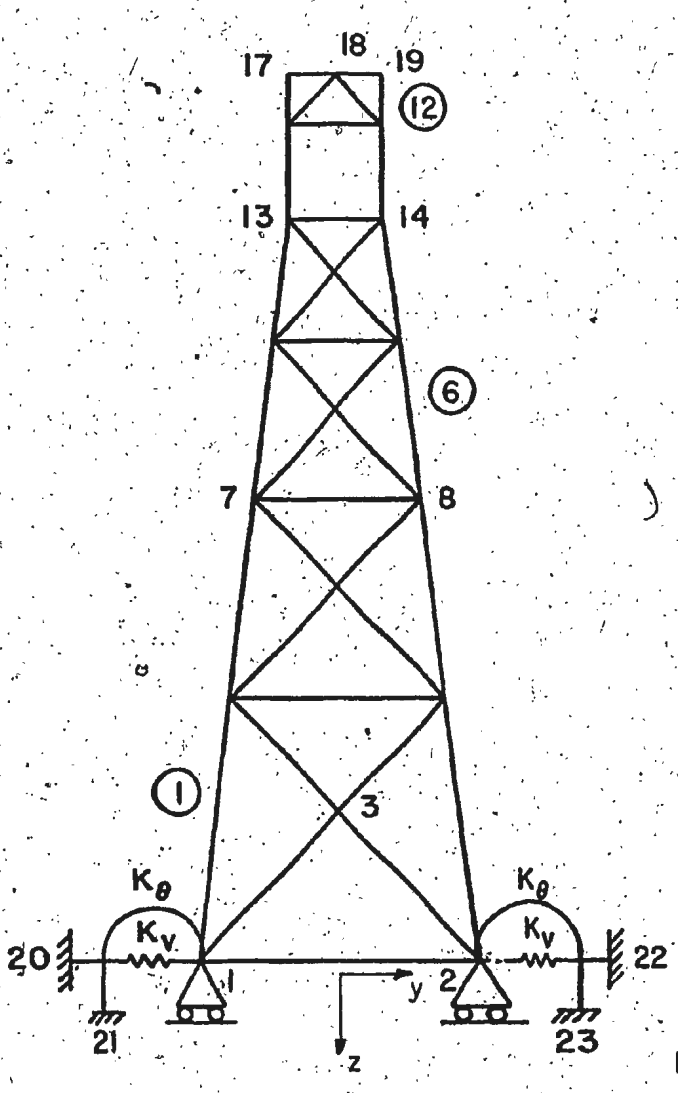

NODAL POINTS: 1, 2, · · ·
ELEMENT NO: (1), (6), · ·

K_θ = ROTATIONAL SPRING
K_v = HORIZONTAL SPRING

Fig. 15(b). Lumped Parameter Foundation Model.

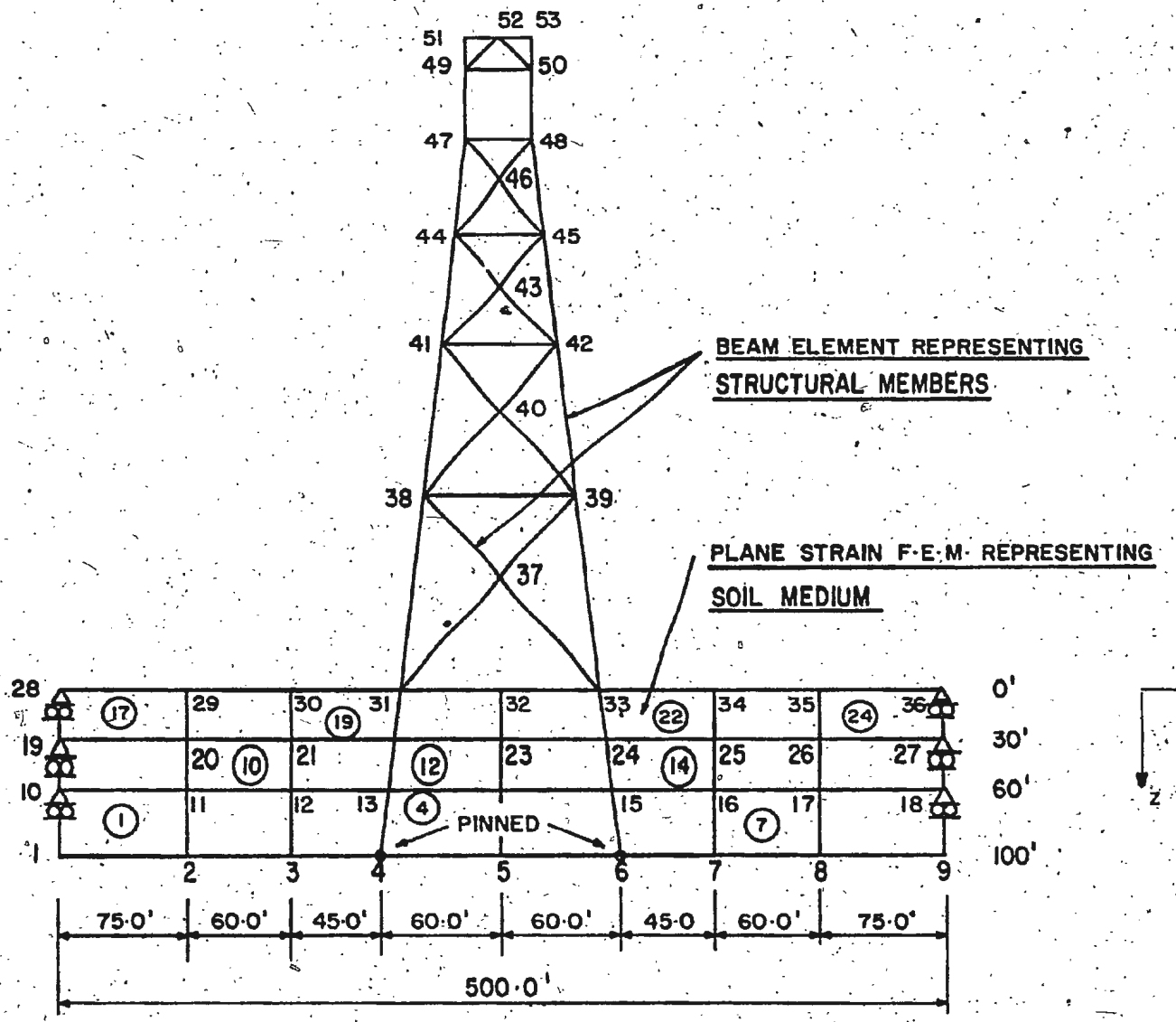

Fig. 15(c). Finite Elemented Foundation Model.

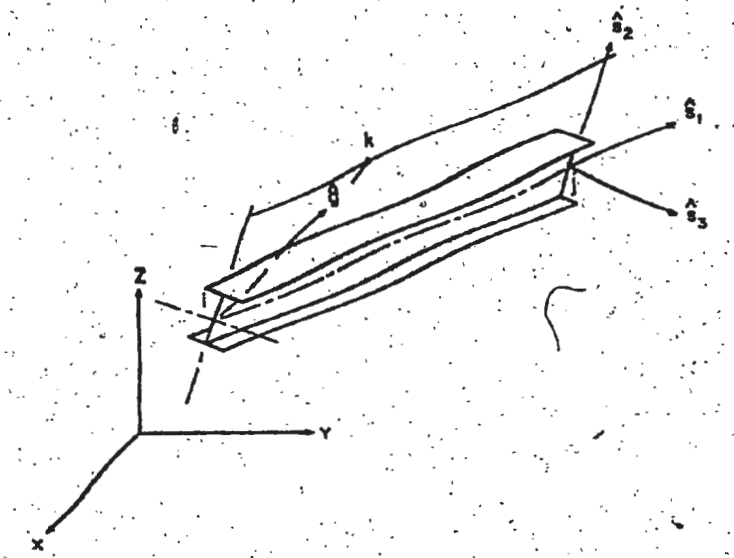

Fig. 16(a). Three-Dimensional Beam Element (Ref. 159).

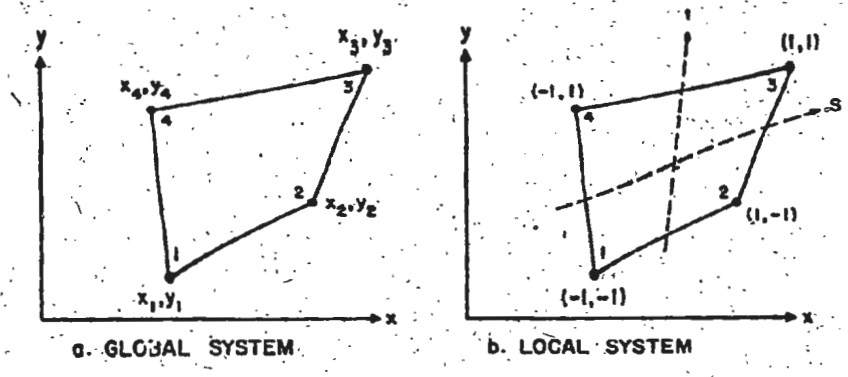

Fig. 16(b). Two-Dimensional Isoparametric Element (Ref. 159).

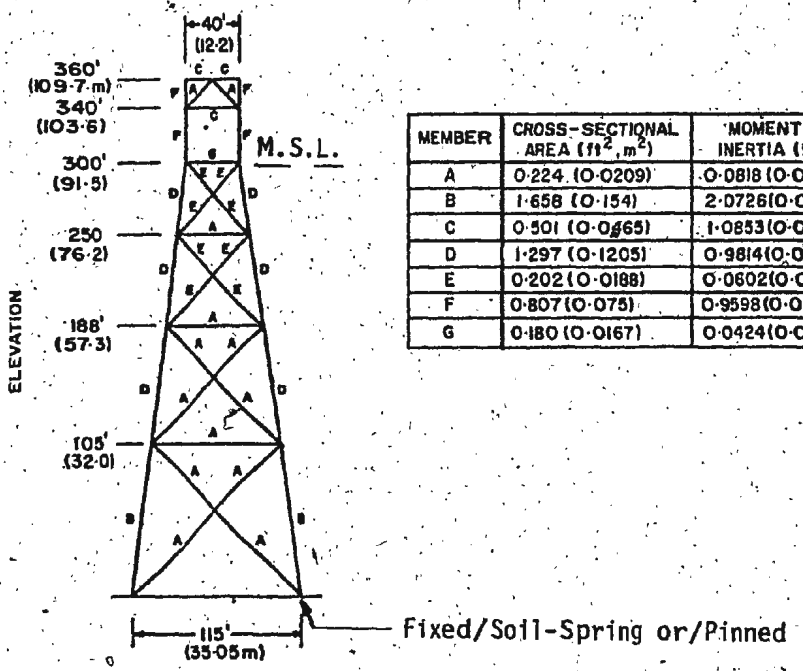

MEMBER	CROSS-SECTIONAL AREA (ft^2, m^2)	MOMENT OF INERTIA (ft^4, m^4)
A	0·224 (0·0209)	0·0818 (0·00071)
B	1·658 (0·154)	2·0726 (0·01788)
C	0·501 (0·0465)	1·0853 (0·00937)
D	1·297 (0·1205)	0·9814 (0·00847)
E	0·202 (0·0188)	0·0602 (0·00052)
F	0·807 (0·075)	0·9598 (0·00828)
G	0·180 (0·0167)	0·0424 (0·00037)

Fig. 17. Two-Dimensional Representation of the Tower-Structural Dimensions and Member Properties (Ref. 25).

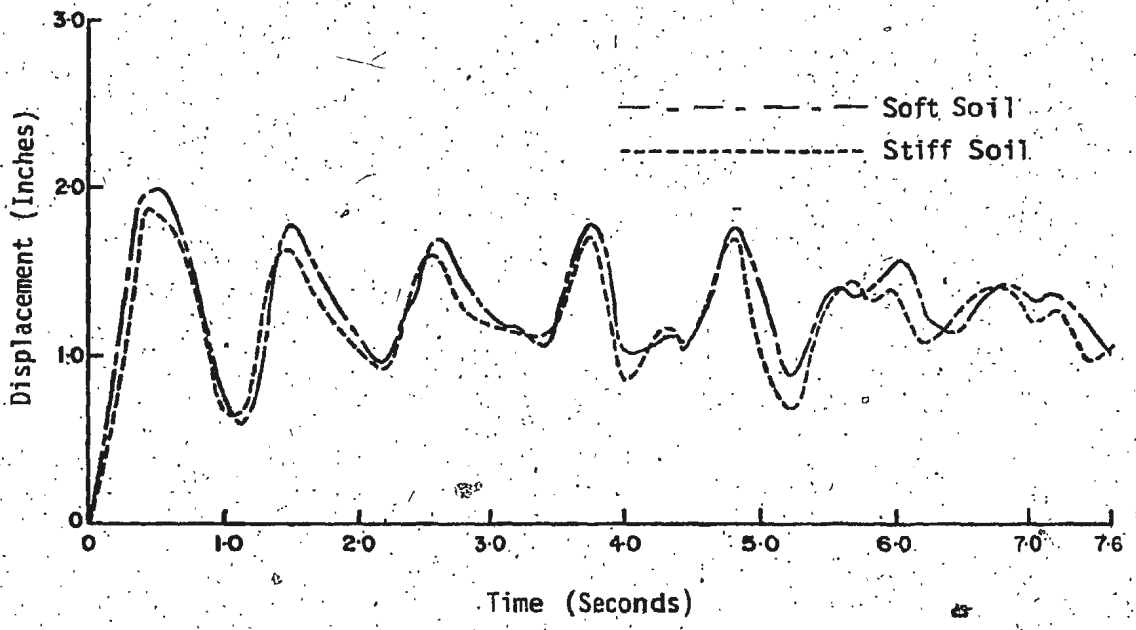

Fig. 18. Time-History for Horizontal Displacements at Node 47 - Finite Elemented Foundation Model with Linear Soil Behaviour.

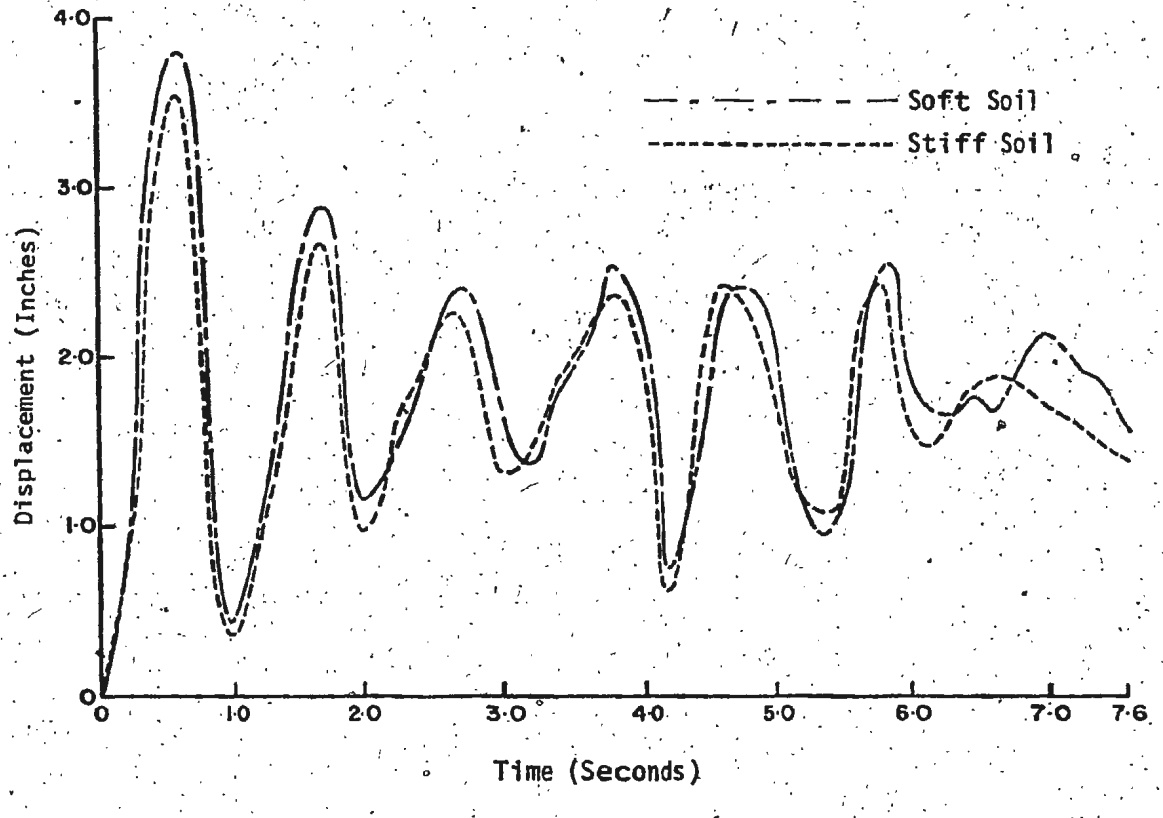

Fig. 19. Time-History for Horizontal Displacements at Node 49 - Finite Elemented Foundation Model with Linear Soil Behaviour.

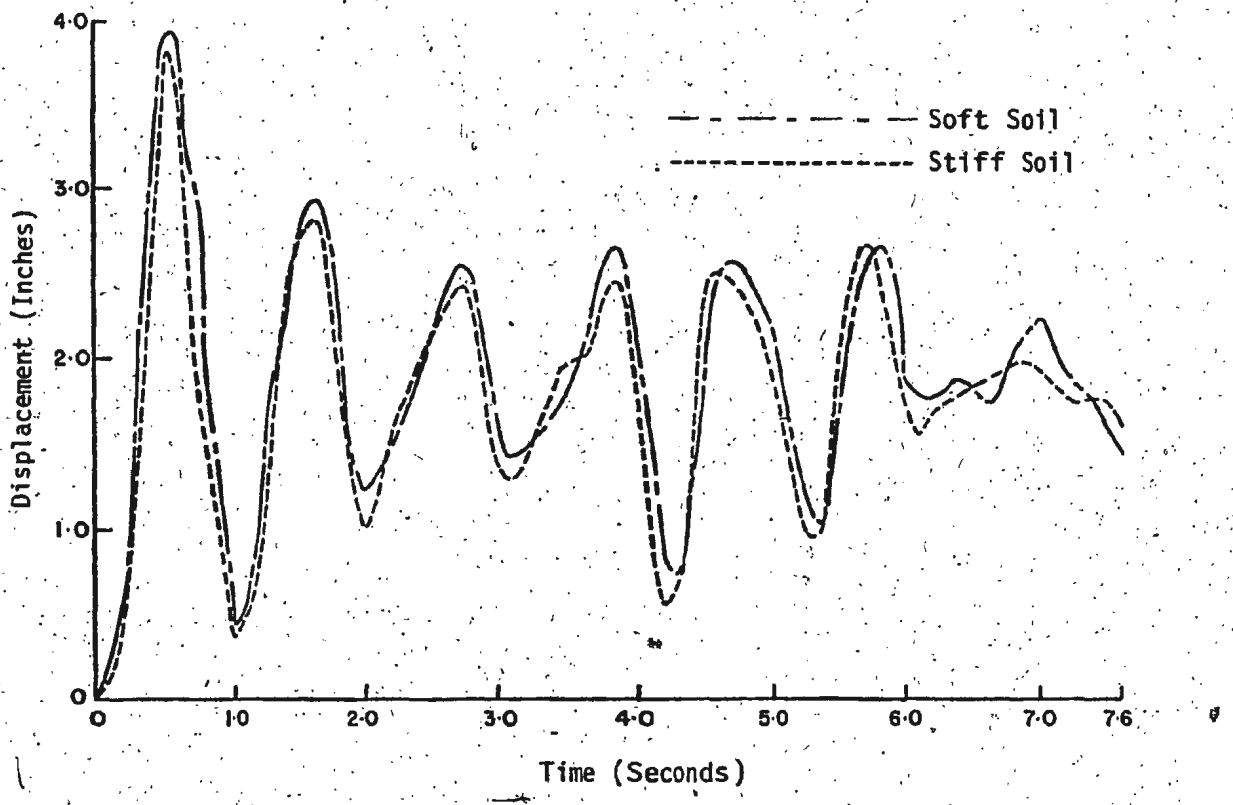

Fig. 20. Time-History for Horizontal Displacements at Node 51 - Finite Elemented Foundation Model with Linear Soil Behaviour.

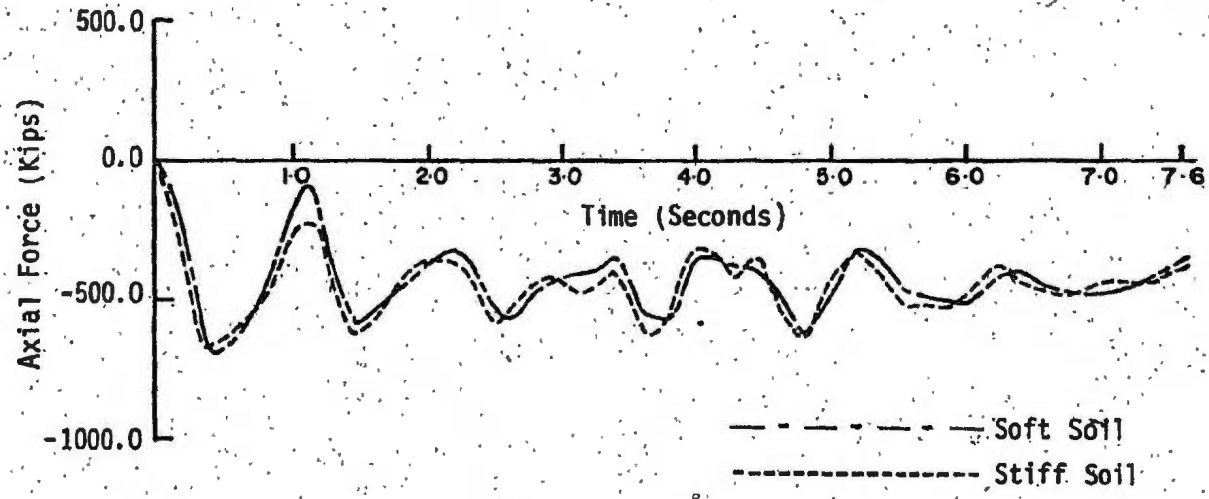

Fig. 21. Time-History for Axial Force in Member 7 at Node 31 - Finite Elemented Foundation Model with Linear Soil Behaviour.

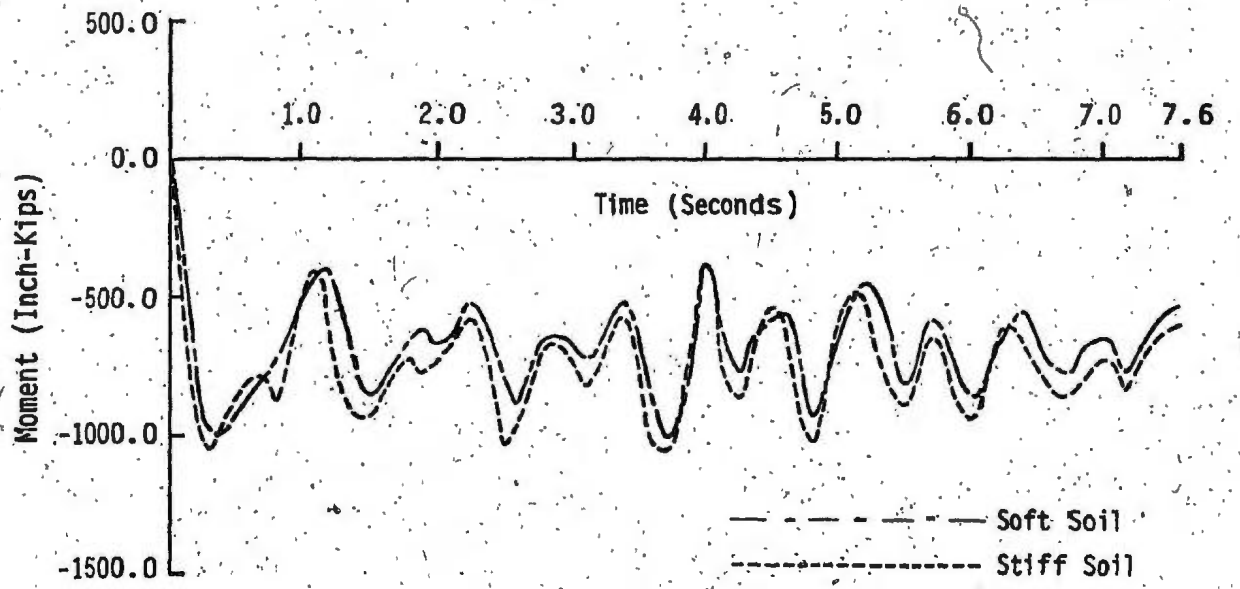

Fig. 22. Time-History for Bending Moment in Member 7 at Node 31 - Finite Elemented Foundation Model with Linear Soil Behaviour.

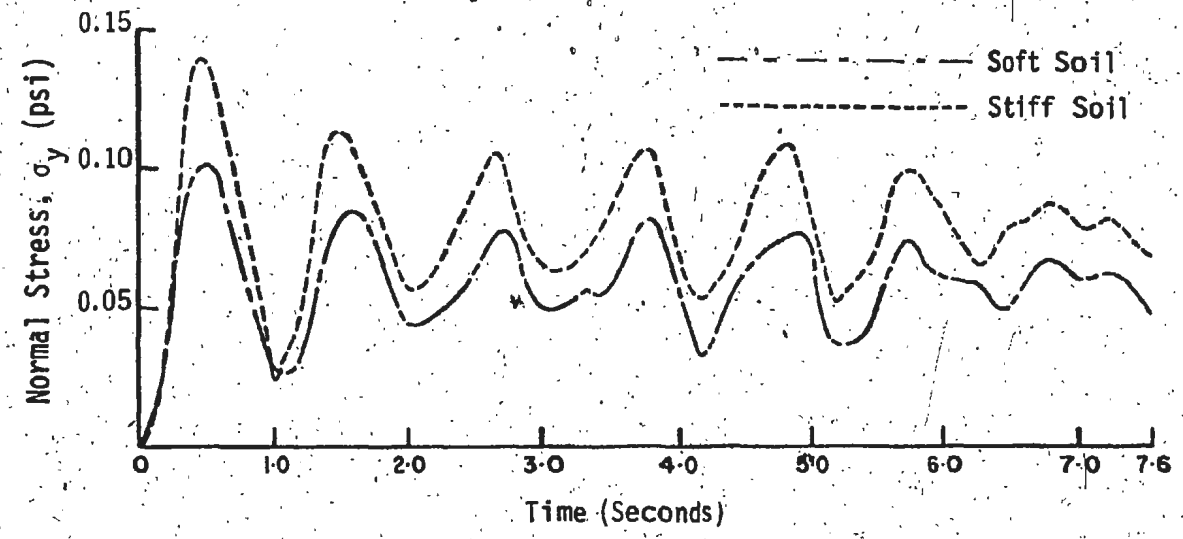

Fig. 23. Time-History for Normal Stresses (σ_y) in Soil Element No. 20 - Finite Elemented Foundation Model with Linear Soil Behaviour.

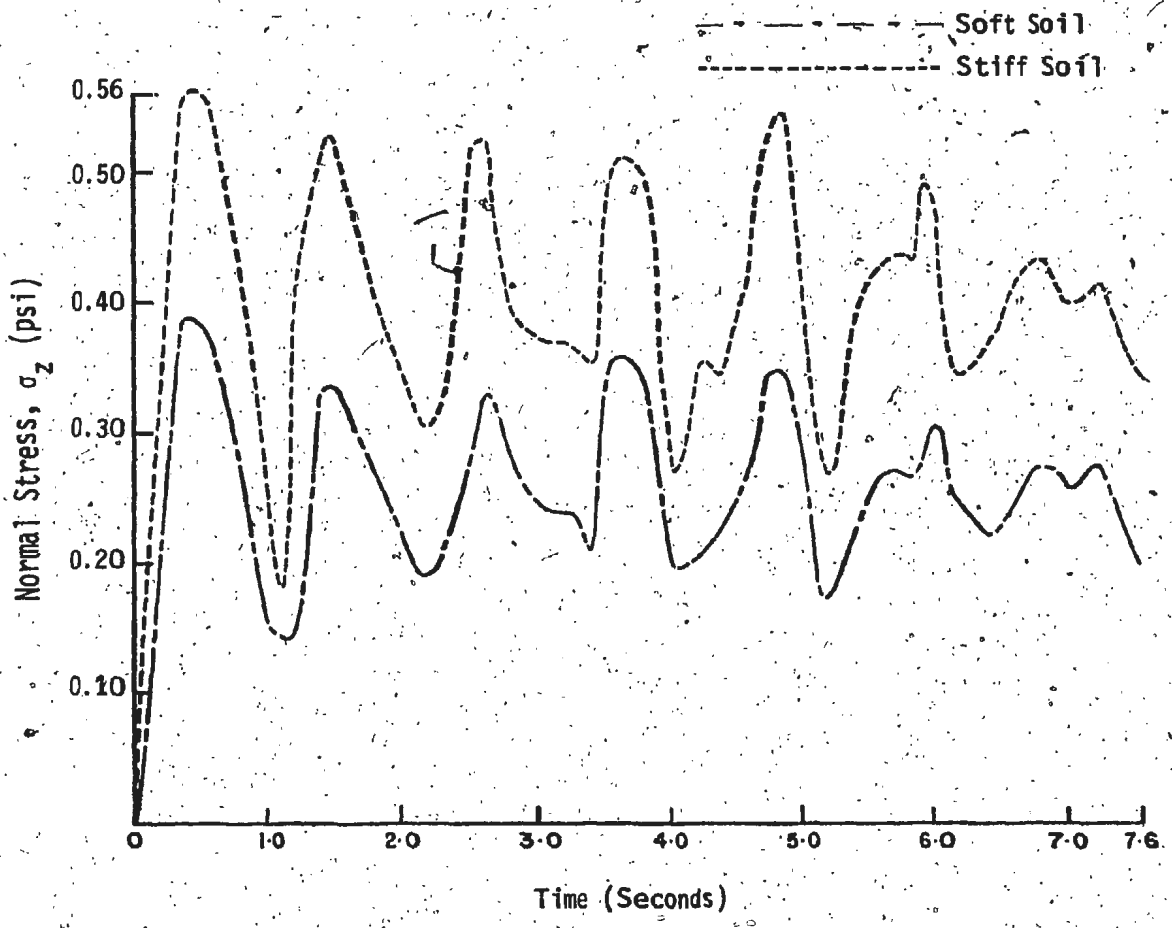

Fig. 24. Time-History for Normal Stresses (σ_z) in Soil Element No. 20 - Finite Elemented Foundation Model with Linear Soil Behaviour.

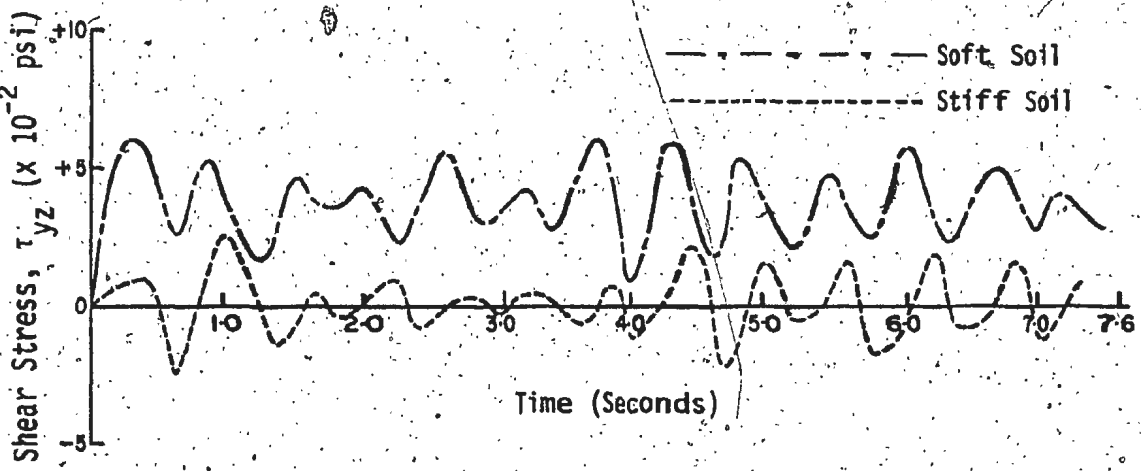

Fig. 25. Time-History for Shear Stresses (τ_{yz}) in Soil Element No. 20 - Finite Elemented Foundation Model with Linear Soil Behaviour.

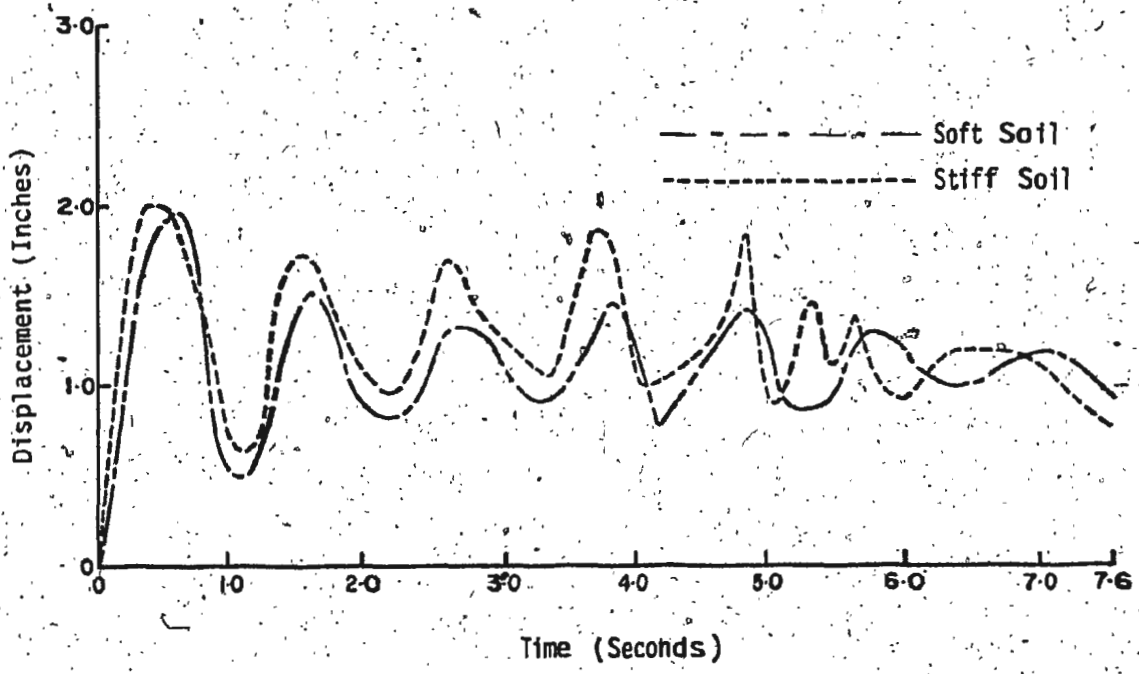

Fig. 26. Time-History for Horizontal Displacements at Node 47 - Finite Elemented Foundation Model with Nonlinear Soil Behaviour.

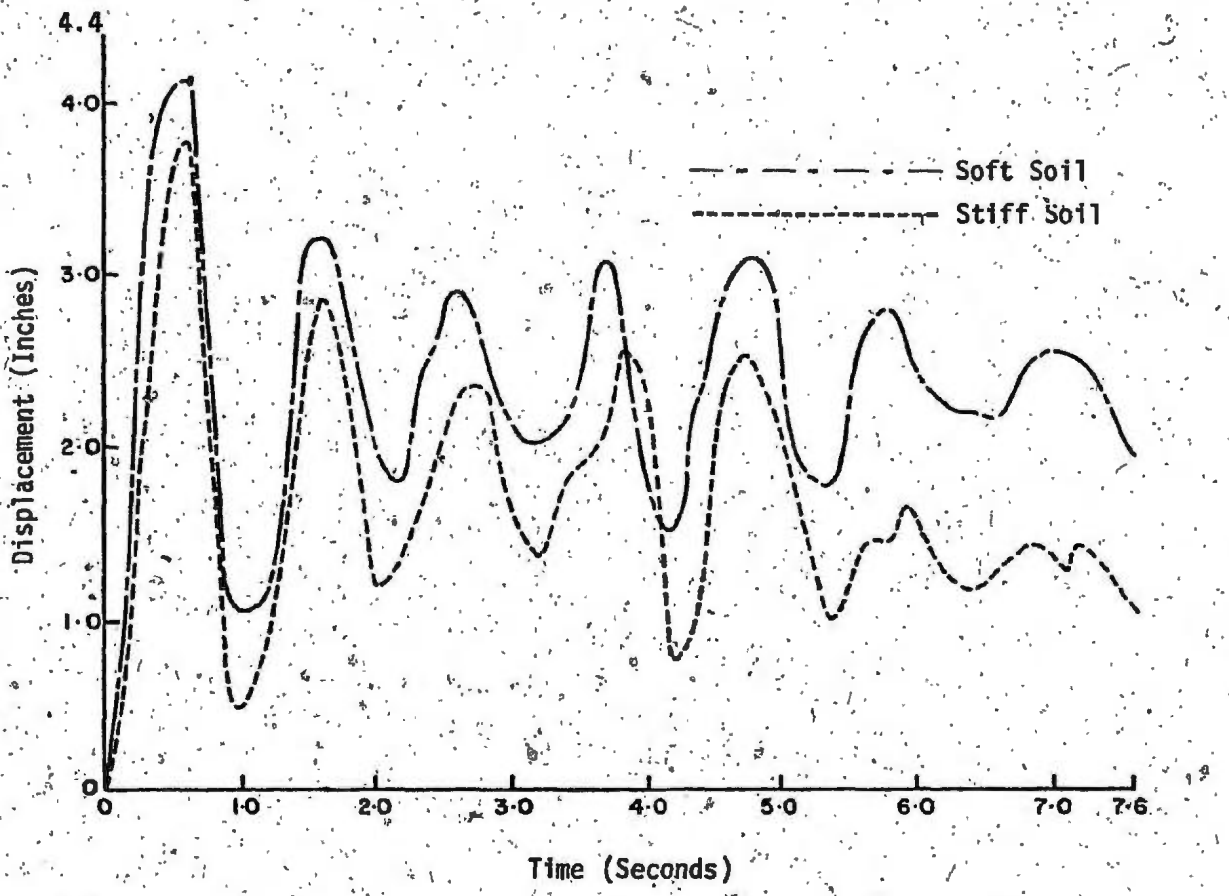

Fig. 27. Time-History for Horizontal Displacements at Node 49 - Finite Elemented Foundation Model with Nonlinear Soil Behaviour.

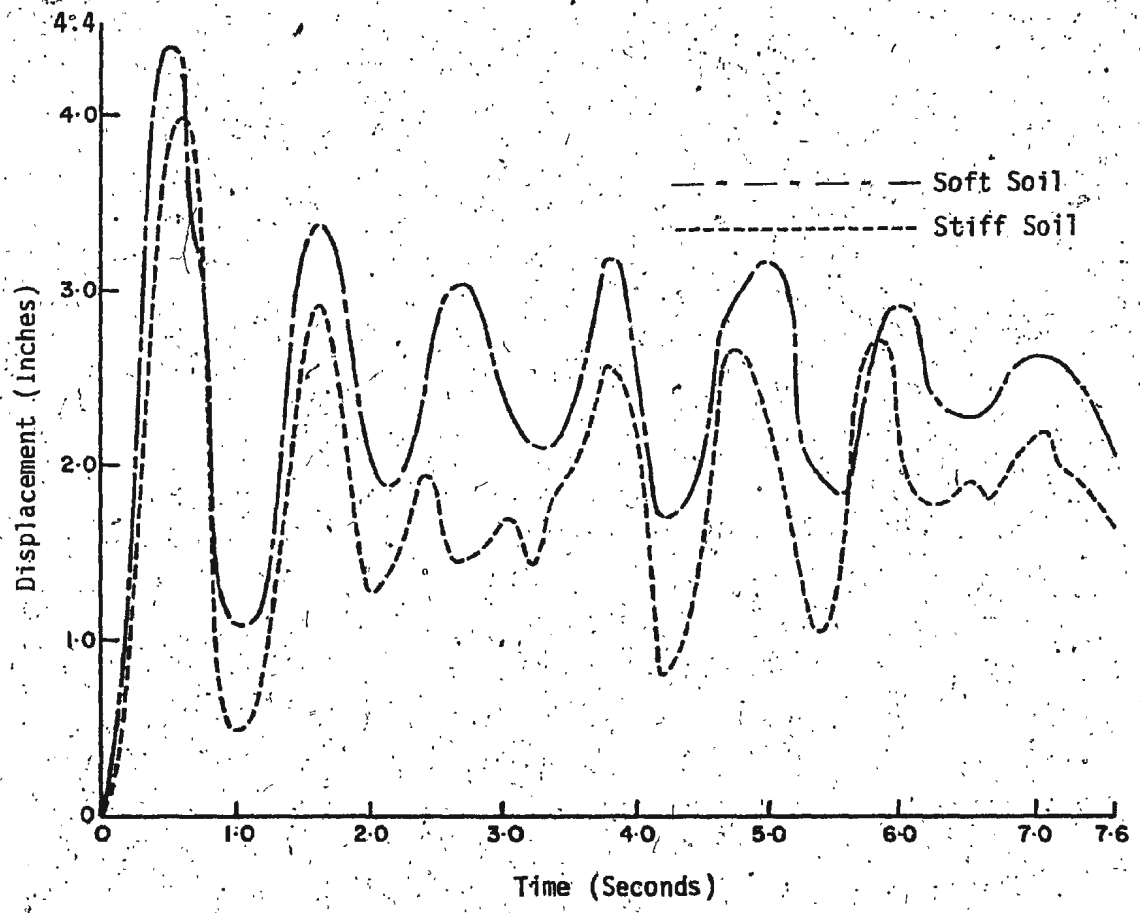

Fig. 28. Time-History for Horizontal Displacements at Node 51 - Finite Elemented Foundation Model with Nonlinear Soil Behaviour.

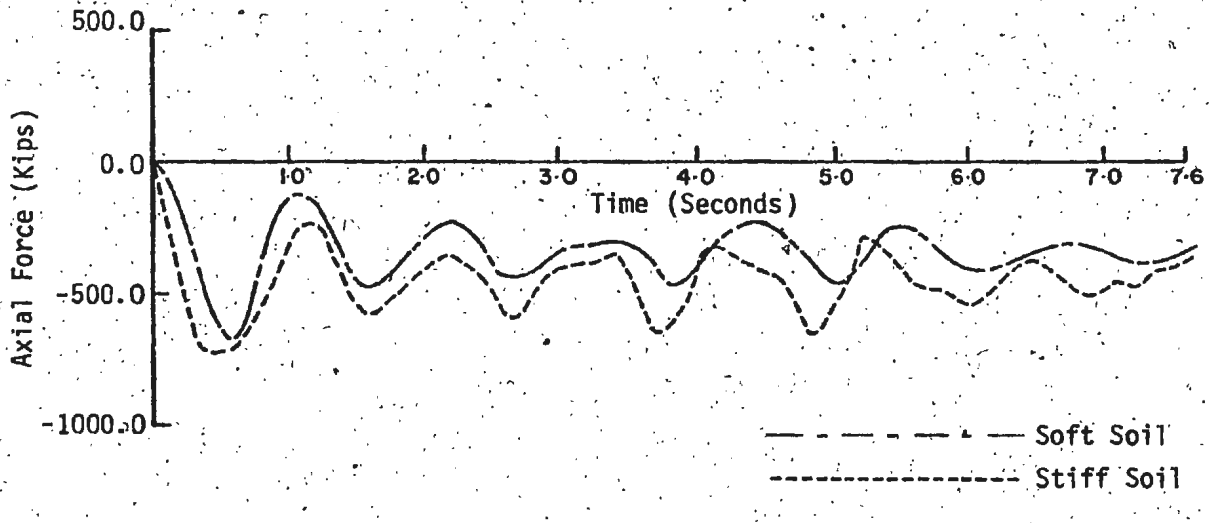

Fig. 29. Time-History for Axial Force in Member 7 at Node 31 - Finite Elemented Foundation Model with Nonlinear Soil Behaviour.

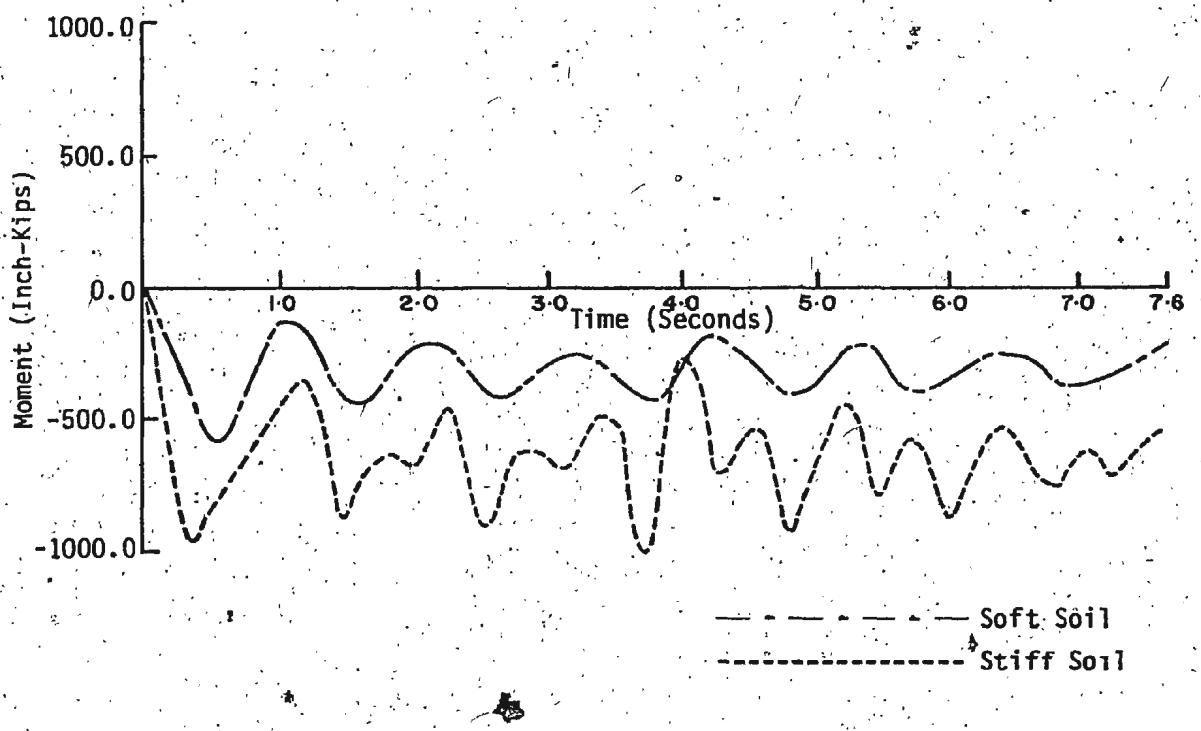

Fig. 30. Time-History for Bending Moment in Member 7 at Node 31 - Finite Elemented Foundation Model with Nonlinear Soil Behaviour.

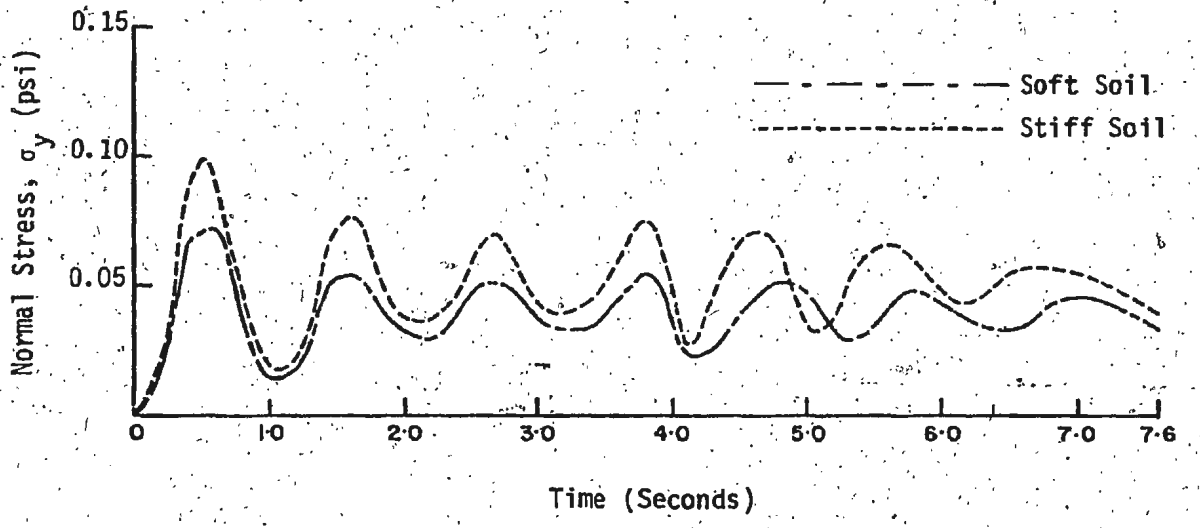

Fig. 31. Time-History for Normal Stresses (σ_y) in Soil Element No. 20 - Finite Elemented Foundation Model with Nonlinear Soil Behaviour.

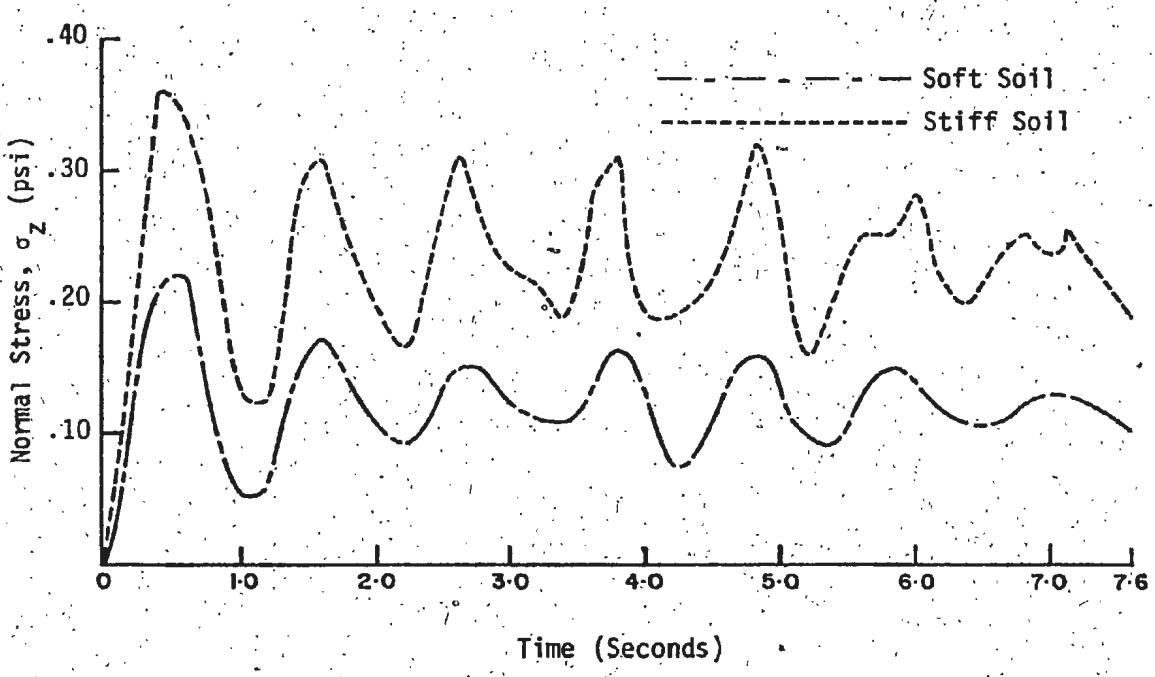

Fig. 32. Time-History for Normal Stresses (σ_z) in Soil Element No. 20 - Finite Elemented Foundation Model with Nonlinear Soil Behaviour.

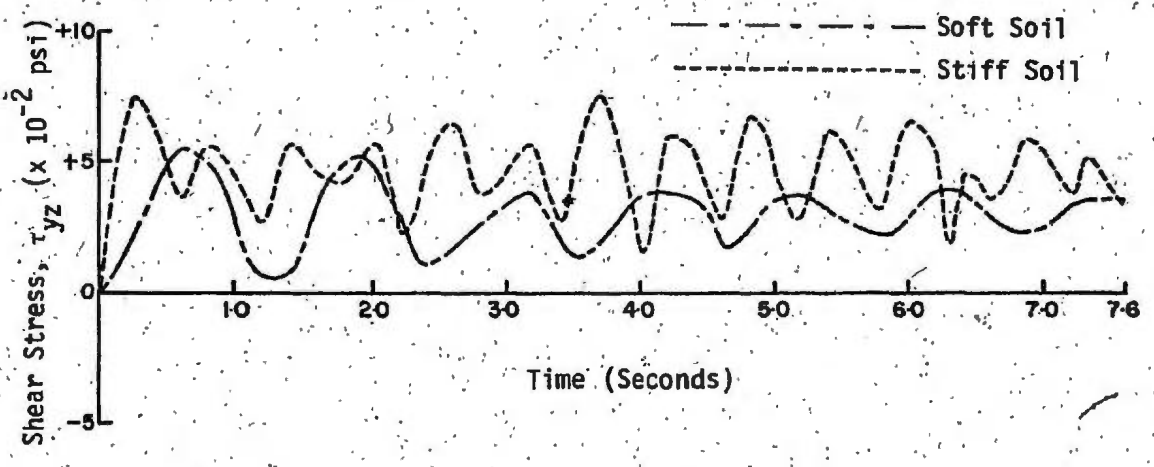

Fig. 33. Time-History for Shear Stresses (τ_{yz}) in Soil Element No. 20 - Finite Elemented Foundation Model with Nonlinear Soil Behaviour.

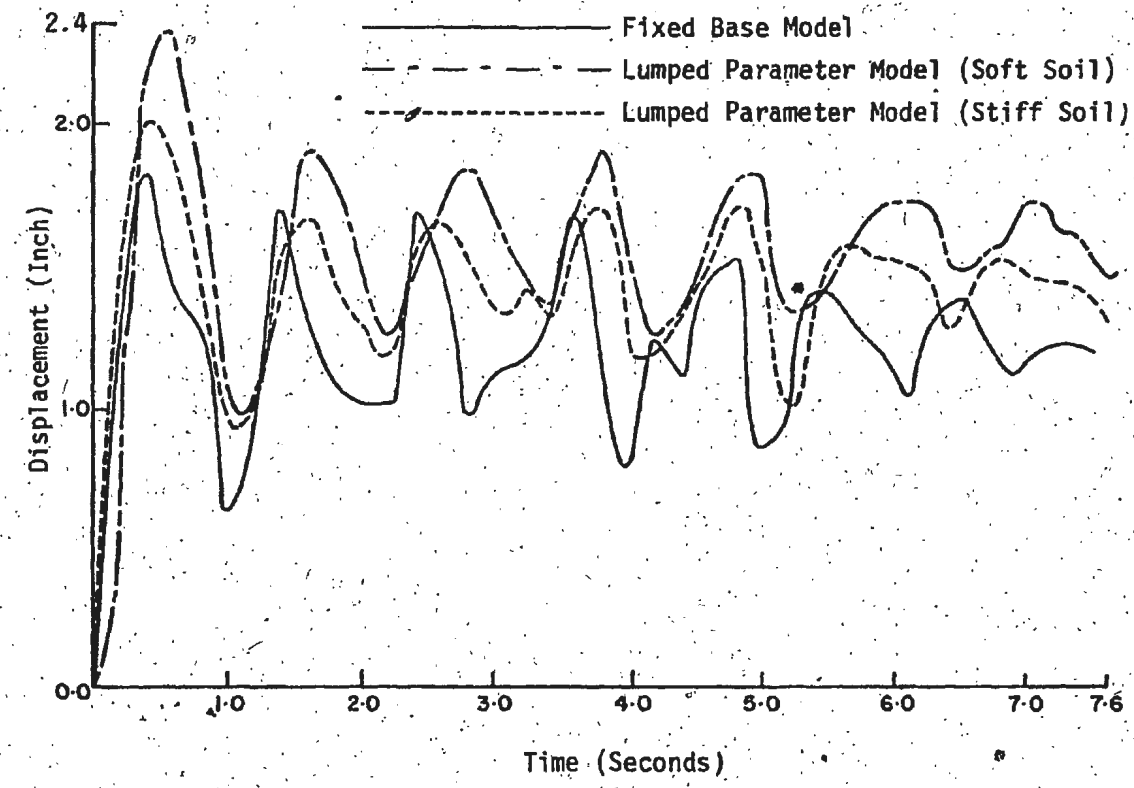

Fig. 34. Time-History for Horizontal Displacements at Node No. 13.

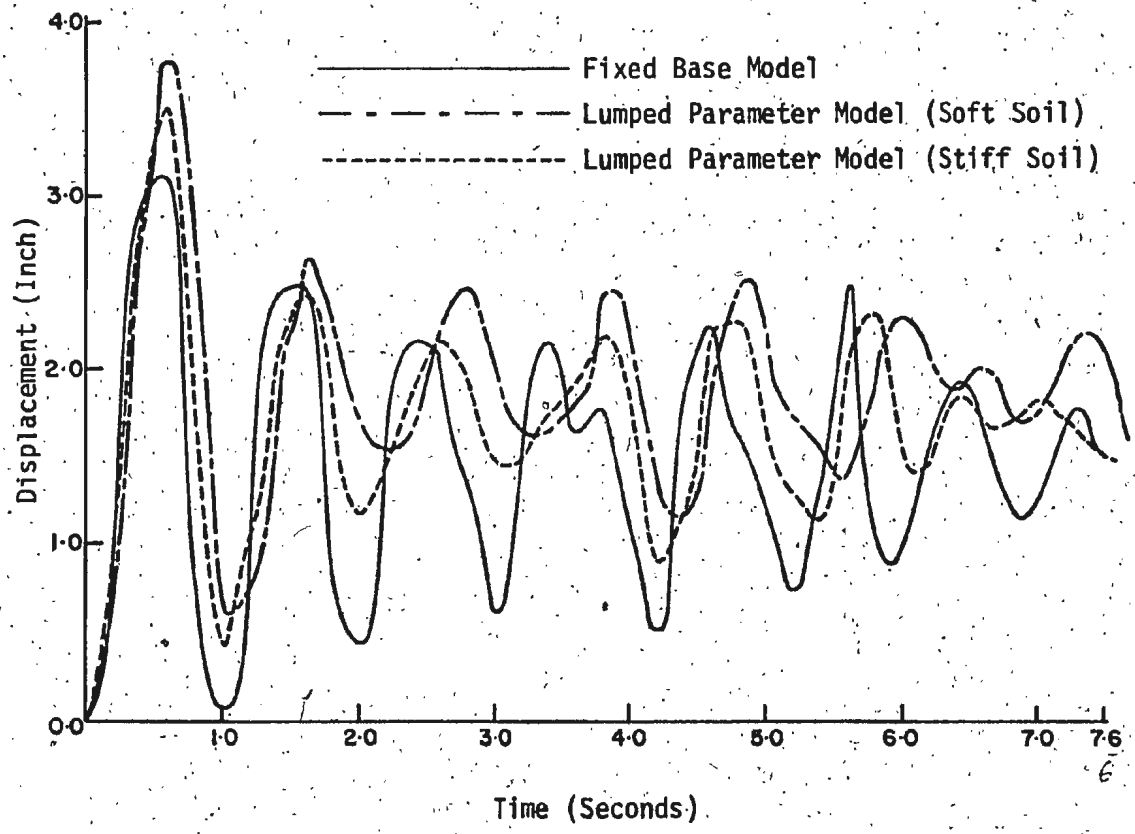

Fig. 35. Time-History for Horizontal Displacements at Node No. 15.

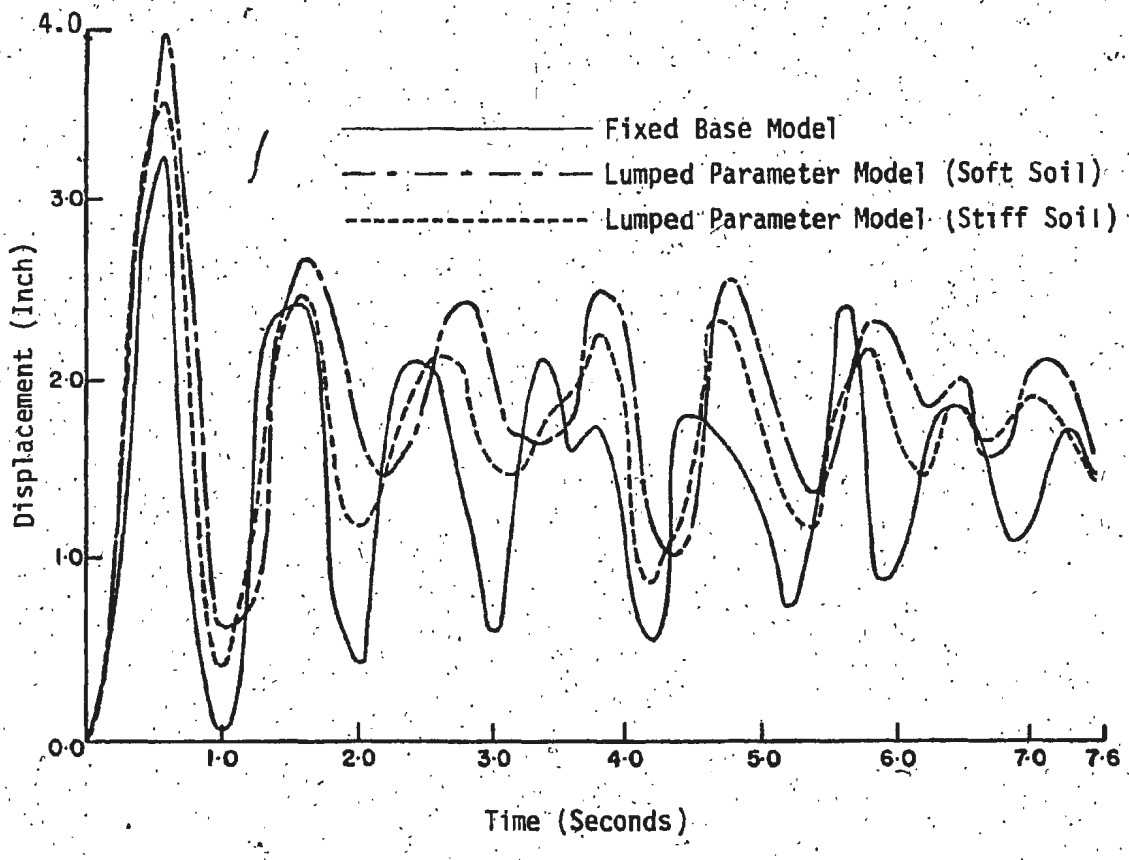

Fig. 36. Time-History for Horizontal Displacements at Node No. 17.

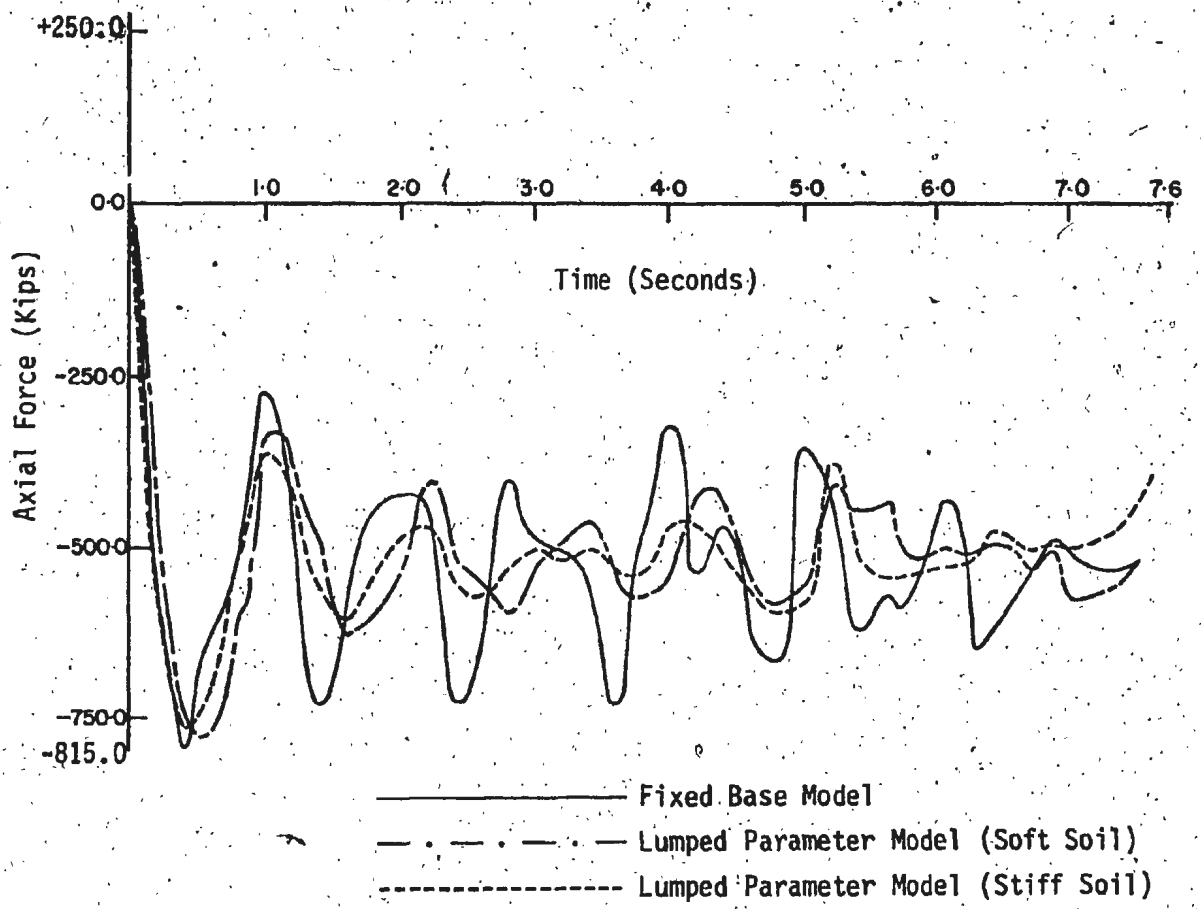

Fig. 37. Time-History for Axial Forces in Member 1 at Node 1.

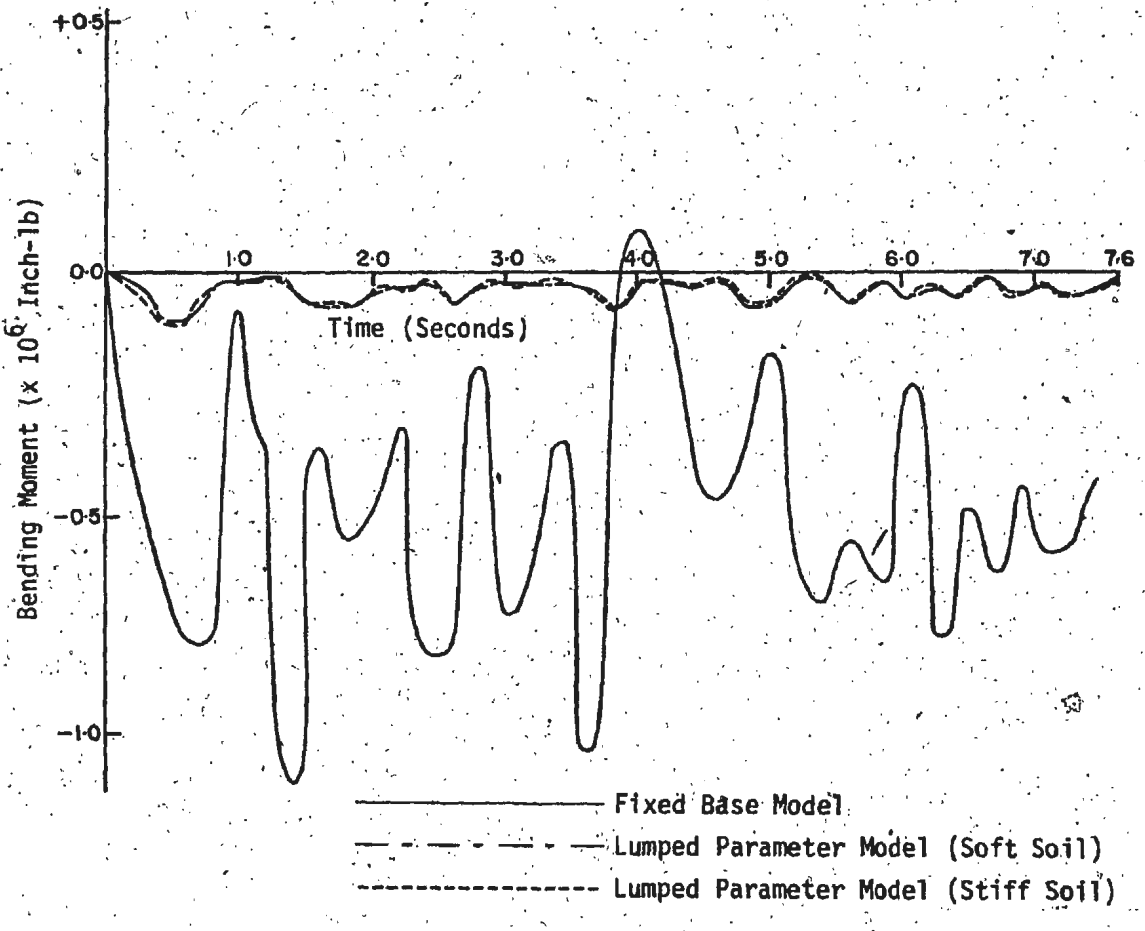

Fig. 38. Time-History for Bending Moment in Member 1 at Node 1.

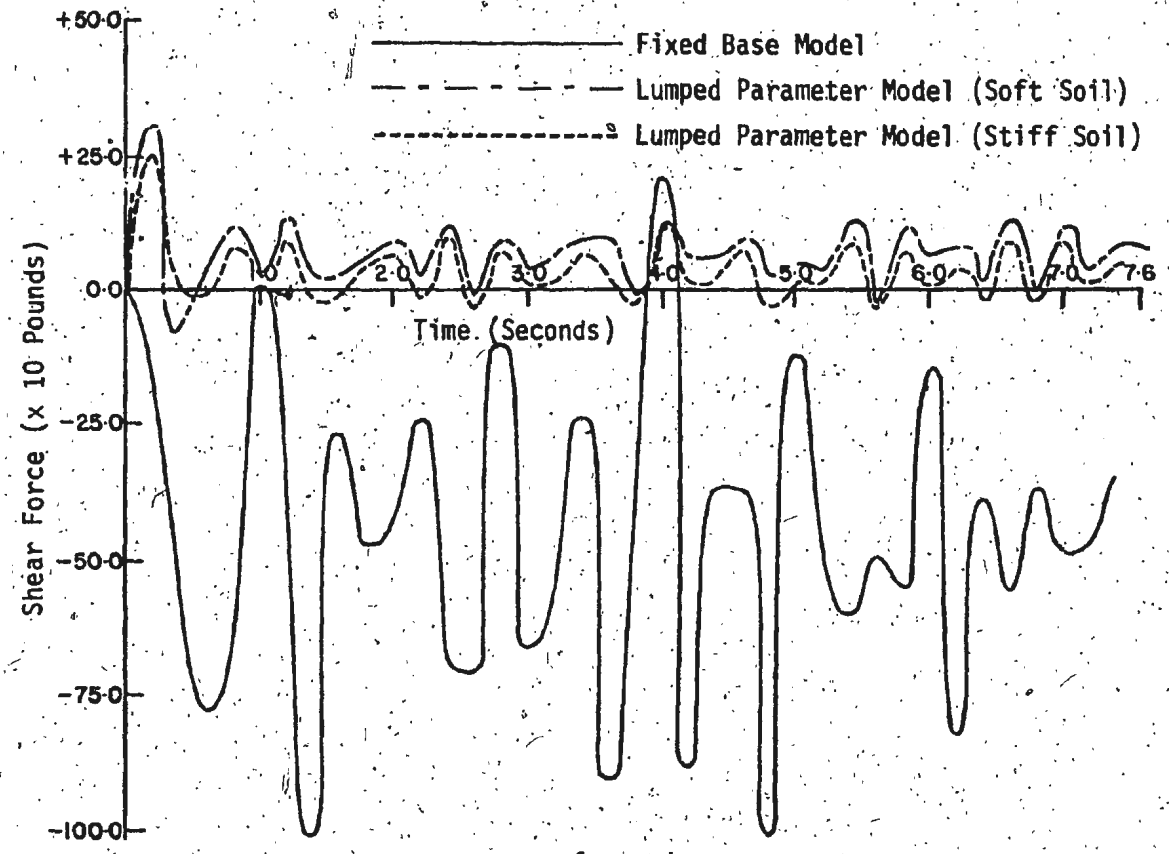

Fig. 39. Time-History for Shear Forces in Member 1 at Node 1.

BIBLIOGRAPHY

1. Afanas'ev, V. P., 1973. Ice Pressure on Vertical Structures. Technical Translations 1708, National Research Council, Ottawa, Canada, 6 pp.

2. Agarwal, S. L., 1973. Discrete Element Analysis and Its Experimental Verification of Vertical Piles under Dynamic Lateral Loads. Proc. Eighth International Conference on Soil Mechanics and Foundation Engineering, Vol. 2, pp. 9-12.

3. American Petroleum Institute, New York, 1971. API Recommended Practice for 'Planning, Designing, and Construction - Fixed Offshore Platforms'.

4. Anderson, R. H., Bartholomew, R. J., and Wong, S. Y., 1967. Fixed Offshore Platform Design Analysis. Unpublished Report, Mechanics Research Inc., 650 North Sepulveda Blvd., El Segundo, California, 33 p.

5. Aschenbrenner, R., 1967. Three-Dimensional Analysis of Pile Foundation. Proc. ASCE, Journal of Structural Division, Vol. 93, No. ST1, Paper No. 5097, February, pp. 201-219.

6. Awoshika, K. and Reese, L. C., 1971. Analysis of Foundation with Widely Spaced Batter Piles. Research Report No. 117-3F. Centre for Highway Research, The University of Texas at Austin, Austin, Texas, February.

7. Barkan, D. D., 1960. Dynamics of Bases and Foundations. Translated from Russian by I. Drashevska, McGraw-Hill Book Co. Inc., New York, 434 p.

8. Bathe, K. J. and Wilson, E. L., 1973. Stability and Accuracy Analysis of Direct Integration Methods. International Journal of Earthquake Engineering and Structural Dynamics, Vol. 1, No. 2.

9. Bergdahl, L. L., 1972. Two Lighthouses Damaged by Ice. Proc. IAHR Ice Symp. and Its Action on Hydraulic Structures, Leningrad, U.S.S.R., pp. 234-238.

10. Bielak, J. and Jennings, P. C., 1973. Dynamics of Building-Soil Interaction. Bulletin of the Seismological Society of America, Vol. 63, pp. 9-48.

11. Billington, D. P., Gaither, W. S., and Ebner, A. H., 1966. Analysis of Four-Legged Tower for Dynamic Load. Proc. ACSE, Journal of Engineering Mechanics Division, Vol. 92, No. EM2, Paper No. 4769, April, pp. 61-73.

12. Blenkarn, K. A. and Knapp, A. E., 1969. Ice Conditions on the Grand Banks. Ice Seminar Sponsored by Petroleum Society of Canadian Institute of Mining and Metallurgy and the American Petroleum Institute, Calgary, Alberta, Canada, 61-72.

13. Blenkarn, K. A., 1970. Measurement and Analysis of Ice Forces on Cook Inlet Structures. Proc. Offshore Technology Conference (OTC), Houston, Texas, Vol. 2, pp. 365-378.

14. Blumberg, R. and Strader, N. R. II, 1969. Dynamic Analysis of Offshore Structures. Proc. Offshore Technology Conference (OTC), Houston, Texas, Vol. 1, Paper No. OTC 1009, pp. 107-126.

15. Botea, E., Manoliu, I., and Abrameseu, T., 1973. Large Diameter Piles under Axial and Lateral Loads. Proc. Eighth International Conference on Soil Mechanics and Foundation Engineering, Vol. 2, pp. 27-33.

16. Brod, J., Fowler, J. N., and Boston, L. A., 1975. A Unified Technique for the Analysis of Structure Soil-Pile Systems. Proc. Offshore Technology Conference (OTC), Houston, Texas, Vol. 2, Paper No. OTC 2262, pp. 199-208.

17. Broms, B. B., 1964. Lateral Resistance of Piles in Cohesive Soils. Proc. ASCE, Journal of the Soil Mechanics and Foundation Division, Vol. 90, No. SM2, Paper No. 3825, March, pp. 27-63.

18. Broms, B. B., 1964. Lateral Resistance of Piles in Cohesionless Soils. Proc. ASCE, Journal of Soil Mechanics and Foundation Division, Vol. 90, No. SM3, Paper No. 3909, May, pp. 123-156.

19. Bycroft, G. N., 1956. Forced Vibration of a Rigid Circular Plate on a Semi-Infinite Elastic Space and on an Elastic Stratum. Philosophical Transactions, Royal Society of London, Series A, No. 948, Vol. 248, January 5, pp. 327-368.

20. Carnahan, F., Zimmer, R. A., and Carnahan, F. L., 1975. Anchor Pile Design for Ocean Floor Environments using Finite Element Method. Proc. Offshore Technology Conference (OTC), Vol. 2, Paper No. OTC 2308, pp. 625-632.

21. Chan, J. H. C. and Matlock, H., 1973. A Discrete Element Method for Transverse Vibrations of Beam Columns Resting on Linearly Elastic or Inelastic Supports. Proc. Offshore Technology Conference (OTC), Houston, Texas, Vol. 2, Paper No. OTC 1841, pp. 205-218.

22. Chan, P. C. and Hirach, T. J., 1966. Soil Dynamics and Soil Rheology. Research Report No. 33-5, Texas Transportation Institute, Texas A & M University, June.

23. Clough, R. W., 1960. The Finite Element Method in Plane Stress Analysis. Proc. Second ASCE Conference on Electronic Computation, Pittsburgh.

24. Clough, R. and Penzien, J., 1975. Dynamics of Structures, McGraw-Hill Book Company Inc., New York.

25. Corotis, R. B. and Martin, C. H., 1975. Approximate Dynamic Modelling of an Offshore Tower, Preprint 2439, ASEC National Structural Engineering Convention, New Orleans.

26. Croasdale, K. R., 1974. Crushing Strength of Arctic Ice. The Coast and Shelf of the Beaufort Sea. Proc. Arctic Institute of North America.

27. Danys, J. V., 1971. Effect of Cone-Shaped Structures on Impact Forces of Ice Floes. Proc. First POAC Conference, Trondheim, Norway, Vol. 1, pp. 609-620.

28. Danys, J. V., 1972. Effect of Ice Forces on Some Isolated Structures in the St. Lawrence River. Proc. IAHR Ice Symp. and Its Action on Hydraulic Structures, Leningrad, U.S.S.R., pp. 229-331.

29. Davisson, M. T. and Salley, J. R., 1970. Model Study of Laterally Loaded Piles. Proc. ASCE, Journal of Soil Mechanics and Foundation Division, Vol. 96, No. SM5, September, pp. 1605-1627.

30. Desai, C. S., 1974. Numerical Design Analysis for Piles in Sands. Proc. ASCE, Journal of Geotechnical Engineering Division, Vol. 100, No. GT6, Paper No. 10617, June, pp. 613-635.

31. Diaj, E. B., 1973. Determination of Forces, Displacements and Soil Reactions of a Group of Piles. Proc. Eighth International Conference on Soil Mechanics and Foundation Engineering, Vol. 2, pp. 83-88.

32. Doherty, W. P., Wilson, E. L., and Taylor, R. L., 1969. Stress Analysis of Axisymmetric Solids Utilizing Higher Order Quadrilateral Finite Elements, Report No. S.E.S.M. 69-3, Structural Engineering Laboratory, University of California, Berkeley, January.

33. Drouin, M., 1966. Static Ice Forces on Extended Structures. National Research Council Technical Memorandum No. 92, NRC No. 9851, Ottawa, Canada, pp. 95-108 (1968).

34. Drouin, M. and Michel, B., 1974. Pressures of Thermal Origin Exerted by Ice Sheets upon Hydraulic Structures. Draft Translations 427 Corps of Engineers, CRREL, Hanover, New Hampshire, 405 pp.

35. Duncan, J. M. and Chang, C. Y., 1970. Non-Linear Analysis of Stress and Strain in Soils. Proc. ASCE, Journal of Soil Mechanics and Foundation Division, Vol. 96, No. SM5, Paper No. 7513, September, pp. 1629-1653.

36. Edge, B. L. and Mayer, P. G., 1969. A Stochastic Model for the Response of Permanent Offshore Structures Subject to Soil Restraints and Wave Forces. Water Resources Research Center, Report No. NRC-0269, Georgia Institute of Technology, Atlanta, 203 pp.

37. Edwards, R. Y., Lewis, J. W., and Benze, D. L., 1971. An Arctic Model Basin - Design, Construction and Operating Experience. Proc. First POAC Conference, Trondheim, Norway, 1, pp. 541-568.

38. Edwards, R. Y. and Wheaton, J. W., 1972. Experimental Determination of Ice Impact Loads on Marine Vehicles. IAHR/AIRH Symp. on Ice and Its Action on Hydraulic Structures, Leningrad, U.S.S.R., pp. 51-60.

39. Feibusch, R. J. and Keith, E. J., 1969. Analysis of Offshore Structures Including Coupled Structure, Pile and Inelastic Soil Supports. Proc. Offshore Technology Conference (OTC), Houston, Texas, Vol. 1, Paper No. OTC 1054, pp. 567-574.

40. Finn, W. D. L. and Khanna, J., 1966. Dynamic Response of Earth Dams. Proc. Third Earthquake Symp., University of Roorkee, India.

41. Fleming, J. F., Serewvala, F. N., and Kondner, R. L., 1965. Foundation Superstructure Interaction under Earthquake Motion. Proc. Third World Conference on Earthquake Engineering, Vol. I, pp. 22-30.

42. Focht, J. A. and Koch, K. J., 1973. Rational Analysis of the Lateral Performance of Offshore Pile Groups. Proc. Offshore Technology Conference (OTC), Houston, Texas, Vol. 2, Paper No. OTC 1896, pp. 701-708.

43. Forehand, P. W. and Reese, J. L., 1964. Prediction of Pile Capacity by Wave Equation. Proc. ASCE, Journal of Soil Mechanics and Foundation Division, Vol. 90, No. SM2, Paper No. 3820, March, pp. 1-25.

44. Francis, A. J., 1964. Analysis of Pile Groups with Flexural Resistance. Proc. ASCE, Journal of Soil Mechanics and Foundation Division, Vol. 90, No. SM3, Paper No. 3887, May, pp. 1-32.

45. Frederking, R. and Gold, L. W., 1971. Ice Forces on an Isolated Circular Pile. Proc. First POAC Conference, Trondheim, Norway, 1, pp. 73-92.

46. Gaul, R. D., 1958. Model Study of Dynamically Laterally Loaded Pile. Proc. ASCE, Journal of Soil Mechanics and Foundation Division, Vol. 84, No. SM1, February.

47. Gold, L. W., 1970. The Failure Process in Columnar-Grained Ice. Ph.D. Thesis, McGill University, Montreal, Quebec, Canada.

48. Hardin, B. O. and Drnevich, V. P., 1972. Shear Modulus and Damping in Soils: Measurement and Parameter Effects. Proc. ASCE, Journal of Soil Mechanics and Foundation Division, Vol. 98[1], No. SM6, June, Paper No. 8977, pp. 603-624.

49. Hardin, B. O. and Drnevich, V. P., 1972. Shear Modulus and Damping in Soils: Design Equations and Curves. Proc. ASCE, Journal of Soil Mechanics and Foundation Division, Vol. 98[2], No. SM7, Paper No. 9006, July, pp. 667-692.

50. Hasselman, T. K., Bronowicki, A., and Chrostowski, J., 1975. Probabilistic Response of Offshore Platforms to Seismic Excitations. Proc. Offshore Technology Conference (OTC), Houston, Texas, Vol. 8, Paper No. OTC 2353, pp. 165-178.

51. Hayashi, S. and Miyajima, N., 1962. Dynamic Lateral Load Tests on Steel H-Piles. Proc. Japan National Symp. on Earthquake Engineering, Tokyo, Japan.

52. Hayashi, S., Miyajima, N., and Yamashita, I., 1965. Horizontal Resistance of Steel Piles under Static and Dynamic Loads. Proc. Third World Conference on Earthquake Engineering, Vol. 2, pp. 146-166.

53. Hays, C. O. and Matlock, H., 1973. Nonlinear Discrete Element Analysis of Frames. Proc. ASCE, Journal of Structural Division, Vol. 99, No. ST10, Paper No. 10091, October, pp. 2011-2030.

54. Hays, C. O., Jr., 1975. Nonlinear Dynamic Analysis of Framed Structures with Pile Foundations. Preprint 2450, ASCE National Structural Engineering Convention, New Orleans.

55. Hirayama, K., Schwarz, J., and Wu, H. C., 1973. Model Technique for the Investigation of the Forces on Structures. Proc. Second POAC Conference, Reykjavik, Iceland, pp. 332-344.

56. Hirayama, K., Schwarz, J., and Wu, H. C., 1974. An Investigation of Ice Forces on Vertical Structures. Iowa Inst. Hyd. Res. Report, No. 158.

57. Howe, R. J., 1955. Design of Offshore Drilling Structures. Trans. ASME, Vol. 77, pp. 827-851.

58. Hrennikoff, A., 1950. Analysis of Pile Foundations with Batter Piles. Trans. ASCE, Vol. 115, Paper No. 2401.

59. Idriss, I. M., Lysmer, J., Hwang, R., and Seed, H. B., 1973. QUAD-4: A Computer Program for Evaluating the Seismic Response of Soil Structures by Variable Damping Finite Element Procedures. Report No. EERC 73-16, July, University of California, Berkeley.

60. Idriss, I. M., Dorby, R., and Power, M. S., 1975. Soil Response Consideration in Seismic Design of Offshore Platforms. Proc. Offshore Technology Conference (OTC), Houston, Texas, Vol. 3, Paper No. OTC 2355, pp. 191-206.

61. Isenberg, J., 1971. Interaction between Soil and Nuclear Reactor Foundations during Earthquakes, Midland Soil Mechanics and Foundation Engineering Society, Birmingham, England, July, pp. 183-195.

62. Jackson, J. G., Jr., 1968. Factors that Influence the Development of Soil Constitutive Relations. U.S. Army Engineer Waterways Expt. Station, Corps of Engineers, Vicksburg, Miss., Misc. Paper No. 4-980.

63. Jackson, J. G., Jr., 1969. Analysis of Laboratory Test Data to Derive Soil Constitutive Properties. U.S. Army Engineer Waterways Expt. Station, Corps of Engineers, Vicksburg, Miss., Misc. Paper No. S-69-16.

64. Kennedy, R. J., 1966. On the Expansion of a Floating Ice Sheet with Temperature Change. Ice Pressure against Structures, National Research Council of Canada, Assoc. Gtec. on Geotechnical Research, Tech. Memo. No. 92, Appendix I, 185-188 (1968).

65. Khanna, J., 1969. Elastic Soil-Structure Interaction. Proc. Fourth World Conference on Earthquake Engineering, Vol. 3, A-16, pp. 143-153.

66. King, R., 1974. Hydroelastic Models and Offshore Design, Civil Engineering, pp. 43-47.

67. Kivisild, H. R., 1968. Ice Impact on Marine Structures. Ice Seminar Sponsored by Petroleum Society of Canadian Institute of Mining and Metallurgy and the American Petroleum Institute, Calgary, Alberta, Canada, 6 pp.

68. Kivisild, H. R., 1971. Year-Round Oil Terminal in Ice-Covered Waters. Proc. First POAC Conference, Trondheim, Norway, 1, pp. 621-631.

69. Kondner, R. L., 1963. Hyperbolic Stress-Strain Response of Cohesive Soils. Proc. ASCE, Journal of Soil Mechanics and Foundation Division, Vol. 89, No. SM1, Paper No. 3429, pp. 115-143.

70. Kondner, R. L. and Zelasko, J. S., 1963. A Hyperbolic Stress-Strain Formulation for Sands. Proc. Second Pan-American Conference on Soil Mechanics and Foundation Engineering, Brazil, Vol. 1, pp. 289-324.

71. Kopaigorodski, E. M., Vershinin, S. A., and Nifontov, S. A., 1972. Model Investigations of the Effect of an Ice Field Pushed Against the Piles of Offshore Oil Platforms. IAHR/AIRH Symp. on Ice and Its Action on Hydraulic Structures, Leningrad, U.S.S.R., pp. 100-102.

72. Korzhavia, K. N., 1962. Action of Ice on Engineering Structures. Novosibirsk 1962. Draft Transl. 260 Corps of Engineers, CRREL, Hanover, New Hampshire, 319 pp. (1971).

73. Kubo, K., 1965. Response of a System of Two-Degree Freedom. Proc. Third World Conference on Earthquake Engineering, Vol. 2, pp. 357-368.

74. Kubo, K., 1965. Experimental Study of the Behaviour of Laterally Loaded Piles. Proc. Sixth International Conference on Soil Mechanics and Foundation Engineering, Vol. 2, Divisions 3-6, pp. 275-279.

75. Kubo, K., 1969. Vibration Test of a Structure Supported by Pile Foundation. Proc. Fourth World Conference on Earthquake Engineering, Vol. 3, A-6, pp. 1-12.

76. Kuhlemeyer, R. L. and Lysmer, J., 1973. Finite Element Method Accuracy for Wave Propogation Problems. Proc. ASCE, Journal of Soil Mechanics and Foundation Division, Vol. 100, No. GT1; Paper No. 10284, pp. 1-3.

77. Kuhlemeyer, R. L., 1976. Static and Dynamic Laterally Loaded Piles. Research Report No. CE76-9, March, University of Calgary.

78. Kuribayashi, E. and Iida, Y., 1974. An Application of Finite Element Method to Soil-Foundation Interaction Analysis. Bulletin of the New Zealand National Society for Earthquake Engineering, Vol. 7, No. 4, December.

79. Lavrov, V. V., 1969. Deformation and Strength of Ice. Hydromef. Publ. House, Leningrad, U.S.S.R. Trans. by Israel Prog. for Scientific Transl., Jerusalem, Israel.

80. Lavrov, V. V., 1971. Deformation and Strength of Ice. Israel Prog. for Scientific Transl., Jerusalem, Israel.

81. Lazier, S. S. and MacLachlan, F. A., 1969. Movements in Continuous Lake Ice Sheets and Temperature Gradients in an Ice Sheet. Ice Engineering and Avalanche Forecasting and Control. Proc. of International Conference held at University of Calgary, Alberta, N.R.C. Tech. Momo 98, pp. 17-35.

82. Lazier, S. S. and Metge, M., 1972. Observations on Thermal Cracks in Lake Ice. IAHR/AIRH Symp. on Ice and Its Action on Hydraulic Structures, Leningrad, U.S.S.R., 6 pp.

83. Liaw, C. Y. and Chopra, A. K., 1973. Earthquake Response of Axisymmetric Tower Structures Surrounded by Water. Report No. EERC 73-25, University of California, Berkeley, 171 pp.

84. Lysmer, J., Udaka, T., Seed, H. B., and Hwang, R., 1974. LUSH: A Computer Program for Complex Response Analysis of Soil-Structure Systems. Report No. EERC 74-4, University of California, Berkeley, April.

85. Matlock, H. and Reese, L. C., 1961. Foundation Analysis of Offshore Pile Supported Structures. Proc. Fifth International Conference on Soil Mechanics and Foundation Engineering, Vol. 2, 3B/14, pp. 91-97.

86. Matlock, H., 1962. Analysis of Several Beam On-Foundation Problems. Presented at the Houston Convention, ASCE, Soil Mechanics and Foundation Division, February.

87. Matlock, H. and Ingram, W. B., 1963. Bending and Buckling of Soil Supported Structural Elements. Paper No. 32. Proc. Second Pan-American Conference on Soil Mechanics and Foundation Engineering, Brazil, July.

88. Matlock, H. and Haliburton, T. A., 1965. A Finite Element Method of Solution for Linearly Elastic Beam Columns. Research Report No. 56-1, Center for Highway Research, The University of Texas at Austin.

89. Matlock, H., 1970. Correlations for Design of Laterally Loaded Piles for Soft Clays. Proc. Offshore Technology Conference (OTC), Houston, Texas, Vol. 2, Paper No. OTC 1204, pp. 579-594.

90. Matlock, H., Dawkins, W. P., and Panak, J. J., 1971. Analytical Model for Ice Structure Interaction. Proc. ASCE, Engineering Mechanics Division, Vol. 97, No. EM4, pp. 1083-1092.

91. Matsumoto, Y. and Tsuchiya, T., 1962. Lateral Load Capacity of Vertical and Bektered Concrete Pile Groups. Proc. Japan National Symposium on Earthquake Engineering, Tokyo, Japan.

92. McClelland, B. and Focht, J. A., 1958. Soil Modulus for Laterally Loaded Piles. Trans. ASCE, Vol. 123, pp. 1049-1086.

93. Michel, B., 1970. Ice Pressure on Engineering Structures. Cold Regions Science and Engineering, Monograph III-Bib, CRREL, Hanover, New Hampshire, U.S.A., 71 pp.

94. Neill, C. R., 1970. Ice Pressure on Bridge Piers in Alberta. Proc. IAHR/AIRH Symp. on Ice and Its Action on Hydraulic Structures, Reykjavik, Iceland.

95. Neill, C. R., 1972. Force Fluctuations during Ice-Floe Impact on Piers. IAHR/AIRH Symp. on Ice and Its Action on Hydraulic Structures, Leningrad, U.S.S.R., 7 pp.

96. Nevel, D. E., 1967. Ice Breaker Simulation. Cold Regions Res. Eng. Lab. Rep., CRREL, Hanover, New Hampshire, U.S.A.

97. Newmark, N. M., 1959. A Method of Computation for Structural Dynamics. Proc. ASCE, Journal of Engineering Mechanics Division, Vol. 85, No. EM3, Paper No. 2094, July, pp. 67-94.

98. Newmark, N. M., 1960. Failure Hypothesis for Soils. SMFD ASCE Research Conference on Shear Strength of Cohesive Soils, Boulder, Colorado.

99. Novak, M., 1974. Dynamic Stiffness and Damping of Piles. Canadian Geotechnical Journal, Vol. 2, No. 4, November, pp. 574-598.

100. Parker, F., Jr., and Cox, W. R., 1970. Experimental and Analytical Studies of Behaviour of Single Piles in Sand under Lateral and Axial Loading. Research Report No. 117-2. Center for Highway Research, The University of Texas at Austin, Austin, Texas, November.

101. Parmelee, R. A., 1967. Building Foundation Interaction Effects. Proc. ASCE, Journal of Engineering Mechanics Division, Vol. 93, No. EM2, Paper 5200, April, pp. 131-152.

102. Penzien, J., Scheffey, C. F., and Parmelee, R. A., 1964. Seismic Analysis of Bridges on Long Piles. Proc. ASCE, Journal of Engineering Mechanics Division, Vol. 90, No. EM3, June, pp. 223-254.

103. Penzien, J., 1975. Seismic Analysis of Platform Structure Foundation System. Proc. Offshore Technology Conference (OTC), Houston, Texas, Vol. 3, Paper No. OTC 2352, pp. 153-164.

104. Peyton, H. R., 1966. Sea Ice Strength. Report No. UAGR-182, Final Report Prepared for Department of the Navy, Office of Naval Research by Geophysical Institute, University of Alaska, College, 273 pp.

105. Peyton, H. R., 1967, Sea Ice Strength. Ph.D. Thesis, University of Alaska.

106. Peyton, H. R., 1968. Ice and Marine Structures, Part I - The Magnitude of Ice Forces Involved in Design. Ocean Industry, 3, pp. 404-444. Also Part II, 3, pp. 59-65, and Part III, Vol. 3, No. 12, pp. 51-58.

107. Poulos, H. G., 1971. Behaviour of Laterally Loaded Piles: I - Single Piles. Proc. ASCE, Journal of Soil Mechanics and Foundation Division, Vol. 97, No. SM5, Paper No. 8092, May, pp. 711-731.

108. Poulos, H. G., 1971. Behaviour of Laterally Loaded Piles: II - Pile Groups. Proc. ASCE, Journal of Soil Mechanics and Foundation Division, Vol. 97, No. SM5, Paper No. 8093, May, pp. 733-751.

109. Poulos, H. G., 1972. Behaviour of Laterally Loaded Piles: III - Socketted Piles. Proc. ASCE, Journal of Soil Mechanics and Foundation Division, Vol. 98, Paper No. SM4, April, pp. 341-360.

110. Prakash, S. and Aggarwal, S. L., 1965. Study of Vertical Pile under Dynamic Lateral Load. Proc. Third World Conference on Earthquake Engineering, Vol. 1, pp. 215-229.

111. Prakash, S. and Chandrasekharan, V., 1973. Pile Foundation under Lateral Dynamic Loads. Proc. Eighth International Conference on Soil Mechanics and Foundation Engineering, Vol. 2, 3/31, pp. 199-202.

112. Proskuryakov, B. V., 1959. The Investigation of Ice Problems in the Construction of Hydro-Engineering Structures in the U.S.S.R. Eighth Congress on the International Association for Hydraulic Research, Montreal, pp. 41.

113. Przemieniecki, J. S., 1968. Theory of Matrix Structural Analysis, McGraw-Hill Book Company Inc., New York.

114. Reddy, D. V. and Cheema, P. S., 1974. Response of an Offshore Structure to Random Ice Forces. Proc. IEEE, International Conference on Engineering in the Ocean Environment, Halifax, Vol. 1, pp. 84-88.

115. Reddy, D. V., Cheema, P. S., and Swamidas, A. S. J., 1975. Ice Force Response Spectrum Modal Analysis of Offshore Towers. Proc. Third POAC Conference, University of Alaska, Alaska, August.

116. Reddy, D. V., Cheema, P. S., Swamidas, A. S. J., and Haldar, A. K., 1975. Stochastic Response of a Three-Dimensional Offshore Tower to Ice Force. IAHR/AIRH Third International Symp. on Ice Problems, Hanover, New Hampshire, U.S.A., pp. 499-514.

117. Reeh, N., 1970. Natural Frequency of the System of a Heavy Elastic Plate Covering Shallow Water. Bygnningsstatistiske Meddelelser, 41, pp. 167-187.

118. Reeh, N., 1972. Impact of an Ice Floe against a Sloping Face. Prog. Report No. 26, Institute of Hydrodynamics and Hydraulic Engineering, Tech. University of Denmark, pp. 23-28.

119. Reinius, E., Haggard, S., and Ernstons, E., 1971. Experience of Offshore Lighthouses in Sweden. Proc. First POAC Conference, Trondheim, Norway, 1, pp. 657-673.

120. Reese, L. C. and Matlock, H., 1956. Non-Dimensional Solutions for Laterally Loaded Piles with Soil Modulus assumed Proportional to Depth. Proc. Eighth Texas Conference on Soil Mechanics and Foundation Engineering, Austin, Texas, pp. 1-42.

121. Reese, L. C., 1968. Discussion on "Soil Modulus for Laterally Loaded Piles" by McClelland, B. Transaction, ASCE, Vol. 123, pp. 1071-1077.

122. Reese, L. C. and Matlock, H., 1960. Numerical Analysis of Laterally Loaded Piles. Proc. Second ASCE Structural Division Conference on Electronic Computation, Pittsburg, Penn.

123. Reese, L. C. and Matlock, H., 1966a. Behaviour of a Two-Dimensional Pile Group under Inclined and Eccentric Loading. Proc. Offshore Exploration Conference, Long Beach, California, February.

124. Reese, L. C. and O'Neill, M. W., 1967. The Analysis of Three-Dimensional Pile Foundations Subjected to Inclined and Eccentric Loads. Proc. ASCE Conference on Civil Engineering in the Oceans, September, pp. 245-276.

125. Reese, L. C., O'Neill, M. W., and Smith, R. E., 1970. Generalized Analysis of Pile Foundations. Proc. ASCE, Journal of Soil Mechanics and Foundation Division, Vol. 96, No. SM1, January, pp. 235-250.

126. Reese, L. C., Cox, W. R., and Koop, F. D., 1975. Field Testing and Analysis of Laterally Loaded Piles in Stiff Clay. Proc. Offshore Technology Conference (OTC), Houston, Texas, Vol. 2, Paper No. OTC 2312, pp. 671-690.

127. Richart, F. E., Jr., 1975. Some Effects of Dynamic Soil Properties on Soil-Structure Interaction. Tenth Terzaghi Lecture, ASCE. UMEE-75R1, April.

128. Robertson, R. N., 1961. Analysis of a Bridge Foundation with Batter Piles. M.Sc. Thesis, The University of Texas, Austin, Texas, January.

129. Ross, H. E., 1970. Dynamic Response of Laterally Loaded Offshore Piling. Sea Grant Program. Texas A & M University, Report No. 132, TAMU-SG-70-224, August.

130. Saul, W. E., 1968. Static and Dynamic Analysis of Pile Foundations. Proc. ASCE, Journal of Structural Division, Paper No. 5936, No. ST5, May, pp. 1077-1100.

131. Schwarz, J., Hirayama, K., and Wu, H., 1973. Model Technique for the Investigation of Ice Force on Structures. Proc. Second POAC Conference, Reykjavik, Iceland.

132. Schwarz, J., Hirayama, K., and Wu, H. C., 1974. An Investigation of Ice Forces on Vertical Structures. Iowa Institute of Hydraulic Research, Report No. 158.

133. Schwarz, J., Hirayama, K., and Wu, H. C., 1974. Effect of Ice Thickness on Forces. Proc. Offshore Technology Conference (OTC), Houston, Texas, Vol. 2, pp. 145-155.

134. Shrivastava, S. P., 1973. Elastic Analysis of Pile Groups in Granular Soil. Proc. Eighth International Conference on Soil Mechanics and Foundation Engineering, Vol. 2, pp. 223-227.

135. Seed, H. B. and Idriss, I. M., 1969. Influence of Soil Conditions on Ground Motion during Earthquakes. Proc. ASCE, Journal of Soil Mechanics and Foundation Division, Vol. 95, No. SM1, pp. 99-137, January.

136. Seed, H. B. and Idriss, I. M., 1970. Soil Moduli and Damping Factors for Dynamic Response Analysis, EERC Report No. 70-10, University of California, Berkeley, December.

137. Seed, H. B., 1975. Soil Structure Interaction Analysis. Proc. ASCE, Journal of Geotechnical Engineering Division, Vol. 101, No. GT5, May, pp. 439-457.

138. Skempton, A. W., 1951. The Bearing Capacity of Clays. Building Research Congress, Division, 1, Part III, pp. 180-189.

139. Spillers, W. R. and Stroll, R. D., 1964. Lateral Response of Piles. Proc. ASCE, Journal of the Soil Mechanics and Foundation Division, Vol. 90, Np. SM6, November, pp. 1-9.

140. Stockard, D. M., 1976. Effects of Pile-Soil-Water Interaction on the Dynamic Response of a Seismically Excited Dynamic Response. Proc. Offshore Technology Conference (OTC), Houston, Texas, Vol. 3, pp. 617-631.

141. Sundararajan, C. and Reddy, D. V., 1973. Stochastic Analysis of Ice Structure Interaction. Proc. Second. POAC Conference, Reykjavik, Iceland, pp. 345-353.

142. Swamidas, A. S. J. and Reddy, D. V., 1976. Dynamic Ice Structure Interaction of Offshore Monopod Towers by Hybridisation of the Computer Programs EATSW and SAP-IV. Proc. First SAP-IV User's Conference, Los Angeles, California, 33 pp.

143. Swamidas, A. S. J., Reddy, D. V., and Purcell, G., 1976. Ice Structure Interaction with Artificially Generated Force Records. Presented at the Symposium on Applied Glaciology Organized by the International Glaciological Society, Cambridge, England, September 12-17, 1976.

144. Szilard, R., 1965. Dynamic Response of Multi-Level Guyed Towers to Earthquake considering Nonlinearity of the Elastic Support. Proc. Third World Conference on Earthquake Engineering, Vol. 2.

145. Tajimi, H., 1965. Dynamic Analysis of a Structure Embedded in an Elastic Stratum. Proc. Third World Conference on Earthquake Engineering, Vol. 3, A-6, pp. 54-69.

146. Terzaghi, K., 1955. Evaluation of Coefficients of Subgrade Reactions. Geotechnique. Institute of Civil Engineering, Vol. V, London, pp. 297-326.

147. Thiers, G. R. and Seed, B. H., 1968. Cyclic Stress Strain Characteristic of Clay. Proc. ASCE, Journal of Soil Mechanics and Foundation Division, Vol. 94, No. SM2, Paper No. 5871, March, pp. 555-569.

148. Tucker, R. L., 1964. Lateral Analysis of Piles with Dynamic Behaviour. Presented at Conference on Deep Foundations, Mexico City, Mexico, December, 10 pp.

149. U.S.S.R. State Committee of the Council of Ministers for Construction, 1966. Instructions for Determining Ice Loads on River Structures, SN76-1966. National Research Council of Canada Tech. Trans. 1663 (1973), Ottawa, 20 pp.

150. Utt, M. E., Durning, P. J., Duthweiler, F. C., and Engle, D. D., 1976. Estimation of the Foundation Condition of a Fixed Platform by Measurement of Dynamic Response. Proc. Offshore Technology Conference (OTC), Houston, Texas, Vol. 3, Paper No. OTC 2625, pp. 65-74.

151. Vandiver, J. K., 1975. Detection of Structural Failure on Fixed Platforms by Measurement of Dynamic Response. Proc. Offshore Technology Conference (OTC), Houston, Texas, Vol. 2, Paper No. OTC 2267, pp. 243-252.

152. Weeks, W. and Assur, A., 1967. The Mechanical Properties of Sea Ice. Report 11-63. U.S. Army, CRREL, Hanover, New Hampshire, U.S.A.

153. Whitman, R. V. and Richart, F. E., 1967. Design Procedures for Dynamically Loaded Foundation. Proc. ASCE, Soil Mechanics and Foundation Engineering, Vol. 93, No. SM6, Paper No. 5569, November, pp. 169-193.

154. Whitman, R. V., 1969. Equivalent Lumped System for Structure Founded upon Stratum of Soil. Proc. Fourth World Conference on Earthquake Engineering, Vol. 3, A-6, pp. 133-142.

155. Whitman, R. V., 1973. Analysis of Dynamic Soil-Structure Interaction for Nuclear Plants. Panel Discussion. The ASCE Speciality Conference, December 17-18, Chicago.

156. Wilson, E. L. and Clough, R. W., 1962. Dynamic Response by Step-by-Step Matrix Analysis. Symposium on Use of Computer in Civil Engineering, Laborotorio National de Engenharia Civil, Lisbon, Portugal.

157. Wilson, E. L., 1969. A Method of Analysis for the Evaluation of Foundation Structure Interaction. Proc. Fourth World Conference on Earthquake Engineering, Vol. 3, A-6, pp. 87-100.

158. Wilson, E. L., Bathe, K. J., Peterson, F. E., and Dorey, H. H., 1973. SAP-IV: A Structural Analysis Program for Linear Systems. Proc. Nuclear Engineering and Design, 25, pp. 257-274. North-Holland Publishing Company. Also, EERC Report No. 73-11. SAP-IV: A Structural Analysis Program for Static and Dynamic Response of Linear Systems (1974).

159. Wilson, E. L., 1971. SOLID SAP: A Static Analysis Program for Three-Dimensional Solid Structures. Report No. UC SESM-1-19, University of California, Berkeley, California.

160. Wilson, S. D. and Dietrich, R. J., 1960. Effect of Consolidation Pressure on Elastic and Strength Properties of Clay. Proc. Research Conference on Shear Strength of Cohesive Soils, ASCE, Boulder, Colarado.

161. Wilson, W. E., 1967. Analysis of Laterally Loaded Long Piles in an Inelastic Soil. Ph.D. Dissertation, Georgia Institute of Technology, Atlanta, Georgia.

162. Workman, G. H., 1969. The Inelastic Behavior of Multistory Braced Frame Structures Subjected to Earthquake Excitation. Ph.D. Dissertation, University of Michigan, Ann Arbor, 1969.

163. Wu, P. K., 1965. The Resistance of Soils in Vibro-Sinking of Precast Reinforced Concrete Pipe Piles of Large Diameter. Proc. Sixth International Conference on Soil Mechanics and Foundation Engineering, Vol. 2, pp. 252-255.

164. Yegian, M. and Wright, S. G., 1973. Lateral Soil Resistance - Displacement - Relationship for Pile Foundations in Soft Clays. Proc. Offshore Technology Conference (OTC), Houston, Texas, Vol. 2, Paper No. OTC 1893, pp. 663-676.

165. Zienkiewicz, O. C., 1971. The Finite Element Method in Engineering Science, McGraw-Hill, London.

166. Zubov, N. N., 1945. Arctic Ice. Izdatel'stvo Glavsevmoi eti, Moscow (1945), Transl. by the U.S. Navy Oceanographic Office and the Americal Meteorological Society (1963), 489 pp.

APPENDIX

APPENDIX

AUTHOR'S PUBLICATIONS

1. "Stochastic Response of Three-Dimensional Offshore Towers to Ice Forces". Coauthored by D. V. Reddy, P. S. Cheema, and A. S. J. Swamidas. Third International Symposium on Ice Problems, Hanover, New Hampshire, U.S.A., August 1975.

2. "Dynamic Ice Force Response of a Gravity-Type Offshore Tower (Monopod) in the Canadian Beaufort Sea". Coauthored by A. S. J. Swamidas and D. V. Reddy. To be published in the Proc. Symposium on Cold Region. Engineering Changes and Development, Univ. of Alaska, Fairbanks, U.S.A., 1976.

3. "Dynamic Ice-Water-Soil Structure Interaction of Offshore Towers including Nonlinear Soil Behavior". Coauthored by A. S. J. Swamidas, D. V. Reddy, and M. Arockiasamy. (Paper accepted for presentation at the Ninth Offshore Technology Conference, Houston, Texas, May 2-5, 1977.)

APPENDIX

4. "Modelling of Offshore Structures for Dynamic Response to Ice Forces considering Water-Soil-Structure Interaction". Coauthored by A. S. J. Swamidas and D. V. Reddy. (Paper accepted to International Conference on Applied Numerical Modelling to be held on 11-15 July, 1977, University of Southampton, England, for presentation.)

5. "Wind Force Response Spectrum Modal Analysis of the C.N. Tower, Toronto". Coauthored by D. V. Reddy, A. S. J. Swamidas, and M. Arockiasamy. (To be published.)

6. "Nonlinear Response Analysis of an Offshore Tower considering Soil-Structure Interaction". Coauthored by A. S. J. Swamidas, M. Arockiasamy, and D. V. Reddy. (Submitted to ASCE National Structural Engineering Convention, 1977, for publication.)

7. "Dynamic Analysis of Wave-Water-Soil-Structure System of Offshore Structures considering Nonlinear Soil Behaviour". Coauthored by D. V. Reddy, M. Arockiasamy, and T. K. Yen. (Paper accepted for presentation at Second SAP-IV Users Conference to be held on June 23 and 24, 1977, University of Southern California, Los Angeles.)

8. "Dynamic Wave-Water-Soil Interaction. Studies of Offshore Structures considering Soil Nonlinearity". Coauthored by M. Arockiasamy, D. V. Reddy, and T. K. Yen. Paper accepted for presentation at Symposium on Applications of Computer Methods in Engineering, University of Southern California, Los Angeles, August 23-26, 1977.

9. "Dynamic Wave-Structure-Soil Interaction Studies of Offshore Structures considering Soil Nonlinearity". Coauthored by M. Arockiasamy and D. V. Reddy. Paper submitted for presentation to Fourth POAC Conference to be held on September, 1977, at M.U.N., St. John's, Newfoundland.

10. "Response of an Offshore Floating LPG Storage Platform to Simulated Wind and Ice Forces". Coauthored by D. V. Reddy, D. S. Sodhi, and M. Arockiasamy. Submitted for presentation to Fourth POAC Conference to be held on September, 1977, at M.U.N., St. John's, Newfoundland.